Acid-base Chemistry of Aquatic Systems

An introduction to the chemistry of acid-base equilibria with emphasis on the carbon dioxide system in natural waters

Keith A. Hunter

Professor in Chemistry
Department of Chemistry
University of Otago
Dunedin, New Zealand
Email: khunter@alkali.otago.ac.nz
Web page: http://telperion.otago.ac.nz:800/rweavers/research/KAH-RES.HTM

PREFACE

The first draft of this book was prepared during a sabbatical leave at the Department of Oceanography, University of Washington, Seattle in 1991. Since then, the subject material has undergone much revision, particular as new research findings have emerged since that time. Therefore, during the summer vacation of 1997/98, I embarked on a major revision, the result of which is the present version. Most of the structure of the book has been changed, and material that had become somewhat dated has been removed.

I am particularly grateful to my colleagues who have assisted with various aspects of this book, but most of all to the many undergraduate and graduate students whose feedback has been the major source of improvements.

Keith A. Hunter
Dunedin, March 1998

TABLE OF CONTENTS

Chapter 1 Basic Concepts of Acid-Base Chemistry

While acid-base reactions are not the only chemical reactions important in aquatic systems, they do present a valuable starting point for understanding the basic concepts of chemical equilibria in such systems. Carbon dioxide, a substance of vital importance to a variety of environmental processes, including growth and decomposition of biological systems, climate regulation and mineral weathering, has acid-base properties that are critical to an understanding of its chemical behaviour in the environment. The phenomenon of acid rain is another example of the importance of acid-base equilibria in natural aquatic systems.

This chapter reviews the basic concepts used to describe and understand the chemistry of acid-base reactions in aquatic systems. The principles developed throughout this book, are generally applicable to other types of chemical equilibria, e.g. the solubility of minerals and oxidation-reduction reactions.

1.1 The Arrhenius Theory of Acids and Bases

In 1887, the Swedish chemist Svante Arrhenius proposed that acids were substances which, when dissolved in water, produced a solution of hydrogen ions. Conversely, bases were substances that produced solutions containing hydroxide ions. In each case, the ions were considered to arise from dissociation reactions of the parent acid or base. For example, the dissociation of hydrochloric acid gives hydrogen ions

$$HA \rightarrow H^+ + A^- \qquad [1.1]$$

Similarly, the dissociation of the base sodium hydroxide gives hydroxide ions

$$NaOH \rightarrow Na^+ + OH^- \qquad [1.2]$$

When acids and bases react according to this theory, the hydrogen and hydroxide ions neutralize each other forming water

$$H^+ + OH^- \rightarrow H_2O \qquad [1.3]$$

The Cl^- and Na^+ ions formed by the dissociation of the acid and the base respectively, were considered to combine to form a *salt* (in this case common salt or sodium chloride). It is important to realize that at the time Arrhenius formulated his theory, the concept of the independent nature of ions in aqueous solutions was still undergoing development (see Section 1.4) and was not widely accepted.

The Arrhenius view of acids and bases explained many of the properties of acidic and basic substances known at the time. However, it has a number of limitations, particularly with respect to how bases react. In fact, the Arrhenius concept is strictly correct only for those acids and bases that are completely dissociated in solution into their constituent ions.

The need to view the reactions of a base as being a result of dissociation to yield hydroxide ions gave rise to the erroneous notion that in an ammonia solution, the active base species was

NH_4OH. In fact, such a species does not exist and the actual base is the NH_3 molecule itself. The same objection applies to many other bases, e.g. organic amines, carboxylate anions etc.

A second problem with the Arrhenius concept is that it accords no specific role to the solvent. Yet even in Arrhenius' day, it was already appreciated that basic properties could be observed in solvents such as aniline, which cannot form hydroxide ions. On the other hand, hydrochloric acid was known to have no acidic properties in what we now recognize as aprotic solvents, e.g. benzene. Finally, it soon became clear that even pure water contains both hydrogen and hydroxide ions. Obviously the solvent plays a critical role in acid-base reactions.

A third problem is that according to the Arrhenius theory, all salts should produce solutions that are neither acidic nor basic. While this is true of many salts, there are also obvious exceptions. For example, sodium acetate is slightly basic while ammonium chloride is slightly acidic. The theory gives no explanation for these properties.

1.2 The Lowry-Brønsted Theory

In 1923, within several months of each other, Johannes Nicolaus Brønsted (Denmark) and Thomas Martin Lowry (England) published essentially the same theory about how acids and bases behave. Their ideas, taken together, overcame many of the problems inherent in the Arrhenius theory. Since they arrived at their conclusions independently of each other, it has become usual to refer to them collectively as the Lowrie-Bronsted theory of acid-base behaviour.

Thomas Lowrie

Johannes Brønsted

The Lowrie-Brønsted theory is based on the idea that an acid base reaction involves a *transfer of protons* from one substance to another. The acid is the *proton donor* and the base is the *proton acceptor*. Thus when HCl is dissolved in water, it transfers a proton to the base H_2O

$$HCl + H_2O \rightarrow H_3O^+ + Cl^- \qquad [1.4]$$

Similarly, with acetic acid (abbreviated as HOAc) and a solution of sodium hydroxide, this time acetic acid is the proton donor and OH^- is the proton acceptor

$$HOAc + OH^- \rightarrow OAc^- + H_2O \qquad [1.5]$$

The acetate OAc^- produced is still a base because it can accept protons from an acid and, in the process, turn back into the original acetic acid:

$$OAc^- + H_3O^+ \rightarrow HOAc + H_2O \qquad [1.6]$$

This simple example demonstrates the principle that acids and bases come in pairs called an *acid-base conjugate pair*. They differ by the proton that is exchanged. Moreover, an acid-base reaction always involves two conjugate pairs, one functioning as an acid and one as a base.

$$HA + B^- \rightarrow A^- + HB \qquad [1.7]$$

In this example, HA/A^- is one conjugate pair and HB/B^- is the other.

Some substances are capable of both accepting and donating protons depending on what they are reacting with

$$HCO_3^- + OH^- \rightarrow CO_3^{2-} + H_2O$$
$$HCO_3^- + H_3O^+ \rightarrow H_2CO_3 + H_2O \qquad [1.8]$$

Some, like H_2O, are even capable of reacting with themselves, one molecule acting as the acid and the other acting as the base, thus explaining the presence of both hydrogen and hydroxide ions in pure water:

$$H_2O + H_2O \rightarrow H_3O^+ + OH^- \qquad [1.9]$$

Lowrie was the first to introduce the terminology H_3O^+ to signify the hydrogen ion in solution, seeking with this formula to emphasize that the hydrogen ion is best regarded as a water molecule to which a proton has been added. This formula also emphasizes that the free proton itself does not itself exist in solution as a discrete species. However, the actual molecular structure of the hydrated proton is not known, but almost certainly it involves more than one water molecule. On thermodynamic grounds, it is not possible through any *macroscopic* measurement to distinguish between any *microscopic* forms of the hydrated proton, i.e. the molecular species H_3O^+, $H_5O_2^+$ ($H^+ + 2\ H_2O$), $H_7O_3^+$ ($H^+ + 3\ H_2O$), etc are all thermodynamically identical. Thus, many textbooks and research papers still make use of the symbol H^+ to refer to the hydrogen ion in aqueous solution, largely for reasons of economy and simplicity.

Following this practice, the terms H_3O^+ and H^+ will be used interchangeably in this book. The simpler form H^+ is used mostly for economy, with the term H_3O^+ used when it is necessary to explicitly refer to the role of water in an acid-base reaction.

While the Lowry-Brønsted concept of acids and bases eliminates most of the confusing aspects of the Arrhenius viewpoint, it does have limitations. Take, for example, the hydrolysis reaction of 2-chloro, 2-methylpropane (*tert*-butyl chloride)

$$C(CH_3)_3Cl + OH^- \rightarrow C(CH_3)_3OH + Cl^- \qquad [1.10]$$

This reaction is considered to proceed via a SN1 mechanism involving the formation of a carbocation. Fundamentally the reaction is identical to that between HCl and OH^- as shown in reaction [1.4]. However, there is no proton transfer. Instead, the 2-chloro,2-methylpropane transfers a *carbocation* to the base OH^-.

Another good example is provided by aqueous solutions of metal cations. We can show by various methods of chemical analysis that solutions of many metal cations, e.g. Fe^{3+}, contain hydrogen ions. In the Lowry-Brønsted scheme of things, this is explained by acid-base reactions of the water molecules coordinated to the metal ion

$$Fe(H_2O)_6^{3+} + H_2O \rightarrow Fe(H_2O)_5OH^{2+} + H_3O^+ \qquad [1.11]$$

However, this reaction is fundamentally the same as any other *ligand substitution reaction* in which proton exchange is not involved

$$Fe(H_2O)_6^{3+} + Cl^- \rightarrow Fe(H_2O)_5Cl^{2+} + H_2O \qquad [1.12]$$

There are many counter-examples of the same type.

1.3 The Lewis Theory of Acid-Base Reactions

The Lowrie and Brønsted concept of acids and bases was generalized by G.N. Lewis, who restated their theory in terms of *electron-pair transfer* rather than proton transfer. In the Lewis scheme, a base is a substance that donates an electron pair while an acid is one that accepts an electron pair. Thus a Lewis base is what organic chemists call a *nucleophile*, while a Lewis acid is an *electrophile*.

The Lewis scheme is valuable because it unites "conventional" acid-base reactions, ligand-metal ion coordination reactions, and substitution reactions in organic chemistry involving electrophiles and nucleophiles, all under the same conceptual framework. However, the important contribution of the Lowry-Brønsted approach is the concept of acid-base conjugate pairs. These key features remain unchanged in the Lewis approach.

In this book we will be concerned only with acid-base reactions taking place in water, so that the Lowry-Brønsted concept is adequate to the task. However the general principles that will be developed are applicable to any acid-base reaction.

1.4 The Nature of Ions in Solution

The English chemist Michael Faraday laid the foundation of our present-day understanding of ions in solution. During his investigations of the nature of electricity, Faraday showed that salt solutions were able to conduct electricity quite effectively, and coined the term *electrolyte* to describe this property. Although the ability of electrolyte solutions to conduct electricity hinted strongly at the existence of ions (charged molecules) in solution, this concept was not readily accepted until much later.

Arrhenius developed his early theory of acid-base behaviour by studying the formation of what we now know as ions in aqueous solution. At the age of 24, he set about examining how the electrical conductivity of aqueous solutions depended on the nature of the solute and its concentration. He showed that for dilute solutions of some solutes, the conductivity was nearly proportional to the solute concentration, meaning that the molar conductivity (conductivity per unit concentration) was almost constant. This situation is represented by the results for HCl, NaOH and NaCl in Table 1.1 below. Below 0.01 M, the molar conductivity of these solutes increases by only a few percent on dilution to 0.001 M.

Table 1.1 Molar conductivity (S cm^2 mol^{-1}) of various aqueous electrolytes at different concentrations in the range 0.001 to 0.5 M

Electrolyte	0.001M	0.005M	0.01M	0.05M	0.1M	0.5M
HCl	377	373	370	360	351	327
NaOH	245	241	238	231	226	210
NaCl	124	121	118	111	107	101
CH_3COOH	41	20	14	6.5	4.6	2.0
CH_3COONa	75	72	70	64	61	49

However, quite different results are found for other solutes. For acetic acid, the molar conductivity is much lower than the solutes already mentioned and increases significantly as the solution is diluted. Sodium acetate is intermediate in behaviour.

Arrhenius interpreted these results to mean that substances differed in their ability to dissociate into ions in solution. Those like HCl, which had nearly constant molar conductivity, were more or less completely dissociated at all concentrations, thus providing a constant fraction of ions to conduct electricity. Others like acetic acid, continued to dissociate further as the solution was diluted, thus accounting for the increase in molar conductivity.

These concepts survive into modern chemistry. Electrolytes that dissociate completely into their constituent ions, such as NaCl, NaOH or HCl are termed *strong electrolytes*, while those that only dissociate partly, in a manner that depends on concentration, are termed *weak electrolytes*. Thus we may also speak of strong acids or bases, and weak acids or bases. Neutral molecules such as acetic acid and ammonia are examples of weak electrolytes. All metal salts formed from reaction of strong acids and strong bases are themselves strong electrolytes. Such a salt may be very insoluble, meaning that very little of it dissolves in water. However, 100% of that which does dissolve is dissociated into its constituent ions.

A further key step in the development of Arrhenius' theory of iondissociation was to link his work on conductivity to the theory of osmotic pressure advanced in 1894 by Jacobus van't Hoff, with whom he later worked. Van't Hoff had shown that the osmotic pressureπ of an aqueous solution depended on temperature T and concentration c in a manner identical to that of ideal gases

$$\pi = cRT \qquad [1.13]$$

However, it was known that for many solutes, the measured osmotic pressure was higher than expected on the basis of this equation. In an 1887 paper, Arrhenius explained this discrepancy by proposing the dissociation of such electrolytes into ions, thus providing more molecular species than in the original solute. For example, sodium chloride would provide two species, sodium ion and chloride ion and, he argued, should exert twice the osmotic pressure of a simple solute like sucrose. He showed that for a large number of substances, there was very good agreement between the osmotic pressure anomaly and the extent of dissociation into ions, as measured by electrical conductivity.

Most of these ideas were put forward by Arrhenius for his Ph.D. dissertation, but they were too revolutionary for his chemistry peers. He received a barely passing grade for his Ph.D. (after a failure on the first submission), an outcome that prevented his securing a professorship in his native Sweden and engendered much bitterness. However, as the existence of charged sub-atomic particles such as the electron and proton became clear in the late 1890's, along with the rapidly-emerging understanding of the nature of the nucleus and atomic structure, the inspirational nature of Arrhenius' work became well-recognized. He was awarded the Nobel prize in Chemistry in 1903, effectively silencing his remaining critics. In an interesting twist of circumstance, he refused to accept the ideas of Lowrie and Brønsted published several years before his death in Stockholm in 1927.

1.5 The Properties of Water as a Solvent

The almost unique physical and chemical properties of water as a solvent are of fundamental concern to the chemical processes discussed in this book. As shown in Table 1.2 below, in the liquid state, water has unusually high boiling point and melting point temperatures compared to its hydride analogues from the periodic table such as NH_3, HF and H_2S. Hydrogen bonding between water molecules means that there are strong intermolecular forces making it relatively difficult to melt or vaporize.

Table 1.2 Melting point and boiling point temperatures (at normal pressure) for hydrides of Groups 15-17 analogous to water.

Melting Points (^oC)					
NH_3	-78	H_2O	0	HF	-83
PH_3	-133	H_2S	-86	HCl	-115
AsH_3	-116	H_2Se	-60	HBr	-89
SbH_3	-88	H_2Te	-49	HI	-51
Boiling Points (^oC)					
NH_3	-33	H_2O	100	HF	20
PH_3	-88	H_2S	-61	HCl	-85
AsH_3	-55	H_2Se	-42	HBr	-67
SbH_3	-17	H_2Te	-2	HI	-35

Figure 1.1 shows the structure of ice, which serves as a basis for understanding that of liquid water. The structure, which is based on the tetrahedral arrangement of diamond, is relatively open and is dominated by hydrogen bonds between adjacent water molecules.

This open structure tends to collapse on melting, accounting for the observed volume expansion on melting of almost 10 percent. At the freezing temperature, 0°C, the densities of liquid and solid water are 0.9998 and 0.9168 g mL^{-1} respectively. Above its melting point, water continues to contract as the ice-like open tetrahedral structure supported by hydrogen bonding is broken down, reaching a maximum density at 4°C (Figure 1.2). These changes result from

opposing effects: the increasing breakdown of the open ice-like structure in opposition to the increasing intermolecular distance caused by higher temperatures. In the liquid state, each water molecule has, on average, 3.4 nearest neighbours, compared to 4 in the tetrahedral ice structure.

Figure 1.1

Representation of the 3D structure of normal ice, characterized by a puckered hexagonal array of H_2O molecules, similar to the chair conformer of cyclohexane. Adjacent water molecules are linked by hydrogen bonds.

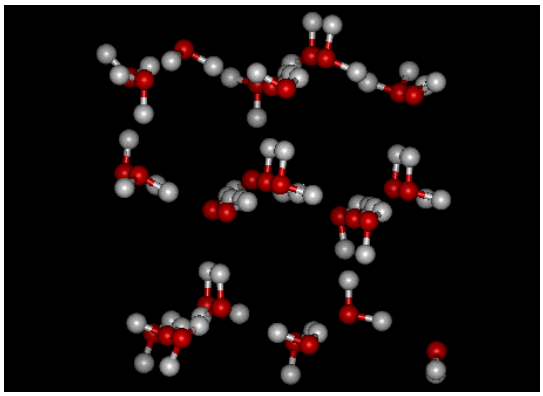

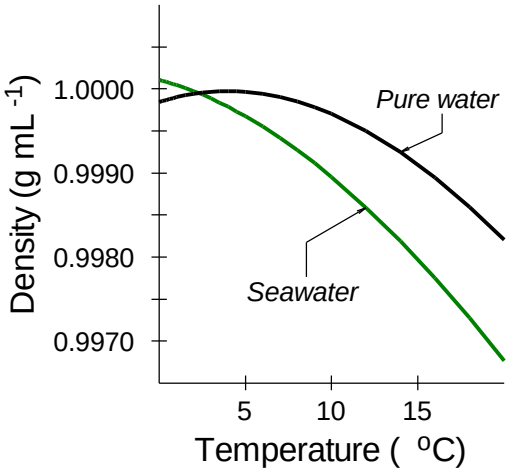

Figure 1.2 *Variation with temperature of the density of pure water and seawater at normal pressure. A constant value of 0.028 has been subtracted from the seawater densities to fit the results onto the same scale as pure water.*

The fact that pure water has its maximum density at 4°C, higher in temperature than its freezing point (0°C), and that ice is substantially less dense than liquid water, is important (and fortunate) in several contexts. Firstly, it means that as water in a lake is cooled at its surface by loss of heat to the atmosphere, the ice structures formed will float. Furthermore, a dynamically stable water layer near 4°C will tend to accumulate at the bottom of the lake, and the overlying, less dense water able to continue cooling down to the freezing point. This means that ice will eventually coalesce at the surface, forming an insulating layer that greatly reduces the rate of freezing of the underlying water. This situation is obviously important for plants and animals that live in lake waters.

As shown in Figure 1.2, the presence of salt components means that the temperature of maximum density for seawater is shifted to lower temperatures: in fact, the density of seawater continues to increase right down to the freezing point. The high concentration of electrolytes in seawater assist in breaking up the open, hydrogen-bonded ice-like structure of water near its freezing point. Because the salt components tend to be excluded from the ice formed by freezing seawater, sea ice is relatively fresh and still floats on water. Much of the salt it contains is not truly part of the ice structure but contained in brines that are physically entrained by small pockets and fissures in the ice.

The dielectric constant of water (78.2 at 25°C) is high compared to most liquids. Of the common liquids, few have comparable values at this temperature, e.g. HCN (106.8), HF (83.6) and H_2SO_4 (101). By contrast, most non-polar liquids have dielectric constants around 2. The high dielectric constant helps liquid water to solvate ions, making it a good solvent for ionic substances, and arises because of the polar nature of the water molecule and its tetrahedrally coordinated structure in the liquid phase.

In many electrolyte solutions of interest, the presence of ions can alter the nature of the water structure. Ions tend to orient water molecules that are near to them. For example, cations attract the negative oxygen end of the water dipole towards them. This reorientation tends to disrupt the ice-like structure further away. This can be seen by comparing the entropy change on transferring ions from the gas phase to water with a similar species that does not form ions. Table 1.3 shows selected values for several ions and argon. Note firstly that all the values are negative because of the choice of states used: the ions/molecules have considerably more entropy when free in the gas phase than when confined to the solution.

Consider now the solution of potassium chloride as an example. This would involve an entropy decrease of (106 + 111) = 217 J mol^{-1} K^{-1}, whereas the corresponding change for 2 argon atoms (each of which has the same electronic structure as the two ions) would be 2× 126 = 252 J mol^{-1} K^{-1}. The net effect of having the two ions, as opposed to the inert gas Ar, is to decrease the entropy loss on solution, i.e. the ions must promote increased disorder in the solution (to the extent of 252 – 217 = 32 J mol^{-1} K^{-1}). This is in spite of the fact that in the immediate neighbourhood of the ions, there must surely be a layer of water molecules that are rather firmly oriented because of the strong local ion-dipole attractions. It has been estimated that this effect alone should cause an entropy loss of about 50 J mol^{-1} K^{-1}. Thus the structure-breaking effect of the ions on water molecules further away is quite substantial, something like 50 + 32 = 82 J mol^{-1} K^{-1}.

Table 1.3 also shows that for both the univalent cations and the univalent anions, the structure-breaking effect increases as the ions get larger in size. For example, from Li^+ through to Cs^+, the entropy loss decreases by 77 J mol^{-1} K^{-1}, with a similar trend occurring from F^- through to I^-. Note also that as the charge increases, the entropy loss on solution also increases (compare K^+, Mg^{2+} and Al^{3+}). Clearly the divalent and trivalent ions promote considerable ordering of the solvent molecules.

Table 1.3 Entropy of solution DS of ions and argon for the change from 1 atm pressure in the gas phase to a hypothetical mole fraction of unity in aqueous solution.

Species	*DS* (J mol^{-1} K^{-1})	*Species*	*DS* (J mol^{-1} K^{-1})
Ar	–126	H^+	–162
		Li^+	–166
F^-	–171	Na^+	–142
Cl^-	–111	K^+	–106
Br^-	–95	Rb^+	–97
I^-	–77	Cs^+	–89
		Mg^{2+}	–352
		Al^{3+}	–556

In a 1 mol L^{-1} solution of a simple salt like NaCl, the average distance between ions, assuming that their distribution approximates to a cubic lattice, is about 1 nm, only a few times larger than the nearest-neighbour distance for pure water. Thus in a solution of this concentration there will be very few water molecules having no ions within a few molecular diameters, and many will have several within that range. Only below about 0.02 mol L^{-1} concentration does the average distance between ions become an order of magnitude greater than the size of a water molecule.

Thus we can regard a dilute electrolyte solution as largely unaltered water containing independent, well-separated ions each carrying a local "atmosphere" of solvating water molecules. On the other hand, in more concentrated electrolytes we would expect to have second-order, short-range effects becoming important because the ions are close enough to interact with each other and because the concept of each ion being independently solvated by different water molecules is no longer applicable.

Further Reading

R.A. Robinson and R.H. Stokes (1959). *Electrolyte Solutions.* Butterworths, London, Ch 1.

W. Stumm and J.J. Morgan (1981). *Aquatic Chemistry: An Introduction Emphasizing Chemical Equilibria in Natural Waters.* Wiley and Sons, New York, Chapter 3.

Chapter 2 Acid-Base Equilibria in Ideal Solutions

Acid-base reactions in aqueous solution are, with few exceptions, very fast reactions that come to chemical equilibrium quickly. Thus the principles of chemical equilibrium apply particularly well to these reactions. This chapter summarizes these basic principles, and their basis in thermodynamics, and then shows how they can be applied specifically to acid-base behaviour in aqueous solution.

2.1 Concentration Scales

As with other types of chemical reactions, any quantitative description of an acid-base equilibrium system is based on consideration of the *concentrations* of the various species participating in the reaction. This is largely because concentration is an *intensive* property, i.e. one that is independent of the actual quantities (volume or mass) of aqueous solution being considered. Concentration, as applied to aqueous solutions, is a parameter that expresses the amount of a particular chemical substance (called the *solute*) in a given quantity of solution. There are several different ways used to express concentration in chemistry, each of which defines a *concentration scale*. All of the chemically useful concentration scales use the SI quantity *amount of substance*, whose unit is the *mole* (abbreviated *mol*) to express the amount of solute. The various concentration scales differ in the way they express the quantity of solution:

Molarity scale

The molarity scale expresses the concentration as the amount of solute (normally in mol) per unit volume of solution (normally in litres, L). Thus it has the base SI unit mol L^{-1}, which historically is often abbreviated by upper case 'M'. The molarity scale is most useful in chemical methods where volumetric equipment is used, since the amount of solute n can be obtained simply by multiplying the concentration c by the volume of solution v, i.e. $n = cv$. Care must be taken to ensure that the volume units used in c and v are coherent with each other.

The main disadvantage of the molarity scale is that it is temperature and pressure dependent because the total solution volume will change through thermal and pressure expansion or contraction. Moreover, since the thermal and pressure expansibilities of solutions generally depend on their total composition, it is often difficult to account for the effects of these changes in T and p accurately. This is particularly relevant in seawater, where the temperature may vary over a range of more than 30°C, and the pressure ranges over several hundred atmospheres throughout its main depth range.

Molality scale

The molality scale expresses the concentration as the amount of solute (normally in mol) per unit mass of solvent (usually in kg). Thus it has the base SI unit mol kg^{-1}, which historically is often abbreviated by lower case 'm'. The latter use is sometimes discouraged because of potential confusion with the SI symbol for the unit of length, the metre. The principal advantage of the molality scale is that it is pressure and temperature independent.

Seawater scale

The seawater concentration scale expresses the concentration as the amount of solute (normally in mol) per unit mass of seawater. This differs from molality in using the mass of solution rather than solvent. This scale is widely used in marine chemistry, and is probably the easiest of all the scales to use in the laboratory.

Converting between Concentration Scales

The concentration scales mentioned above can be readily inter-converted provided the overall composition of the solution, and its density, i.e. mass per unit volume, are both known. The density of simple aqueous solutions can often be obtained from standard tables. For seawater, the density is readily calculated from the salinity[1], which is usually known. Density is easily measured using a density bottle of calibrated volume, or even a small volumetric flask.

To convert between the molarity and molality scales, the total ionic composition of the solution must be known because each solute contributes to the total mass of the solution. Solutions containing more than one solute are easiest to deal with on a case-by-case basis. In the common case where the solution contains only a single solute, explicit conversion formulae are available. These are shown in [2.1] and [2.2], which use the following terminology:

molarity	c	mol L^{-1} solution
molality	m	mol kg^{-1} water
seawater scale	c_{SW}	mol kg^{-1} seawater
density	ρ	g mL^{-1}
molar mass of solute	M	g mol^{-1}

$$c = \frac{\rho m}{1 + \frac{mM}{1000}} \qquad [2.1a]$$

$$m = \frac{c}{\rho - \frac{cM}{1000}} \qquad [2.1b]$$

Conversion between molarity and the seawater scale is made using the density

$$c = \rho\, c_{SW} \qquad [2.2a]$$

Finally, conversion between the molality and seawater scales can be made using the salinity S, since the ionic composition of seawater is nearly constant

$$m = \frac{c_{SW}}{1 - 0.001005\, S} \qquad [2.2b]$$

The expressions in [2.2a] and [2.2b] are valid for any seawater solution.

---

[1] The *salinity* of seawater is a quantity defined in terms of electrical conductivity, but is numerically very close to the total concentration of salt in grams per kg of seawater.

2.2 Thermodynamic Basis of Chemical Equilibria

The form of what is now referred to as the *Law of Chemical Equilibrium* was first arrived at by the study of reaction rates. In 1862, Marcellin Berthelot and Péan de St. Gilles reported results from a study of the hydrolysis of esters. They mixed together 1 mol of acetic acid (HOAc) with varying amounts of ethanol (EtOH) and, after a suitable reaction time, determined the amounts of ethanol and ethyl acetate (EtOAc) present in the mixture as a result of the reaction

$$EtOH + HOAc \rightarrow EtOAc + H_2O$$

Some of their results are shown in Table 2.1 below.

*Table 2.1 Data of Bertholet and St. Gilles for the esterification of ethanol and acetic acid (published in Annal. Chim. Phys. **65**, 385, 1862).*

Initial EtOH (mol)	Ester produced (mol)	$K = \frac{[EtOAc][H_2O]}{[EtOH][HOAc]}$
0.05	0.049	2.6
0.18	0.171	3.9
0.50	0.414	3.4
1.00	0.667	4.0
2.00	0.858	4.5
8.00	0.966	3.8

These results showed a clear relationship between the concentration of product formed and that of the reactant, ethanol. This relationship was expressed in a general form in 1863 by the Norwegian chemists C.M. Guldberg and P. Waage. They argued that a reacting system maintained chemical equilibrium in a dynamic manner by the balancing of the rates of reaction in both directions. Thus for the general chemical reaction

$$A + B \quad C + D \qquad [2.3]$$

the rate of the forward reaction would be proportional to the concentrations of A and B, while the rate of the backward reaction would be proportional to those of C and D. At equilibrium, forward and backwards rates would be equal

$$k_{forward}[A][B] = k_{backward}[C][D] \qquad [2.4]$$

which easily rearranges to

$$K = \frac{[C][D]}{[A][B]} \qquad [2.5]$$

Equation [2.5] became known as the *Law of Chemical Equilibrium*, and the constant K as an *equilibrium constant*. It provides a quantitative expression for relating the concentrations of reactant and product species in a chemical reaction that is at equilibrium. Obviously this is a

powerful paradigm for understanding equilibrium systems. The right column in Table 2.1 shows the calculated K value for the data reported by Bertholet and St Gilles, revealing that the experimental K value is indeed approximately constant over a wide range of compositions.

Although a very important development, the Law of Chemical Equilibrium as put forward by Guldberg and Waage is not a general one applicable to all chemical reactions because its derivation depends on the assumption of a particular type of kinetic rate law that will not be universally valid. However, it turns out that their law is well founded, and can be demonstrated using the principles of chemical thermodynamics. We now consider a derivation of the Law using this approach.

For the general reaction in [2.3], the change in Gibbs free energy ΔG from reactants to products is given by

$$\Delta G = \Delta G^{\emptyset} + RT \ln Q \qquad [2.6]$$

where Q is the reaction quotient and $\Delta G^{\emptyset}$ is the *standard Gibbs free energy change*, i.e. the value of ΔG under standard conditions when all reactants and products are present in their standard states. The standard states are chosen arbitrarily as a matter of convention. For solution species, the usual standard state is unit concentration. Note that this gives rise to two *different* standard state conventions depending on whether molarity or molality is used to express solute concentration. For the molarity scale, the standard state is denoted $c^{\emptyset}$ and has the value 1 mol L^{-1}. For the molality scale, the standard state is denoted $m^{\emptyset}$ and has the value 1 mol kg^{-1}. For solids, the standard state is the pure solid, while for liquids it is the pure liquid and for gases it corresponds to a partial pressure of the gas equal to a standard atmosphere, $p^{\emptyset}$ = 101.3 kPa.

Equation [2.6] arises by considering the individual terms for the chemical potential of each product and reactant as they contribute to Q. For each species X in solution, this will be an expression of the type (assuming a molarity concentration scale)

$$\mu_X = \mu_X^{\emptyset} + RT \ln \frac{c_X}{c^{\emptyset}} \qquad [2.7]$$

where $\mu^{\emptyset}$ denotes the chemical potential of the species X in its standard state (i.e. when $c = c^{\emptyset}$). Note that in [2.7], the argument to the natural logarithm must be a dimensionless quantity, so that the concentration c_X is divided by the standard state concentration $c^{\emptyset}$. In many chemistry publications, an equation like [2.7] is often written in the form

$$\mu = \mu^{\emptyset} + RT \ln [X] \qquad [2.8]$$

In this case, the term in square brackets, which is conventionally regarded as a symbol for the concentration of the species X, must actually represent a dimensionless concentration that has been obtained by dividing the concentration by the standard state value $c^{\emptyset}$. Therefore, care must be taken in interpreting equations like [2.8] and those derived from it. Since the standard state concentration for solutes is always unit concentration, there is usually no difficulty when doing calculations. However, for reactions involving gases, this is not the case unless the pressure is expressed in atmospheres, thus special care is needed.

For the general equilibrium reaction [2.3], the form of Q is

$$Q = \frac{[C][D]}{[A][B]} = \frac{(c_C / c^{\varnothing})(c_D / c^{\varnothing})}{(c_A / c^{\varnothing})(c_B / c^{\varnothing})} \qquad [2.9]$$

Note that Q is a dimensionless quantity.

Equation [2.6] shows that when the reaction is at chemical equilibrium, a condition fulfilled when $\Delta G = 0$, the reaction quotient assumes a special value dependent on $\Delta G^{\varnothing}$. This is none other that the equilibrium constant of our Law of Chemical Equilibrium

$$0 = \Delta G^{\varnothing} + RT \ln K \qquad (\text{at equilibrium}, Q = K)$$
$$K = \exp\left(-\frac{\Delta G^{\varnothing}}{RT}\right) \qquad [2.10]$$

Equation [2.10] is the usual formal definition of the *thermodynamic equilibrium constant*. It reveals that K is a constant whose value, like $\Delta G^{\varnothing}$, depends only on temperature and the choice of standard states (unlike Q which may assume any value).

Combination of [2.9] and [2.10] shows that the equilibrium constant can be related to the quotient of product and reactant concentrations *at equilibrium*.

$$K = \frac{[C]_e[D]_e}{[A]_e[B]_e} \qquad [2.11]$$

where the 'e' subscript denotes an equilibrium concentration. Equation [2.11] is obviously identical to GuldBerg and Waage's Law derived earlier in equation [2.5]. The real power of the thermodynamic approach is that no assumptions needed to be made about a particular form of the reaction rate law.

Solution equilibria that obey equation [2.11] are termed *ideal* in a thermodynamic sense. As will become apparent in Chapter 4, real aqueous solutions do not obey equation [2.11] exactly because of interactions that take place between ions, and between ions and the solvent, that are not accounted for in the theory presented in this section. Nonetheless, the thermodynamic treatment presented here provides a conceptual framework for understanding real chemical equilibria that is so powerful in its predictive capabilities that its importance is hardly diminished.

This role is rather similar to that of the equation of state for ideal gases. Accordingly, we also refer to the notion of *ideal solutions* with respect to chemical equilibria in solutions: these are reactions in solution that obey equation [2.11]. In the discussion that follows in this chapter, such ideal behaviour will be assumed, with the consequences of non-ideal behaviour in real solutions dealt with in Chapter 3.

2.3 Self-Dissociation Equilibrium of Water

Hydrogen and hydroxide ions are formed in all aqueous solutions by a proton transfer reaction between two water molecules

$$H_2O + H_2O \quad H_3O^+ + OH^- \qquad [2.12]$$

The equilibrium constant for this *self-dissociation* reaction is usually symbolized K_w and has the well-known equilibrium expression

$$K_w = [H_3O^+][OH^-] \qquad [2.13]$$

K_w has a value very close to $1x10^{-14}$ at the standard temperature of 25°C.

In equation [2.13] it has been implicitly assumed that water itself is in its standard state and is therefore not included in the equilibrium expression, even though this refers strictly only to the pure solvent and not a solution containing another substance. For dilute aqueous solutions, the concentration of water is scarcely changed by the addition of the solute, so that the term $(c/c^\emptyset)$ for water is unity. However, in more concentrated solutions, this simplification is not good enough for accurate work and the concentration term for water must be explicitly included.

The water self-dissociation equilibrium is significant because it is omnipresent in aqueous solution, which means that it applies to all solutions, regardless of other solutes that may affect the concentrations of hydrogen and hydroxide ions. The form of equation [2.13] shows that the concentrations of these two ions are never independent of each other, i.e. fixing a value for one allows the other to be calculated. This simplification (which is a natural result for all equilibrium constants) is of great assistance in calculating the composition of acid-base solutions at equilibrium (see Chapter 5).

2.4 Sorenson's 'p' Notation

The values encountered for both the concentrations of species in equilibria and the equilibrium constants vary over a very large range. It is often convenient to compress this large range of numbers by employing 'p' notation, a transformation in which the negative of the base 10 (common) logarithm of the quantity is taken. This was originally introduced by Sorenson as part of his definition of pH:

$$pH = -\log [H^+] \qquad [2.14]$$

The same operation may be carried out on the equilibrium constant K_a

$$pK_a = -\log K_a \qquad [2.15]$$

This conversion to a logarithmic form is also convenient because it simplifies calculations involving multiplication and division: in 'p' notation these become addition and subtraction operations. Thus expression [2.13] for the water self-dissociation equilibrium can be written in 'p' notation as

$$pK_w = pH + pOH \qquad [2.16]$$

This particular feature of 'p' notation was rather more important in the years before electronic calculators became readily available than it is today. However, its use is already well established by historical precedence.

It should be noted that in [2.14] the concentration term $[H^+]$ is dimensionless, as it is in the reaction quotient and equilibrium constant expressions mentioned earlier. Thus, an alternative form of [2.14] is

$$pH = -\log_{10} \frac{c_H}{c^{\varnothing}} \qquad [2.17]$$

2.5 Acid-Dissociation Equilibria

The dissociation of a generic weak acid HA is simply a special case of the general chemical equilibrium discussed in the previous section:

$$HA + H_2O \quad H_3O^+ + A^- \qquad [2.18]$$

The equilibrium constant for this reaction is usually termed an *acid dissociation constant* (sometimes an *acidity constant*), symbolized K_a. It is related to the equilibrium concentrations of the species involved as follows

$$K_a = \frac{[H_3O^+][A^-]}{[HA]} \qquad [2.19]$$

As with the water self-dissociation equilibrium treated earlier, it has been implicitly assumed that the water in the solution is in its standard state.

In many textbooks, reaction [2.19] will be written in an equivalent form that uses the simpler form H^+ as the symbol for the hydrogen ion; in this case the role of water is implicit and the reaction resembles the simple ionization scheme originated by Arrhenius

$$HA \quad H^+ + A^- \qquad [2.20]$$

In this case, the expression for the equilibrium constant has the form

$$K_a = \frac{[H^+][A^-]}{[HA]} \qquad [2.21]$$

Degree of Dissociation α

The acid dissociation constant K_a provides information about how readily a weak acid reacts with water and other bases, allowing comparison of the reactivity (proton-donating ability) of different acids. It also provides a measure of how much the acid dissociates as the solution is made acidic or alkaline. Historically, this information has often presented in the form of the *degree of dissociation* α_1, which is the fraction of the weak acid present in its dissociated, conjugate base form:

$$\alpha_1 = \frac{[A^-]}{[HA]+[A^-]} = \frac{[A^-]}{c_{HA}} \qquad [2.22]$$

where $c_{HA} = [HA] + [A^-]$ is the total, analytical concentration of the weak acid and [HA] and $[A^-]$ are the equilibrium concentrations of the acid and its conjugate base respectively. Obviously one can also define α_0, the fraction of the weak acid that is *not* dissociated

$$\alpha_0 = \frac{[HA]}{[HA]+[A^-]} = \frac{[HA]}{c_{HA}} \qquad [2.23]$$

from which it is clear that since the acid must be present either in the acid or base form:

$$\alpha_0 + \alpha_1 = 1 \qquad [2.24]$$

This leads to the following simplifications:

$$K_a = [H^+]\frac{\alpha_1}{\alpha_0}$$
$$\alpha_0 = \frac{[H^+]}{[H^+]+K_a} \qquad [2.25]$$
$$\alpha_1 = \frac{K_a}{[H^+]+K_a}$$

In 'p' notation, [2.25] becomes

$$\log\frac{\alpha_1}{\alpha_0} = pH - pK_a \qquad [2.26]$$

The use of fractional concentrations is convenient because it allows the dissociation behaviour of different acids and/or different concentration conditions to be directly compared.

The Dissociation Diagram

Equation [2.26] shows that the degree of dissociation of a weak acid depends only on the pK_a of the acid (which has a constant value at a particular temperature), and on the pH of the solution. Since the latter can be adjusted almost at will by the addition of strong acid or alkali to the solution, the degree of dissociation of a weak acid can be adjusted experimentally.

Some interesting features can be deduced by considering the properties of equation [2.25]. Figure 2.1 shows how both the degree of dissociation α_1, and its converse α_0, vary with pH for the case where the weak acid HA is acetic acid (pK_a = 4.76 at 25°C). As indicated by [2.22] and [2.23], these parameters correspond to the fractions of conjugate base A^- (α_1) and weak acid HA (α_0) respectively. The curves for α_0 and α_1 cross each other when the pH is equal to the pK_a of the weak acid. At this point

$$\log\frac{\alpha_1}{\alpha_0} = pH - pK_a = 0 \qquad [2.27]$$
$$\alpha_0 = \alpha_1 = 0.5$$

which corresponds to exactly 50% dissociation, i.e. when the concentrations of the free acid HA and its conjugate base A^- are exactly equal. This represents to a buffer solution having equimolar amounts of acid and base.

At pH values lower than pK_a (more acidic), α_0 increases rapidly to unity and the solution is dominated by the undissociated acid form HA. Conversely, at pH values higher than pK_a (more alkaline), α_0 decreases rapidly to zero and the solution is dominated by the dissociated conjugate base form A^-. The profile of the dissociated fraction α_1 is opposite to this.

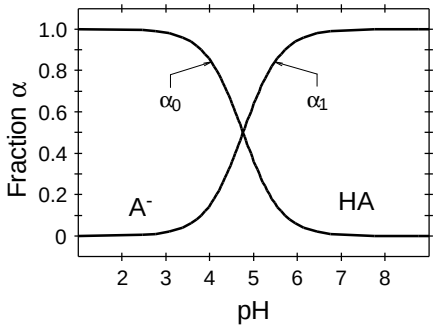

Figure 2.1 Dissociation diagram for acetic acid, pK_a = 4.76 at 25°C

Figure 2.1 is termed a *dissociation diagram* because it describes how the dissociation of a weak acid depends on pH. The general shape of the curves for α_0 and α_1, which correspond to the fractions of conjugate base A^- and weak acid HA respectively, are independent of the nature of the acid, i.e. its pK_a value; this parameter determines only where the two curves are positioned along the horizontal pH axis. Note also that the shape of the diagram is also independent of the analytical concentration of the weak acid c_{HA}, since this quantity does not figure in equation [2.25]. The same kind of information could be conveyed by plotting the concentrations of the species A^- and HA as a function of pH, however such a diagram would be specific for a particular value of c_{HA} and is therefore less general in applicability.

The Composition-pH Diagram

A second type of diagram that does make use of concentrations, rather than α, is also useful because it conveys information about the acid and base species in equilibrium in such a way that the contributions of different reactions may be compared. This type, termed a *composition-pH diagram*, uses a logarithmic scale for the vertical axis, allowing comparison of concentrations over a wide range of values.

Figure 2.2 shows the composition-pH diagram for acetic acid at a total concentration of 0.01 mol L^{-1}. Also plotted on the diagram are the concentrations of H^+ and OH^-, both of which relate directly to the self-dissociation of water.

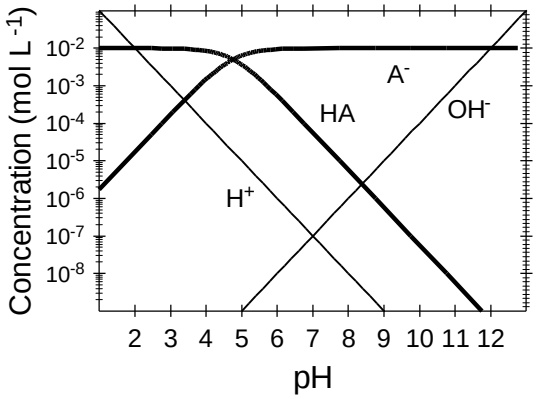

Figure 2.2 *Composition-pH diagram for acetic acid, pK_a = 4.76 at 25°C*

The plot for H^+, which is linear with a slope of -1, is trivially related to pH

$$pH = -\log [H^+] \qquad [2.28]$$

while that for OH^- has a slope of +1 resulting from the expression

$$pOH = pK_w - pH \qquad [2.29]$$

These two lines, which will be the same in any aqueous solution, cross at the pH of a neutral solution, which results from the condition

$$pH = pOH = \tfrac{1}{2}\, pK_w \qquad [2.30]$$

This corresponds to a pH of 7.00 for water at 25°C.

The main significance of the lines for $[H^+]$ and $[OH^-]$ in the composition-pH diagram is that they represent all of the solution compositions that are possible, i.e. every aqueous solution can be represented by a single point on each line, each at the same pH value.

Interpreting the Composition-pH Diagram

Examination of Figure 2.2 shows that regions of the curves for the weak acid HA and it conjugate base A^- are also close to linear, having simple slope values and crossing, as expected, at pH = pK_a. This simplified nature of the diagram (compared to the dissociation-pH diagram in Figure 2.1) results from the use of a logarithmic scales on both axes.

These features can be easily explained using equation [2.26]. When the pH is several units *smaller* than pK_a then α_0 is close to unity (Figure 2.1)

$$\log \frac{\alpha_1}{\alpha_0} = pH - pK_a << 0, \quad \alpha_0 \approx 1$$
$$\log \alpha_1 \approx pH - pK_a \qquad [2.31]$$

This corresponds to the situation where almost none of the weak acid has dissociated. In this case the curve for $[A^-]$ (corresponding to α_1) increases with pH with a slope of +1, while that for [HA] (corresponding to α_0) remains approximately constant at a value corresponding to the total concentration c_{HA}.

On the other hand, when the pH is several units *larger* than pK_a then α_1 is now very close to unity (Figure 2.1):

$$\begin{aligned} \log\frac{\alpha_1}{\alpha_0} &= pH - pK_a >> 0 \\ \alpha_1 &\approx 1 \\ \log \alpha_0 &\approx pK_a - pH \end{aligned} \qquad [2.32]$$

Now almost all of the weak acid has dissociated, the curve for $[A^-]$ is approximately constant, and that for [HA] decreases with pH with a slope of –1.

2.5 Base-Dissociation Equilibria

The dissociation of a generic weak base B^- is also a chemical equilibrium reaction:

$$B^- + H_2O \quad \rightleftharpoons \quad HB + OH^- \qquad [2.33]$$

The equilibrium constant for this reaction is usually termed a *base dissociation constant*, symbolized K_b, and is related to the equilibrium concentrations of the species involved as follows

$$K_b = \frac{[HB][OH^-]}{[B^-]} \qquad [2.34]$$

This equilibrium constant provides a measure of the base strength, i.e. its ability to react with proton donors.

A well-known result is the relationship between the acid dissociation constant for a weak acid and the corresponding base dissociation constant for its conjugate base, obtained as follows:

$$\begin{aligned} K_aK_b &= \frac{[H^+][A^-]}{[HA]} \times \frac{[HA][OH^-]}{[A^-]} \\ &= [H^+][OH^-] \\ &= K_w \end{aligned} \qquad [2.35]$$

Alternatively, in 'p' notation

$$pK_a\, pK_b = pK_w \qquad [2.36]$$

From [2.35] and [2.36] it follows that for an acid-base conjugate pair, the acid and base dissociation constants (and their equilibria) are not independent, i.e. only one or the other needs to be considered, but not both. For this reasons, tables of thermodynamic data normally only tabulate the pK_a values for the conjugate acid form. If pK_b is required instead, it is easily calculated using [2.36].

Figure 2.3 shows the dissociation and composition-pH diagrams for the NH_4^+-NH_3 system, for which pK_a = 9.24 at 25°C. It is seen that this system has very similar properties to those of acetic acid shown earlier in Figures 2.1 and 2.2, except that the curves are displaced to a much higher pH in the ammonia system because NH_4^+ is a much weaker acid.

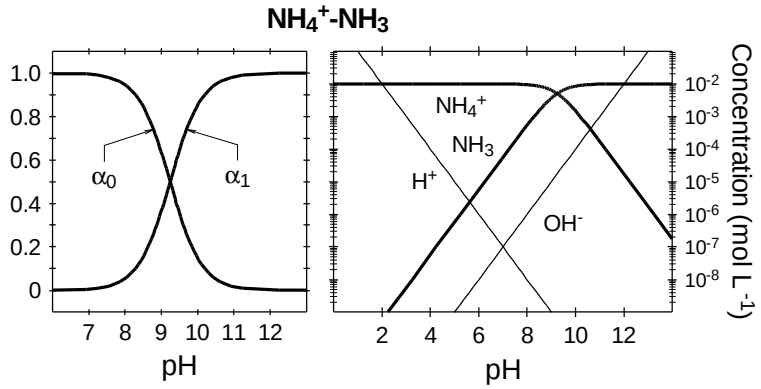

Figure 2.3 *Dissociation (left) and Composition-pH (right) diagrams for the NH_3-NH_4^+ system, pK_a = 9.24 at 25°C*

2.5 Diprotic Acids

Some acids have two or more protons available for transfer to bases and are termed *polyprotic acids.* These have a separate dissociation equilibrium for each proton they are able to donate. Thus the generic *diprotic* acid H_2A has 2 dissociation equilibria, each having a corresponding acid dissociation constant:

$$H_2A \qquad HA^- + H^+ \qquad [2.37]$$

$$HA^- \qquad A^{2-} + H^+ \qquad [2.38]$$

The dissociation constants for each step are

$$K_{a1} = \frac{[HA^-][H^+]}{[H_2A]} \qquad [2.39]$$

$$K_{a2} = \frac{[A^{2-}][H^+]}{[HA^-]} \qquad [2.40]$$

Sometimes it is convenient to refer to the overall reaction involving dissociation of both protons in a single reaction step, for which the equilibrium constant is the product of those for each step

$$H_2A \qquad A^{2-} + 2\,H^+ \qquad [2.41]$$

$$K = \frac{[A^{2-}][H^+]^2}{[H_2A]} = K_{a1}K_{a2} \qquad [2.42]$$

In this case, by analogy with [2.22] and [2.23], we are interested in the fraction of the total acid concentration c_{H2A} that is present in each of the three forms H_2A, HA^- and A^{2-}

$$\alpha_0 = \frac{[H_2A]}{[H_2A]+[HA^-]+[A^{2-}]} = \frac{[H_2A]}{c_{H_2A}} \quad [2.43]$$

$$\alpha_1 = \frac{[HA^-]}{[H_2A]+[HA^-]+[A^{2-}]} = \frac{[HA^-]}{c_{H_2A}} \quad [2.44]$$

$$\alpha_2 = \frac{[A^{2-}]}{[H_2A]+[HA^-]+[A^{2-}]} = \frac{[A^{2-}]}{c_{H_2A}} \quad [2.45]$$

As with [2.24] for the monoprotic acid, these three dissociation fractions must sum to unity:

$$\alpha_0 + \alpha_1 + \alpha_2 = 1 \quad [2.46]$$

Combination of the equilibrium expressions [2.39] and [2.40] with the definitions in [2.43] through [2.46] lead to a set of simple equations for expressing the α values in terms of $[H^+]$ as the only variable:

$$\alpha_0 = \frac{1}{1+\frac{K_{a1}}{[H^+]}+\frac{K_{a1}K_{a2}}{[H^+]^2}} \quad [2.47]$$

$$\alpha_1 = \frac{K_{a1}}{[H^+]}\alpha_0 \quad [2.48]$$

$$\alpha_2 = \frac{K_{a1}K_{a2}}{[H^+]^2}\alpha_0 \quad [2.49$$

Equations [2.47] through [2.49] may be used to construct a dissociation diagram for any diprotic acid. Figure 2.4 shows the diagram for phthalic acid $C_6H_4(COOH)_2$. This shows features that can be readily understood by comparison with the simpler case of a monoprotic acid already discussed.

Note, for example, that the diagram divides into three regions, each corresponding to the preponderance of the forms H_2A, HA^- and A^{2-} respectively. The transition from H_2A to HA^- (α_0 to α_1) occurs where the α_0 and α_1 curves cross each other at pH = pK_{a1} = 2.95, while the corresponding transition from HA^- to A^{2-} occurs at a pH = pK_{a2} = 5.41 where the α_1 and α_2 curves cross each other.

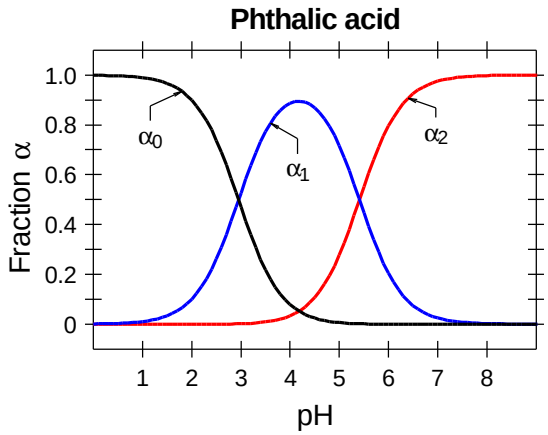

Figure 2.4 *Dissociation diagram for the diprotic acid, phthalic acid (ortho isomer); pK_{a1} = 2.95 and pK_{a2} = 5.41, at 25°C*

The other crossing point in Figure 2.4, at pH = 4.2 where the α_0 and α_2 curves cross each other, and where α_1 has its maximum value, is of particular interest. This corresponds to the solution that would result from dissolving a salt of the species HA^- in water (in this case, this would be a salt like potassium hydrogen phthalate). Reference to equation [2.49] shows that when the condition $\alpha_0 = \alpha_2$ is fulfilled

$$[H^+]^2 = K_{a1} K_{a2} \qquad [2.50]$$

or, in 'p' notation

$$2\,pH = p\,K_{a1} + pK_{a2}$$

$$pH = \frac{pK_{a1} + pK_{a2}}{2} \qquad [2.51]$$

from which the pH value for a solution of potassium hydrogen phthalate is readily calculated:

$$pH = \frac{2.95 + 5.41}{2} = 4.18 \qquad [2.52]$$

Note also that this value is independent of the concentration of the salt, one of the reasons why potassium hydrogen phthalate, as the intermediate acid/base form of a diprotic acid, is chosen as a standard buffer for pH measurements.

The dissociation diagrams for polyprotic acids differ in one important respect from those of monoprotic acids. Equations [2.47]-[2.49] for a diprotic acid contain *two* dissociation constants, and the shape of the corresponding dissociation diagram (e.g. Figure 2.4) depends on the relative values of these constants. In other words, different diprotic acids will have dissociation diagrams differing in appearance. By contrast, the dissociation diagram for all monoprotic acids has the same general shape, differing only in the position of the diagram along the pH axis. This arises because the equations [2.22] defining the monoprotic acid contain only a *single* dissociation constant parameter.

This is illustrated by Figure 2.5, which shows the dissociation diagram for sulfurous acid H_2SO_3. In this case, the central pH region in which the species HSO_3^- is predominant is much wider than it is for phthalic acid (Figure 2.4) because the two pK_a values of H_2SO_3 differ more from each other than is the case for phthalic acid.

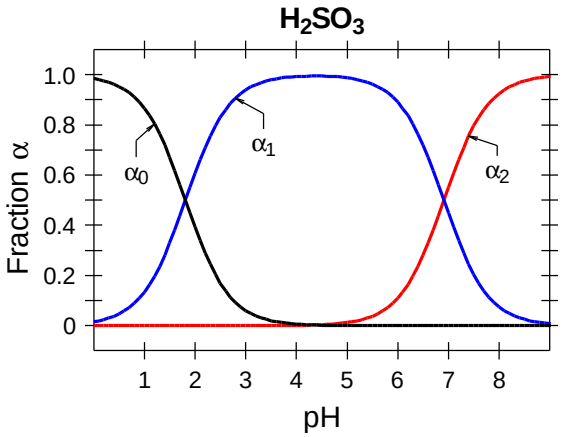

Figure 2.5 *Dissociation diagram for the diprotic acid, sulfurous acid H_2SO_3; having pK_{a1} = 1.81 and pK_{a2} = 6.91 at 25°C*

Composition-pH diagram for diprotic acids

Figure 2.5 shows the composition-pH diagram for phthalic acid at a total concentration of 0.01 mol L^{-1}. This has many features in common with the diagrams already presented for monoprotic acids. The fully protonated acid form H_2A predominates at pH < pK_{a1} = 2.95, while the fully deprotonated base form A^{2-} predominates at pH > pK_{a2} = 5.41. The intermediate species HA^- is the main form only over a relatively narrow pH range between the latter twovalue.

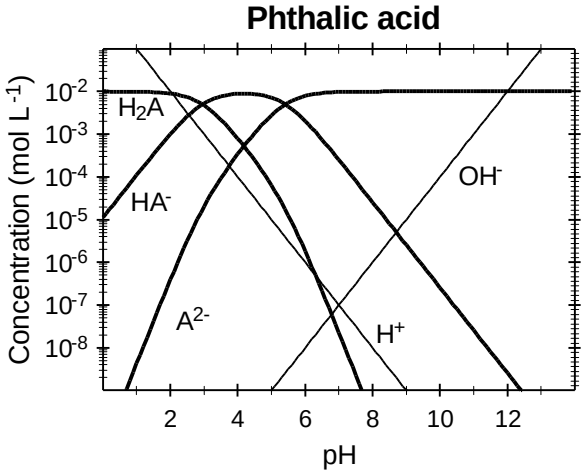

Figure 2.6 *Composition-pH diagram for 0.01 mol L^{-1} phthalic acid at 25°C*

Note that at pH values above pK_{a1} = 2.95, the curve for the fully protonated acid H_2A decreases with a slope of –1, as observed for the monoprotic acid (see equation [2.26]). However, once the pH exceeds pK_{a2} = 5.41, at which point the fully deprotonated base form A^{2-} begins to predominate, the slope of the curve for H_2A becomes *more negative*, in fact it quickly assumes a value of –2. This can be explained by examining equation [2.49] for the case where α_2 becomes approximately unity

$$\alpha_2 = \frac{K_{a1}K_{a2}}{[H^+]^2}\alpha_0 \qquad \alpha_2 \approx 1 \text{ when } pH > pK_{a2} = 5.41$$
$$\log \alpha_0 \approx pK_{a1} + pK_{a2} - 2\,pH \qquad [2.53]$$

A similar change in slope occurs for the fully deprotonated base A^{2-} when the pH is low and the species H_2A dominates. In this case, the curve for A^{2-} increases in slope from +1 to +2

$$\alpha_2 = \frac{K_{a1}K_{a2}}{[H^+]^2}\alpha_0 \qquad \alpha_0 \approx 1 \text{ when } pH < pK_{a1} = 2.91$$
$$\log \alpha_1 \approx 2\,pH - pK_{a1} - pK_{a2} \qquad [2.54]$$

From these two examples, and those discussed earlier for monoprotic acids, it is clear that the slope of the composition-pH diagram results directly from the *stoichiometry* of the acid-base reaction linking the species of interest to that which is currently predominant at any particular pH. This property makes it fairly simple to construct a composition-pH diagram.

Composition-pH diagrams for further diprotic acid-base systems of relevance to natural aquatic systems will be considered in Chapter 4.

2.6 Triprotic acid systems

The dissociation equilibria for triprotic acids are developed by a logical extension of the treatment given in the previous section for diprotic acids. Only an outline will be presented here. A generic triprotic acid H_3A will have *three* dissociation equilibria, each having an associated equilibrium constant

$$H_3A \rightarrow H_2A^- + H^+ \qquad K_{a1} = \frac{[H_2A^-][H^+]}{[H_3A]} \qquad [2.55]$$

$$H_2A^- \rightarrow HA^{2-} + H^+ \qquad K_{a2} = \frac{[HA^{2-}][H^+]}{[H_2A^-]} \qquad [2.56]$$

$$HA^{2-} \rightarrow A^{3-} + H^+ \qquad K_{a3} = \frac{[A^{3-}][H^+]}{[HA^{2-}]} \qquad [2.57]$$

This, in turn, means that there are *four* α terms, α_0 through α_3, corresponding to the fractions of H_3A, …, A^{3-} respectively

$$\alpha_0 = \frac{1}{1+\frac{K_{a1}}{[H^+]}+\frac{K_{a1}K_{a2}}{[H^+]^2}+\frac{K_{a1}K_{a2}K_{a3}}{[H^+]^3}} \qquad [2.58]$$

$$\alpha_1 = \frac{K_{a1}}{[H^+]}\alpha_0 \qquad [2.59]$$

$$\alpha_2 = \frac{K_{a1}K_{a2}}{[H^+]^2}\alpha_0 \qquad [2.60]$$

$$\alpha_3 = \frac{K_{a1}K_{a2}K_{a3}}{[H^+]^3}\alpha_0 \qquad [2.61]$$

Equations [2.58] through [2.61] may be used to construct the dissociation and composition-pH diagrams for a triprotic acid. Figure 2.7 shows the example of citric acid, a common constituent of citrus fruits. The dissociation constants for this acid are not greatly different, with the result that in the intermediate pH region there is not a single dominant species. In fact, neither H_2A^- nor HA^{2-} exceed 80% of the total concentration at any point, and there is a significant pH range over which both of these species co-exist in reasonable concentration.

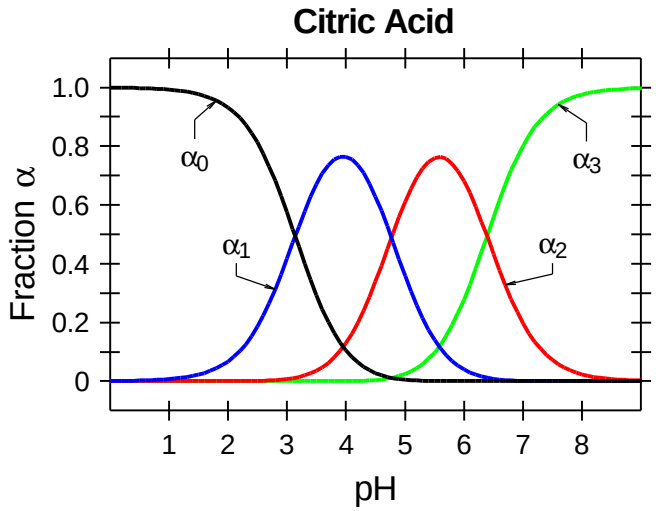

Figure 2.7 *Dissociation diagram for the triprotic acid, citric acid, having dissociation constants pK_{a1} = 3.14, pK_{a2} = 4.77 and pK_{a3} = 6.39 at 25°C*

Further examples of dissociation-pH and composition-pH diagrams may be found in Chapter 4.

Further Reading

W. Stumm and J.J. Morgan (1981). *Aquatic Chemistry: An Introduction Emphasizing Chemical Equilibria in Natural Waters.* Wiley and Sons, New York, Chapters 2 and 3.

Chapter 3 Acid-Base Equilibria in Real Solutions

This chapter discusses how acid-base equilibria in real solutions depart from the ideal behaviour underlining the Law of Chemical Equilibrium, and what practical measures are used to overcome the consequences of this non-ideality. Included is a discussion of the practical meaning of solution pH and how it is measured.

3.1 Non-ideal Behaviour of Aqueous Solutions

As discussed in Section 2.2, the Law of Chemical Equilibrium is based on expressions of type [3.1] which describe how the chemical potential of a species X depends on its concentration in solution c_X

$$\mu_X = \mu_X^{\varnothing} + RT \ln \frac{c_X}{c^{\varnothing}} \qquad [3.1]$$

This equation is not obeyed very well by real solutions because it is based on the assumption that the molecules/ions of X in the solution are independent of each other, and of the other chemical species in the solution, excepting actual chemical reactions between the species. However, as discussed in Chapter 1, only in solutions that are very dilute is this assumption likely to be realistic. In most solutions, interactions between species, especially charged ions, can be expected because of the polar nature of the solvent and the close proximity of the ions in moderately concentrated solutions.

The non-ideal behaviour of electrolyte solutions can be conveniently illustrated using a galvanic cell of the following type:

$$\text{Pt, } H_2(g) \mid H^+, Cl^- \mid \text{AgCl, Ag} \qquad [3.2]$$

This cell can be recognized as that which defines the *standard electrode potential* $E^{\varnothing}$ of the Ag-AgCl electrode system. The Nernst equation for this cell is

$$\begin{aligned} E &= E^{\varnothing} - k \log \frac{[H^+][Cl^-]}{f(H_2)} \\ k &= 2.303 \frac{RT}{F} \end{aligned} \qquad [3.3]$$

where $f(H_2)$ is the fugacity of H_2. If we assume that the H_2 is in its standard state and has unit fugacity, and that the only source of both H^+ and Cl^- ions is hydrochloric acid of molarity c_{HCl} this simplifies as follows:

$$\begin{aligned} E &= E^{\varnothing} - k \log [H^+][Cl^-] \\ &= E^{\varnothing} - 2k \log \frac{c_{HCl}}{c^{\varnothing}} \\ &= E^{\varnothing} - 2k \log [HCl] \end{aligned} \qquad [3.4]$$

Rearranging this so that only measurable or known terms are collected on the right hand side

$$E^{\varnothing} = E + 2k \log [HCl] \qquad [3.5]$$

Equation [3.5] implies that if the cell were filled with a series of solutions of different HCl concentration and the potential E measured, then calculation of [3.5] using the results obtained should yield a set of constant values equal to the standard potential $E^{\varnothing}$. In fact, experiment shows that this is far from the case, as seen in Figure 3.1 below.

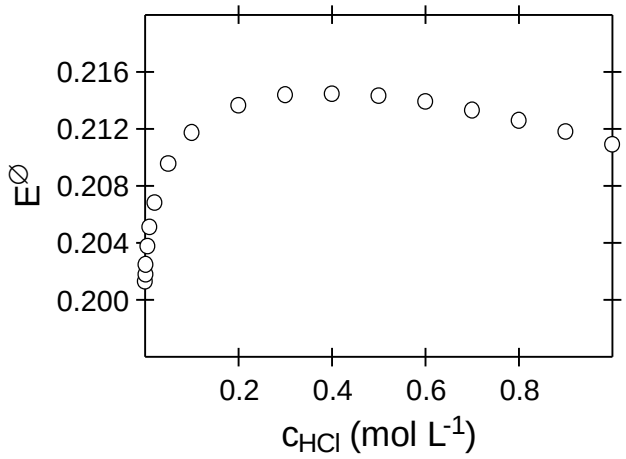

Figure 3.1 *Plot of equation [3.5] made using potential measurements at different molarities of HCl at 25°C.*

At HCl concentrations above 0.1 mol L^{-1}, the apparent value of the standard cell potential is approximately constant, but at lower concentrations it undergoes significant changes towards smaller (less positive) values. The precision of such cell measurements is typically 0.1 mV, so these potential changes are far larger than expected from any known experimental errors.

Another way of viewing what these results mean is to calculate the *apparent* HCl concentration that would satisfy equation [3.5] at each of the data points. To do this, first of all we extrapolate the calculated values of equation [3.5] to zero HCl concentration to obtain the standard cell potential $E^{\varnothing}$. This is done in the Figure 3.2(a). For reasons to be explained later, the horizontal axis used for this extrapolation uses the square root of the HCl concentration. The effect of this is to expand the lower concentration range, making it easier to carry out the extrapolation. The result of this is $E^{\varnothing} = 0.2001$ V.

Next, equation [3.4] is rearranged to calculate the *apparent* HCl concentration from the extrapolated $E^{\varnothing}$ value and the measured potentials for each concentration value.

$$c_{app} = \text{a}\log\left(\frac{E^{\varnothing} - E}{2k}\right) \qquad [3.6]$$

where **alog** is the inverse of the common logarithm function, i.e. alog (x) = 10^{x}.

The results of this calculation are shown in Table 3.1, from which it is clear that the apparent concentration of HCl at each point that satisfies the Nernst equation [3.5] is significantly lower than the actual concentration, especially as the concentration becomes higher. This is also made clear by Figure 3.2(b) shows the ratio of the apparent and true HCl concentrations.

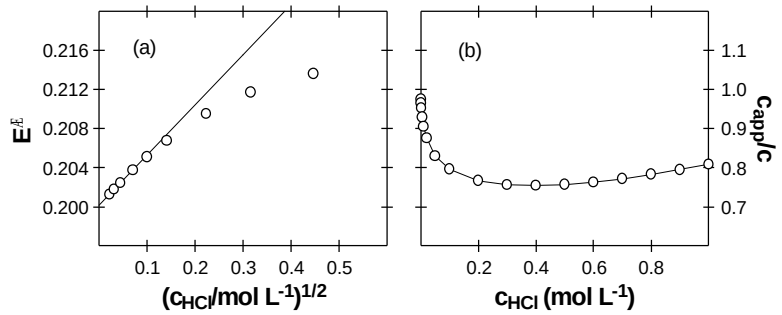

Figure 3.2 *(a) Extrapolation of apparent standard cell potential from equation [3.5] to zero HCl concentration (b) Comparison of actual HCl molarities and apparent values deduced from the Nernst equation [3.4].*

Table 3.1 Cell potential of HCl solutions at different concentrations in the range 0.001 to 1.0 mol L^{-1}, standard cell potential according to [3.5] and the apparent HCl concentration from [3.6].

c (mol L^{-1})	E_{cell} (V)	E+2k log[HCl]	c_{app} (mol L^{-1})	Ratio c_{app}/c
0.001	0.5568	0.2018	0.00097	0.966
0.005	0.4760	0.2038	0.00465	0.929
0.01	0.4418	0.2051	0.00905	0.905
0.05	0.3635	0.2095	0.0415	0.831
0.2	0.2963	0.2136	0.153	0.767
0.4	0.2615	0.2144	0.302	0.755
0.6	0.2402	0.2139	0.458	0.763
0.8	0.2240	0.2126	0.626	0.783
1.0	0.2109	0.2109	0.809	0.809

A second experimental demonstration of the deviation of real solutions from ideal thermodynamic behaviour can be made using a modified version of the galvanic cell in [3.2]. This experiment reveals a further, important feature of real solutions. Suppose that the aqueous solution in cell [3.2] contains both a constant molarity 0.01 mol L^{-1} of HCl and variable concentrations of an inert electrolyte, e.g. $NaClO_4$. The defined cell reaction for the cell is

$$\tfrac{1}{2}H_2 + AgCl \rightarrow H^+ + Ag + Cl^- \qquad [3.7]$$

Since neither of the ions contributed by the inert electrolyte $NaClO_4$, Na^+ and ClO_4^- take part in this reaction, their effect on the Nernst cell potential should be nil. Thus, if the HCl molarity is held constant while the $NaClO_4$ molarity is changed, both the measured potential E and the apparent standard potential $E^{\varnothing}$ calculated using [3.5] should have constant values. As shown by

the results in Figure 3.3, this is again not the case. It is clear that the cell potential E varies substantially with $NaClO_4$ concentration, even though this electrolyte is supposedly inert. As with the case in Figure 3.1, the largest changes take place at low concentrations, with the potential becoming relatively constant at higher values.

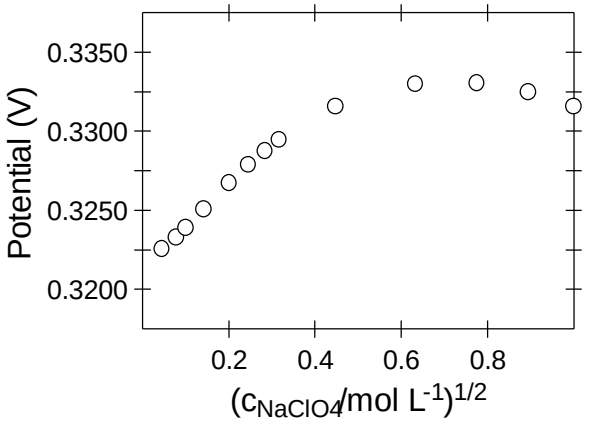

Figure 3.3 *Measured cell potential (V) for cell [3.2] containing 0.01 mol L^{-1} HCl and different concentrations of $NaClO_4$ at 25°C. The horizontal axis scale uses the square root of $NaClO_4$ molarity.*

The important conclusion to be gained from this particular experiment is that the departure from the ideal behaviour predicted by the Nernst equation seems to be caused by the presence of *any ions*, not just ions participating in the galvanic cell reaction.

3.2 Activity and the Activity Coefficient

The same types of deviation from ideal thermodynamic behaviour are observed with other physical properties that also depend, in one way or another, on the chemical potential equation [3.1]. Examples include the osmotic pressure of an electrolyte solution, boiling point elevation and freezing point depression and, naturally, the values of chemical equilibrium constants.

These experimental findings imply that in real solutions, interactions between the any ions in the electrolyte, and between the ions and the solvent, have the effect of decreasing the apparent concentrations that apply to the concentration dependence of the chemical potential, as expressed by equation [3.1]. The results presented in Figures 3.1 and 3.2(b) tend to imply that the solution needs to be very dilute before the electrolyte ions are sufficiently far apart for the resulting deviations to become small. They also imply that at high concentration ($c > 0.1$ mol L^{-1}), the interaction effect appears to saturate.

Because the thermodynamic description of electrolyte properties is extremely valuable in its predictive abilities, scientists have been reluctant to abandon the concept because of the non-ideality of real solutions. Instead, it has become conventional to link the concept of chemical potential, as expressed by equation [3.1], in a quantitatively correct way to experimental measurements made on real solutions. This is done by the sort of method outlined above in connection with Table 3.1 and Figure 3.2, i.e. by introducing an apparent concentration that

exactly satisfies equation [3.5]. This apparent concentration is termed the *activity a*, and is analogous to the fugacity of a gas. Thus for real solutions, equation [3.5] for the chemical potential becomes

$$\mu = \mu^{\varnothing} + RT \ln a_X \qquad [3.8]$$

The activity a_X of the species X is related to its concentration c_X through the *activity coefficient* γ_X

$$a_X = \gamma_X \frac{c_X}{c^{\varnothing}} = \gamma_X [X] \qquad [3.9]$$

Note that in [3.9], the convention is used that [X] is the dimensionless 'molarity' of X, i.e. the quotient of the molarity and the standard state concentration, 1 mol L^{-1}. Both the activity and the activity coefficient are dimensionless quantities. The activity coefficient is the ratio of activity to [X], and is unity in the case of an ideal solution.

$$\gamma_X = \frac{a_X}{[X]} \qquad [3.10]$$

This equation shows that the quantity c_{app}/c used in the rightmost column in Table 3.1, and in Figure 3.2(b), actually corresponds to the activity coefficient for HCl.

It should be noted that although activity is defined as a dimensionless quantity, its value depends on the standard state in use. Therefore, we must distinguish between the concentration scales, molarity and molality. Thus, we can also define activity in terms of the molality scale as follows

$$a_X = \gamma_X \frac{m_X}{m^{\varnothing}} \qquad [3.11]$$

where $m^{\varnothing}$ = 1 mol kg^{-1} is the standard state concentration in the molality scale. The activities defined by [3.11] and [3.9] are physically distinct and cannot be mixed together in an equation without converting all terms to the same concentration scale.

We are now in a position to apply this concept to the galvanic cell [3.2] used above as an example. First, we replace the concentrations of H^+ and Cl^- in the Nernst equation [3.4] with the corresponding activities, and then we express each activity in terms of the concentration of the ion and its corresponding activity coefficient using [3.10]

$$\begin{aligned} E &= E^{\varnothing} - k \log (a_H a_{Cl}) \\ &= E^{\varnothing} - k \log \left(\frac{\gamma_H c_H}{c^{\varnothing}} \frac{\gamma_{Cl} c_{Cl}}{c^{\varnothing}}\right) \end{aligned} \qquad [3.12]$$

This equation is readily simplified to

$$E = E^{\varnothing} - 2k \log[HCl] - k \log(\gamma_H \gamma_{Cl}) \qquad [3.13]$$

If this expression [3.13] is rearranged so that it has the same right-hand side as [3.5], the quantity that was plotted in Figures 3.1 and 3.2(a), we obtain

$$E^{\varnothing} - k \log(\gamma_H \gamma_{Cl}) = E + 2k \log[HCl] \qquad [3.14]$$

Equation [3.14] reveals why the quantity E + 2k log [HCl] does not exhibit a constant value in Figures 3.1 or 3.2(a). It suggests that the observed variations may be due to changes in the values of the activity coefficient terms on the left-hand side of [3.14].

Can we use this extended equation [3.14] to deduce values for both the activity coefficient term log ($\gamma_H\gamma_{Cl}$) and the standard cell potential $E^{\varnothing}$ from the experimental data in Table 3.1? This is only possible if we can firstly obtain an independent estimate of one of these terms. Even though $E^{\varnothing}$ is presumed constant, we can still not solve by the method of simultaneous equations because we do not know how log ($\gamma_H\gamma_{Cl}$) varies with concentration.

The only solution to this problem is to *adopt* a value for the activity coefficient term that seems reasonable under particular conditions. The conditions that immediately come to mind are when the solution is extremely dilute, at which point we might expect that the interactions between the ions of the solute that have caused the non-ideal behaviour might start to become more or less negligible. In other words, we would make the assumption that as the HCl concentration approaches zero, the activity coefficients of H^+ and Cl^- would both approach unity and the logarithmic term log ($\gamma_H\gamma_{Cl}$) would become zero. This assumption is known as the *infinitely dilute solution convention*, and is discussed in more detail in Section 3.4.

3.3 Mean Ionic Activity Coefficient

This assumption that the solution approaches ideal behaviour as it becomes very dilute justifies calculation of the standard cell potential $E^{\varnothing}$ by extrapolating values calculated from [3.14] to zero HCl concentration, as carried out in Figure 3.2(a). Once $E^{\varnothing}$ is known, individual values for log ($\gamma_H\gamma_{Cl}$) for each data point may then be calculated by rearranging [3.14].

$$k \log(\gamma_H \gamma_{Cl}) = E^{\varnothing} - E - 2k \log[HCl] \qquad [3.15]$$

Equation [3.15] illustrates a crucial point. The results can only be used to determine the product ($\gamma_H\gamma_{Cl}$) of the activity coefficients, not the individual values for each ion. In more general terms, since it is not possible to have a galvanic cell (or a solution) that contains only a single ion, it follows that it is only possible to measure the activity coefficient of a *complete electrolyte* (i.e. cation *plus* anion). For this reason, the quantity ($\gamma_H\gamma_{Cl}$) is normally expressed in terms of the *mean ionic activity coefficient* that is defined in the case of a 1:1 electrolyte HCl as the geometric mean of the individual coefficients

$$\gamma_{\pm} = (\gamma_H \gamma_{Cl})^{1/2} \qquad [3.16]$$

The mean ionic activity coefficient is a property of a complete electrolyte. For the case under consideration, [3.15] may be rewritten in terms of $\gamma_{\pm}$ for HCl

$$2k \log(\gamma_{\pm}) = E^{\varnothing} - E - 2k \log[HCl] \qquad [3.17]$$

This equation can also be expressed in terms of the original activities

$$\begin{aligned} E^{\varnothing} - E &= 2k \log(\gamma_{\pm}[HCl]) \\ &= 2k \log(a_{HCl}) \end{aligned} \qquad [3.18]$$

which rearranges, after taking antilogarithms, to a form identical to [3.6]

$$a_{HCl} = \text{a log}\left(\frac{E^{\varnothing} - E}{2k}\right) \qquad [3.19]$$

demonstrating that the activity of HCl can be identified, as expected, with the apparent HCl concentration c_{app} that was calculated earlier in Table 3.1. It also shows that the ratio of apparent to true concentration, c_{app}/c, can itself be identified with the mean ionic activity coefficient $\gamma_{\pm}$, which values are shown in Table 3.1 and Figure 3.2(b). This analysis confirms the basis of activity as the apparent electrolyte concentration needed to satisfy the chemical potential equation [3.1] and equations derived directly from it, such as the Nernst equation.

General case of the Mean Ionic Activity Coefficient

For an electrolyte of general stoichiometry X_mY_n, where X^{n+} is the cation and Y^{m-} is the anion, the dissociation of the electrolyte into its ions would be

$$X_mY_n \rightarrow m\,X^{n+} + n\,Y^{m-} \qquad [3.20]$$

Thus the activity a of the electrolyte is related to those of the constituent ions, and the mean ionic activity $a_{\pm}$ by

$$a = (a_X)^m (a_Y)^n = (a_{\pm})^{m+n} \qquad [3.21]$$

Similarly the activity coefficients are related by

$$(\gamma_{\pm})^{m+n} = (\gamma_X)^m (\gamma_Y)^n \qquad [3.22]$$

3.4 The Reference State for Activity Scales

In calculating the activity of HCl in the example just presented, it was necessary to assume that the behaviour of the HCl solution approached that of the ideal solution as it became extremely dilute (or, more exactly, infinitely dilute). The assumption of such a condition for ideal behaviour is known as the *reference state* for the activity scale, and it has some similarities with the assumption of a standard state that defines a concentration scale. The reference state for a particular solute X, is the solution in which X is assumed to behave ideally in the sense that the equation for the chemical potential [3.1] is exactly obeyed. Thereference state has the properties

$$a_X = [X] \quad \text{and} \quad \gamma_X = 1 \qquad [3.23]$$

We need to define the ideal solution because the experimental measurements that we make, such as cell potentials, can only provide information about *changes* in the chemical potential, not its absolute value. In the previous section, it was argued that a very dilute solution ought to approximate ideal behaviour because it seems reasonable to assume that interactions between the ions in the solution ought to become negligible as the solution is greatly diluted. However, the fact remains that this choice for the ideal solution is an arbitrary one. Thus, as with the concept of the standard state, there is no uniquely correct way to define thereference state for an activity scale, and the actual choice becomes a matter of convention. Several conventions are in common use.

The Infinitely-dilute Solution Convention

The most common is that already discussed, the *infinitely dilute solution convention*, in which the activity coefficients of all solutes approach unity as the concentrations of *all species* in the solution themselves approach zero. Obviously such a solution is not experimentally accessible except by extrapolating measured results in real solutions to zero concentration of all electrolytes.

This convention has the conceptual advantage that, like a gas under very low pressure, it is easy to understand how interactions between solute ions and molecules would become very small at high dilution. As we shall see later, this provides a useful starting point for theoretical treatments of activity.

The practical application of this convention is seen in Figure 3.2(a), in which the standard cell potential $E^{\varnothing}$ is obtained by extrapolating equation [3.14] to zero HCl concentration. As already discussed, this procedure assumes that $\log (\gamma_H \gamma_{Cl})$ approaches zero under these conditions.

The Constant Ionic Medium Convention

Another commonly-used method is the *constant ionic medium convention*, in which the activity coefficient of a particular solute approaches unity as the solute concentration approaches zero *in the ionic medium*, i.e. with all other species remaining present at the constant concentrations of the medium. This convention is particularly applicable to solutions like seawater, which has an ionic composition that is extremely constant and dominated by only 6 or 7 so-called major ions (Table 4.2):

Table 4.2 Concentrations, on molality and seawater scales, of the 12 most concentrated ionic species in seawater of salinity 35.

Ion	*c* (mol kg^{-1} SW)	*c* (mol kg^{-1} H_2O)
Cl^-	0.54586	0.56576
Na^+	0.46906	0.48616
Mg^{2+}	0.05282	0.05475
SO_4^{2-}	0.02824	0.02927
Ca^{2+}	0.01028	0.01065
K^+	0.01021	0.01058
HCO_3^-/CO_3^{2-}	0.00203	0.00210
Br^-	0.00084	0.00087
$B(OH)_4^-/ B(OH)_3$	0.00042	0.00043
Sr^{2+}	0.00009	0.00009
F^-	0.00007	0.00007
OH^-	0.00001	0.00001

This convention also confers practical advantages. As suggested by the results in Figure 3.3, the activity coefficient of an electrolyte is strongly concentration-dependent at low electrolyte concentrations, but less so in more concentrated solutions. Thus, it is often convenient to carry out physical measurements in the presence of a high concentration of an inert electrolyte. This has the effect of holding, or 'buffering', changes in activity coefficients to a minimum. While this generally makes measurements more reliable, it also usually makes it more difficult to extrapolate to zero electrolyte concentration to obtain the reference state value. Therefore, defining the reference state to be a concentrated inert electrolyte solution *in the first place* avoids the need for uncertain extrapolations.

The constant ionic medium convention also has certain peculiarities not found in the simpler, infinitely dilute solution convention. These involve interactions that take place between the species of interest and a solute component of the medium. For example, in seawater, the hydrogen ion reacts to a measurable extent with the sulfate ion, one of the ionic medium components

$$H^+ + SO_4^{2-} \rightarrow HSO_4^- \qquad [3.24]$$

Should we regard this as a separate chemical equilibrium, or as part of the interaction between the hydrogen ion and the solvent (which, in the constant ionic medium convention, includes the sulfate ion)? There is no 'correct' answer to this question, but each approach gives rise to a different activity scale. Thus, if we choose to regard reactions like [3.24] explicitly as chemical equilibria, we develop a convention in which we consider only the activity of the free hydrogen ion, i.e. the proton combined with one, or more H_2O molecules. On the other hand, we can regard reactions like [3.24] as interactions between the hydrogen and the solution, in which case our scale concerns both free and combined protons

$$[H^+]_T = [H^+] + [HSO_4^-] \qquad [3.25]$$

These distinctions are really only important in a complex medium like seawater, and will be discussed in more detail in Section 3.8. Commonly, an electrolyte like $NaClO_4$, which does not interact with protons in solution, is used as the base electrolyte in this convention.

3.5 Activity Coefficients of Typical Electrolytes

The activity coefficients of electrolytes are found to depend on several factors: the ionic strength and composition of the solution, taking all ions into account, and the electrical charge and chemical nature of the ions.

The *ionic strength I* is a parameter that is related to the extent of ion-ion interactions in a solution, and is defined as follows

$$I = \frac{1}{2}\sum_i c_i |z_i|^2 \qquad [3.26]$$

where z_i is the charge on ion i having concentration c_i, and the summation extends over all anions and cations. The ionic strength is seen to be the concentration of all ions, weighted according to the square of the charge on each ion. This arises because the electrostatic interaction between two ions of a given charge is proportional to the square of that charge. For a simple 1:1 electrolyte

like NaCl, the ionic strength is identical to the electrolyte concentration. For other electrolytes, it depends on the stoichiometry of the salt.

In seawater, ionic strength is related to salinity S by the equation

$$I = 19.92\frac{S}{1000 - 1.0049S} \qquad [3.27$$

Figure 3.4 compares measured value of the mean ionic activity coefficients of univalent chloride electrolytes at different concentrations up to 5 mol kg^{-1}. In all cases, $\gamma_{\pm}$ decreases sharply from unity at zero concentration up to about 0.2 mol kg^{-1}. Above that, $\gamma_{\pm}$ for the larger cations becomes approximately constant, whereas for the smaller cations, H^+ and Li^+, it increases steadily with concentration to values greater than 2. While the attainment of activity coefficients larger than unity may seem to be puzzling, this is only because of the arbitrary nature of the reference state at infinite dilution. What these results mean is that in concentrated solutions of HCl and LiCl, the *apparent* concentration of the electrolyte is larger than it would be in a hypothetical solution of the same concentration in which all the ions are assumed to behave completely independently of each other. In Section 1.5 it was noted that in concentrated electrolytes, the ions are actually quite close together, making the assumption of independent action somewhat dubious.

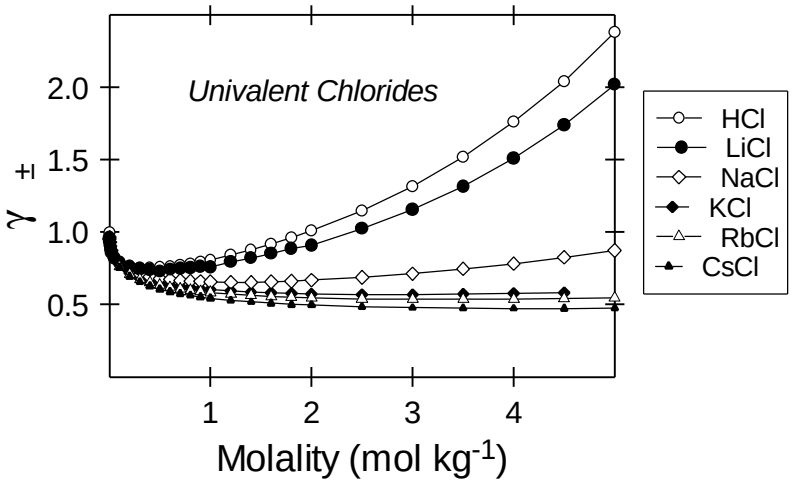

Figure 3.4 *Measured mean ionic activity coefficients of various univalent chloride salts as a function of concentration in water at 25°C.*

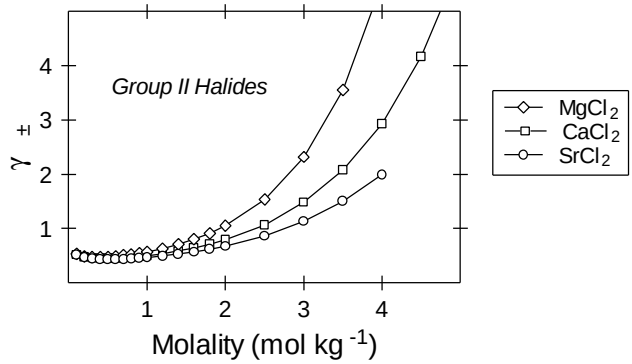

Figure 3.5 *Measured mean ionic activity coefficients of chloride salts of various Group II metal ions as a function of concentration in water at 25°C.*

Figure 3.5 shows similar data for Group II divalent chlorides. This shows uniformly lower values as the cation gets larger (Mg^{2+} through to Sr^{2+}), but with the same overall trend as the smaller univalent cations (H^+, Li^+).

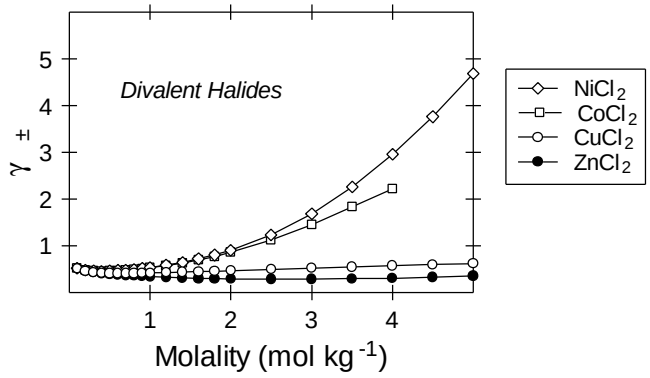

Figure 3.6 *Measured mean ionic activity coefficients of chloride salts of various divalent transition metal ions as a function of concentration in water at 25°C.*

One of the factors that will affect activity coefficients is a specific interaction between the cation and anion in the electrolyte. This is seen in Figure 3.6, which shows similar data for divalent chlorides from the first transition series. Comparison with Figure 3.5 shows that the curves for $CoCl_2$ and $NiCl_2$ are very similar to that for $MgCl_2$, whereas those for $CuCl_2$ and $ZnCl_2$ exhibit much lower activities throughout. This is largely because the cations Cu^{2+} and Zn^{2+} both form moderately strong coordination complexes with the chloride ion.

3.6 Single-ion Activities and Activity Coefficients

In Section 3.3 it was demonstrated that physical measurements can only reveal the activity coefficient for a complete electrolyte, not for a single ion. Therefore, activity coefficients for

single ions cannot be deduced from these measurements without further information. One approach is to use one of the several theories that have been developed to calculate single-ion activities from first principles. These are discussed in the next section.

A second approach is to calculate activity coefficients for single ions from experimental values for whole electrolytes by assuming, for a particular choice of electrolyte, that the single ion values can be assigned equally to the cation and the anion. This convention, first suggested by MacInnes in 1919, assumes that the single ion activity coefficients for K^+ and Cl^- are both equal to the mean ionic activity coefficient of KCl in the particular solution of interest:

$$\gamma(K^+) = \gamma(Cl^-) = \gamma_\pm(KCl) \qquad [3.28]$$

Once this convention is adopted, the activity coefficients of other cations may then be calculated from measured values of the mean ionic activity coefficients of their chloride salts. Similarly, the activity coefficients of anions may be calculated from measured values of the mean ionic activity coefficients of their potassium salts.

Consider the following example as an illustration of this method: we will calculate the mean ionic activity coefficient of NaBr. At a concentration of 0.1 mol kg^{-1}, the mean ionic activity coefficient of KCl is 0.775, which is therefore the single ion activity coefficient for both K^+ and Cl^- in the MacInnes convention. Similarly, the measured mean ionic activity coefficients for NaCl and KBr are 0.788 and 0.772, respectively. Thus we estimate the activity coefficients for Na^+ and Br^- as follows:

$$\begin{aligned}\gamma_+(Na) &= \frac{[\gamma_\pm(NaCl)]^2}{\gamma_-(Cl)} \\ &= \frac{[0.788]^2}{0.775} = 0.801 \\ \gamma_-(Br) &= \frac{[\gamma_\pm(KBr)]^2}{\gamma_+(K)} \\ &= \frac{[0.772]^2}{0.775} = 0.769\end{aligned} \qquad [3.29]$$

From these two values, we calculate the mean ionic activity coefficient for NaBr

$$\begin{aligned}\gamma_\pm(NaBr) &= \sqrt{\gamma_+(Na) \times \gamma_-(Br)} \\ &= \sqrt{0.801 \times 0.769} \\ &= 0.785\end{aligned} \qquad [3.30]$$

This value compares quite favourably with the experimental value of 0.782 at this concentration. Figure 3.7 shows values for NaBr calculated using the same method in the concentration range 0.1–4.0 mol kg^{-1}, from which it is clear that the MacInnes approach works only up to about 1 mol kg^{-1}, after which there are substantial deviations. Furthermore, the agreement is even worse for other electrolytes. The MacInnes convention is not especially good for accurate work.

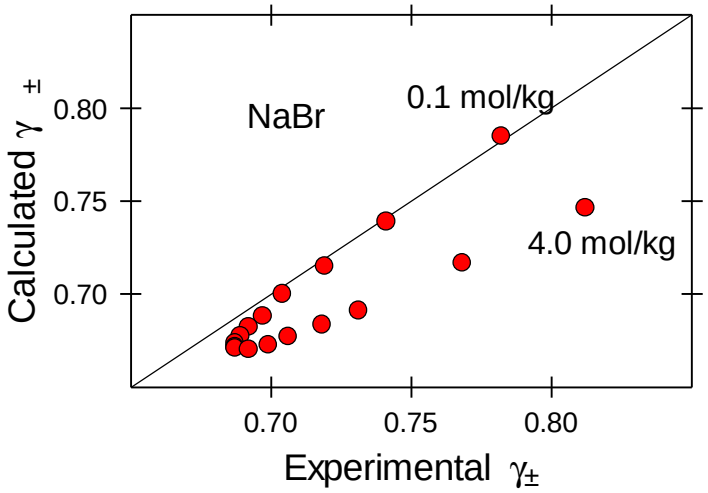

Figure 3.7 *Comparison of measured mean ionic activity coefficients of NaBr with values calculated using the MacInnes convention as a function of concentration in water at 25°C.*

3.7 Theoretical Calculations of Activity Coefficients

In the previous section we saw that experimental methods for the measurement of single ion activity coefficients are not possible, and that conventional approaches (e.g. the MacInnes convention) are not always reliable. A number of attempts have been made to determine activity coefficients for both single ions and electrolytes by theoretical means. These approaches attempt to model the interactions that take place between solute ions, and between ions and the solvent, that lead to departures from ideal behaviour.

The classical starting point for this approach is that of Debye and Huckel, who treated an ionic solution by assuming that the ions are independent point charges and considered the electrical effects of the "atmosphere" of ions surrounding a given ion in the solution. This treatment leads to the *Debye-Huckel equation* for estimating the activity coefficient of an ion:

$$\log \gamma = -Az^2 \sqrt{I} \qquad [3.31]$$

where z is the charge on the ion, I is the ionic strength and A is a constant having a value of 0.509 at 25°C. As we shall see shortly, this equation is somewhat limited in accuracy above concentrations of 0.01 mol kg^{-1}. However, it has been extended to take account of the finite size of ions in the *extended Debye-Huckel equation* [3.32]

$$\log \gamma = -Az^2 \frac{\sqrt{I}}{1 + Ba\sqrt{I}} \qquad [3.32]$$

where B = 0.33 at 25°C and a is an adjustable parameter corresponding to the size of the ion. Various other extensions to this have been proposed, including the *Davies equation* [3.33]

$$\log \gamma = -Az^2 \left(\frac{\sqrt{I}}{1+\sqrt{I}} - 0.2I \right) \qquad [3.33]$$

In this case, the second term linear in I helps to improve the fit of the equations at higher ionic strengths.

Figure 3.8 shows values of the mean ionic activity coefficient for NaCl calculated using the three equations presented above, [3.31]-[3.33] in the concentration range 0–2.5 mol kg^{-1}. The results show that the Davies equation provides quite good agreement up to about 0.7 mol kg^{-1}, and the extended Debye-Huckel only to about 0.1 mol kg^{-1}. The original Debye-Huckel equation [3.31] gives poor agreement at all reasonable concentrations and is of historical interest only.

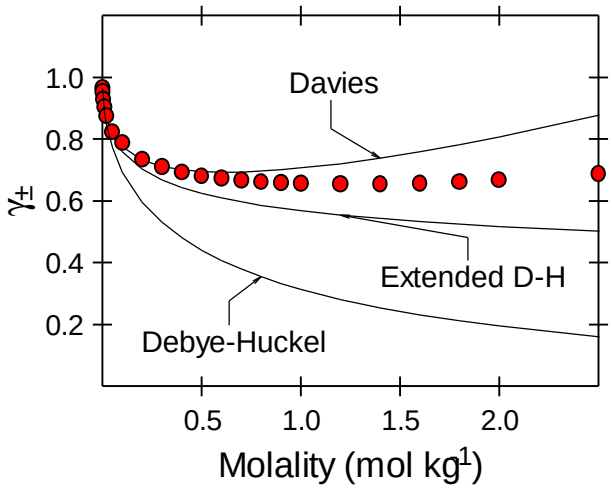

Figure 3.8 *Comparison of measured mean ionic activity coefficient of NaCl with values calculated using the Debye-Huckel, extended Debye-Huckel and Davies equations as a function of concentration in water at 25°C.*

Although the Davies equation gives the best agreement with experimental data in the concentration range up to 0.7 mol kg^{-1}, it has no parameters dependent on the type of ion other than charge. Thus the calculated mean ionic activity coefficients for all salts of a given stoichiometry are the same. As we saw in the previous section, this is usually not the case. As an example, Figure 3.10 compares the calculated values for a 1:2 electrolyte with experimental values for three cases, $Mg(ClO_4)_2$, $MgCl_2$ and $CuCl_2$. For the perchlorate salt, the agreement is quite good up to about 0.7 mol kg^{-1}, while the two chloride salts both deviate from the calculated values above only 0.2 mol kg^{-1}. Indeed, both show *lower* activity coefficients than $Mg(ClO_4)_2$, which is almost an "ideal" Davies electrolyte. As discussed below, this deviation is often interpreted in terms of the formation of *ion pairs* between the cation and anion of the electrolyte, in this case Mg^{2+} or Cu^{2+} and Cl^-.

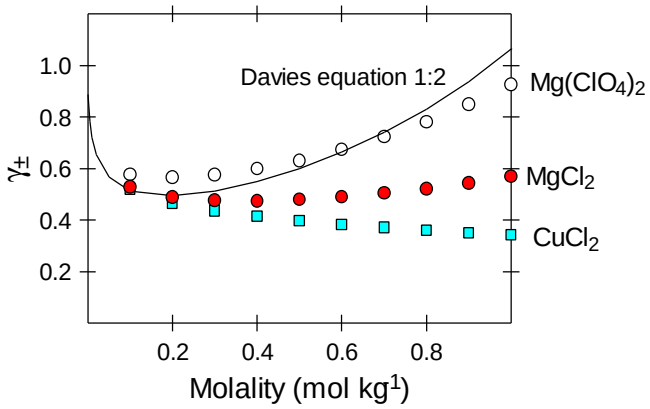

Figure 3.9 *Comparison of measured mean ionic activity coefficients of $Mg(ClO_4)_2$, $MgCl_2$ and $CuCl_2$ with values calculated using the Davies equation for a 1:2 electrolyte as a function of concentration in water at 25°C.*

Ion Association Models

In cases where the measured activity coefficients of an electrolyte are lower than those calculated by a simple equation based on the Debye-Huckel theory, such as the Davies equation, it is natural to ask whether a specific interaction between the ions is responsible. Such an interaction would have precedents. Many metal ions are known to form coordination complexes with simple anions like chloride. By contrast, the perchlorate ion is not considered to form coordination complexes readily and should therefore behave in a nearly ideal way, as observed in Figure 3.9.

How valid is this approach? In a strict sense, the use of ion pairing to explain activity coefficient variations is only valid if the existence, and formation constant, of the ion pair can be validated by some independent means, e.g. spectroscopy. Often, this has not been done, or is impractical. A useful approach adopted by some for metal ions is to use measurements in a supposedly non-complexing electrolyte that is considered not to form ion pairs (e.g. $NaClO_4$) to establish the non-specific behaviour of the ion, and to then ascribe activity coefficient variations in the presence of other anions to ion pairs. While this does not usually have the support of spectroscopic evidence, and does not of itself provide evidence for the existence of ion pairs, it is a perfectly legitimate procedure to adopt.

Specific Ion Interaction Models

An alternative approach to using ion pairs to explain the behaviour of different electrolytes is the specific ion interaction model formulated by Brønsted and Guggenheim. In this model, interactions between *specific pairs* of ions are considered. These interactions are expressed as interaction parameters B_{MX} that are measured in single electrolyte solutions containing only the ions M and X. Thus this model becomes particularly useful for dealing with mixed electrolyte solutions such as seawater. The simplest form of this treatment gives rise to an equation that extends the basic Debye-Huckel approach. For the electrolyte MX

$$\log \gamma_{\pm} = \log \gamma_{el} + \frac{\nu_M}{\nu_M + \nu_M} \sum_{X^*} B_{MX^*}[X^*]_T + \frac{\nu_X}{\nu_M + \nu_M} \sum_{M^*} B_{M^*X}[M^*]_T$$
$$\log \gamma_{el} = -Az^2 \frac{\sqrt{I}}{1+\sqrt{I}} \qquad [3.34]$$

The first term $\log \gamma_{el}$ is essentially the *non-specific* electrostatic interaction term arising from the Debye-Huckel theory. The remaining two terms are summations over all anions, or all cations, respectively of the B_{MX} interaction terms. More detailed versions of [3.34] have been developed by Pitzer and co-workers, and these have been extremely successful at predicting the activity coefficients of electrolytes in mixed solutions, including seawater and concentrated brines. A more detailed discussion of these models is beyond the scope of this book.

Finally, we should note that some authors (e.g. Millero and Schreiber, Millero and Hawke) have combined the concepts of specific ion pairing with the ionic interaction model of Pitzer to treat the behaviour of trace metals in seawater and related media with considerable success. Thus the two model approaches should not be treated as mutually exclusive, but rather as complementary ways of looking at the complicated phenomenon of ion-ion interactions in solution.

3.8 The Concept of pH

pH is an extremely common parameter in experimental science, yet it is one whose physical significance is usually poorly understood. The original definition of pH due to Sorenson was introduced in Section 2.4:

$$pH = -\log [H^+] \qquad [3.35]$$

pH is usually measured using a Galvanic cell, one that incorporates the H^+-responsive glass electrode. For the purposes of discussion, the following much simpler cell incorporating the hydrogen electrode will suffice:

$$Pt, H_2(g) \mid H^+ \parallel Cl^- \mid AgCl, Ag \qquad [3.36]$$

If we assume that the H_2 is in its standard state and has unit fugacity, then the Nernst equation for this cell takes the form

$$\begin{aligned} E &= E^{\varnothing} - k \log (a_H a_{Cl}) \\ &= E^{\varnothing} - k \log \frac{c_{Cl}\gamma_{Cl}}{c^{\varnothing}} - k \log a_H \\ &= E_o - k \log a_H \end{aligned} \qquad [3.37]$$

where the constant E_o is the combination of the standard cell potential and the logarithm term involving the chloride ion. At first glance it might seem that [3.37] achieves what was earlier stated to be impossible: the ability to measure the activity of a single ion, H^+. However, it is clear that if this cell is to be used to measure the activity of H^+ ions, firstly a value for the constant E_o must be obtained. Clearly there are only 2 ways to do this:

1. Obtain a value for the activity coefficient of the other single ion, chloride; or
2. Measure E_o in a solution of known H^+ activity.

Clearly, neither method is achievable without recourse to some non-thermodynamic assumption, e.g. the calculation of an activity coefficient from theory.

The IUPAC Practical pH scale

The standard convention for making equation [3.37] yield measurements that approximate the hydrogen ion activity was formulated by the International Union of Pure and Applied Chemistry (IUPAC). This convention *defines* the pH value of a series of standard buffer solutions (method 2 above). These defined values are based on measurements using a cell like that in [3.36], with the activity coefficient of the chloride ion estimated using the Davies equation. Because this approach is arbitrary (since other choices could be made), it is termed a *practical definition* of pH. The original measurements that gave rise to the defined pH values of the standard buffers were made at the U.S. National Institute of Standards and Technology NIST (formerly the National Bureau of Standards, NBS). For this reason, the pH scale is often referred to as the *NBS pH scale*.

In these circumstances, the Nernst equation [3.37] can be rewritten

$$E = E_o + k\,pH \qquad [3.38]$$

If the measured cell potential in a standard buffer of defined $pH = pH_S$ is E_S, then

$$E_S = E_o + k\,pH_S \qquad [3.39]$$

Subtracting these two equations and rearranging then leads to the defining equation for the IUPAC pH scale

$$E - E_s = k(pH - pH_S)$$
$$pH = pH_s + \frac{E - E_s}{k} \qquad [3.40]$$

The treatment just presented allows us to identify the quantity pH defined by [3.40] as based on the activity of the H^+ ion only to the extent that the defined pH values are themselves satisfactory in this respect. This depends, in turn, on the estimation of the chloride ion activity using the Davies equation. The discussion presented earlier on the validity of this equation might suggest that the correspondence between pH and H^+ activity might be good up to an ionic strength of about 0.7 mol kg^{-1}. However, other factors intrude to limit the usefulness to ionic strengths less than only 0.1 mol kg^{-1}.

The main factor is that the cell [3.36] contains a *liquid-liquid junction*, needed to separate the standard KCl solution in the right-hand half-cell from the compartment containing the test solution or standard buffer. Because the compositions of the electrolytes on each side of this junction will never be the same, a small *liquid-junction potential* E_j will develop across the junction whose magnitude is, in principle, impossible to determine. Thus [3.40] needs to be rewritten to include the difference in liquid junction potentials between when the standard buffer is measured and when the unknown solution is measured:

$$pH = pH_s + \frac{E - E_s}{k} + \Delta Ej \qquad [3.41]$$

The quantity ΔE_j is termed the *residual liquid junction potential*. The best that can be done is to minimize its value by filling the salt bridge making up the liquid junction with a concentrated solution of KCl, whose ions have very nearly equal electrical mobilities. It is also important to minimize changes in ionic strength and composition between the test solution and the standard buffer. However, this is not always possible. Uncertainties in the residual liquid junction potential mean that for solutions having $I < 0.1$ M, the measured pH corresponds to the free H^+ activity to within ± 0.002, while at higher ionic strengths this correspondence is lost and pH becomes just a number (albeit still very reproducible.

pH Scales based on concentration

In Sections 3.5 and 3.6 we saw that in concentrated electrolytes, changes in activity coefficient often become rather small. This is particularly true where a solution contains a large excess of "inert" electrolyte, as is the case in seawater. If, under these circumstances, changes in activity coefficient of H^+ can be neglected, the Nernst equation for cell [3.36] reduces to a form resembling the ideal case:

$$E = E_o - k \log [H^+] \qquad [3.42]$$

where the constant term E_o now incorporates the activity coefficient terms for both chloride ion and H^+. However, unlike the case described earlier for the activity of H^+, we *can* measure the constant E_o simply by measuring the cell potential with the left-hand cell compartment filled with a solution of known H^+ *concentration*. By this procedure, we can define a concentration based pH scale

$$p^C H = -\log [H^+] \qquad [3.43]$$

This approach corresponds to the constant ionic medium convention mentioned in Section 3.4. It is particularly important in seawater, whose ionic composition varies very little in the main parts of the ocean, making it an almost ideal constant ionic medium. Several pH scales are in common use in marine chemistry in addition to the NBS scale.

Goyet and Poisson made measurements of the dissociation constants for carbonic acid in seawater. They defined a concentration-based pH scale by calibrating their H^+ electrode system using solutions of seawater medium containing known concentrations of standard HCl. Because the seawater medium contained sulfate and fluoride ions, both of which can react with the added HCl, their pH scale (termed the *seawater scale*, pH_{sws}) corresponds to the combined concentrations of free H^+ (i.e. protons associated with solvent molecules) and those combined with both sulfate and fluoride:

$$[H^+]_{sws} = [H^+]_{free} + [HSO_4^-] + [HF] \qquad [3.44]$$

Some years earlier, Hansson completed a series of similar acid-base equilibrium constant measurements using a synthetic seawater solution that contained sulfate ion, but not fluoride, arguing that the effects of fluoride ion could be dealt with explicitly as a competing chemical equilibrium. This is known as the *total proton scale* pH_T and corresponds to

$$[H^+]_T = [H^+]_{free} + [HSO_4^-] \qquad [3.45]$$

The difference between these two scales is rather small and almost constant, $pH_F - pH_{sws} = 0.0092$ in normal seawater, which corresponds to about 2% of H^+ bound as HF. This is only significant in very precise work.

The proportion of H^+ associated with sulfate is also rather constant, which lead Bates and Macaskill to propose the use of a third pH scale based on the free proton only. This scale must be calibrated using a seawater medium containing neither sulfate nor fluoride. For normal seawater, pH_{free} is higher than pH_T by 0.0913, which corresponds to about 23% of the H^+ bound as HSO_4^-.

The relationship between these three scales is as follows

$$[H^+]_{free} = \frac{[H^+]_T}{1+\frac{[SO_4^{2-}]}{K_S}} = \frac{[H^+]_{SWS}}{1+\frac{[SO_4^{2-}]}{K_S}+\frac{[F^-]}{K_F}} \qquad [3.46]$$

where K_s is the dissociation constant for HSO_4^- and K_F is the corresponding value for HF. It well be shown in the next chapter that under the conditions of normal seawater, the fraction α_0 of both total sulfate S_T and total fluoride F_T that is protonated is negligible, equation [3.46] may be converted to the pH-independent form

$$[H^+]_{free} = \frac{[H^+]_T}{1+\frac{S_T}{K_S}} = \frac{[H^+]_{SWS}}{1+\frac{S_T}{K_S}+\frac{F_T}{K_F}} \qquad [3.47]$$

The detailed use of these three scales will be considered further in Chapter 7, which deals with acid-base equilibria in seawater.

3.9 Equilibrium Constants in Real Solutions

As discussed in Section 2.2, the law of chemical equilibrium is founded on the chemical potential of the reactant and product species in a reaction. Thus, equilibrium constants must also be expressed in terms of the activities of the species involved, not their concentrations. Thus for the general chemical reaction

$$A + B \quad C + D \qquad [3.48]$$

the expression for the equilibrium constant is

$$K = \frac{a_C\, a_D}{a_A\, a_B} \qquad [3.49]$$

The equilibrium constant defined in this way is termed a *thermodynamic equilibrium constant.* If we dissect this into the constituent activity coefficients and concentrations, we obtain

$$\begin{aligned} K &= \frac{[C][D]}{[A][B]} \times \frac{\gamma_C\, \gamma_D}{\gamma_A\, \gamma_B} \\ &= K' \times \frac{\gamma_C\, \gamma_D}{\gamma_A\, \gamma_B} \end{aligned} \qquad [3.50]$$

where K' is termed the *apparent* or *conditional* equilibrium constant based on species concentrations. It is a quantity that is valid only for the specific conditions under which it is measured. The second term in [3.50] involving the activity coefficients of the reaction species can be regarded as describing the deviation from the ideal, thermodynamic value under (specific) real conditions.

Equation [3.50] has important implications for the use of equilibrium constants. If we wish to carry out a calculation to determine the equilibrium composition of an real solution, then clearly we need the conditional K' constant for the particular conditions involved. There are two approaches to this problem:

1 Measure the value of K' for the relevant conditions experimentally; or

2 Use a tabulated thermodynamic value, and estimate the activity coefficient terms using as theory such as the Davies equation or the specific ion interaction model.

Both approaches are commonly used, depending on the nature of the problem and the degree of required accuracy. For the best accuracy, method 1 is preferable.

Acid-base equilibria

In the specific case of acid-base equilibria, the definition of the pH scale used becomes part of the measurement of any equilibrium constant. The same pH scale must be used for both the measurement of acid-dissociation constants and their use in a calculation. To illustrate this, we consider the case of a coloured acid-base indicator. The concentrations of the acid and base forms of such a substance can be readily measured in solution using a spectrophotometer. Thus, we could measure the acid dissociation constant pK_a by measuring both concentrations in a series of solutions of known pH:

$$pK_a = pH - \log \frac{[base]}{[acid]} \qquad [3.51]$$

If we subsequently placed the indicator in a solution of unknown pH and measured the concentrations of acid and base forms, the unknown pH could then be calculated by rearranging [3.51]. The resultant pH would be on the same scale as that used to measure pK_a. Moreover, if equation [3.51] were used to compute the composition of the indicator solution at a given pH, any uncertainties as to the meaning of the pH scale, i.e. whether it corresponds exactly to the free H^+ ion activity or not, are irrelevant because they become factored out through the double use of the equation. This, of course, assumes no change in the activity coefficients of the species involved between measurements and application.

The same experiment could equally have been carried out using standard solutions of known H^+ concentration, in which case the indicator would then be calibrated to measure H^+ concentration in unknown solutions.

It follows that any consideration of acid-base equilibria in real solutions must specify the pH scale appropriate to the equilibrium constants being used. In Chapter 6 we shall consider the measurement of acid dissociation constants in some detail and re-address this issue.

Further reading

General

R.A. Robinson and R.H. Stokes (1959). *Electrolyte Solutions.* Butterworths, London, Chapters 2 and 3.

W. Stumm and J.J. Morgan (1981). *Aquatic Chemistry: An Introduction Emphasizing Chemical Equilibria in Natural Waters.* Wiley and Sons, New York, Chapters 2 and 3.

More specific

R.G. Bates, *The determination of pH*, Wiley and Sons, New York, 1973.

R.G. Bates and C.H. Culberson, Hydrogen ions and the thermodynamic state of marine systems, in: "*The fate of fossil-fuel CO2 in the oceans*", N. Andersen and R. Malahoff, eds., pp. 45-61, Plenum Press, New York, 1976.

R.G. Bates and J.B. Macaskill, Acid-base measurements in seawater, in: "*Analytical Methods in Oceanography*", T.P.R. Gibb, ed., pp. 110-123, American Chemical Society, Washington D.C., 1975.

C. Goyet and A. Poisson (1989). New determination of carbonic acid dissociation constants in seawater as a function of temperature and salinity. *Deep-sea Research* 36: 1635-1654.

I. Hansson, A new set of pH scales and standard buffers for sea water, *Deep-sea Research* 20, 479-491, 1973.

Chapter 4 Some Examples of Acid-Base Equilibria

This chapter looks at some examples of acid-base equilibria relevant to natural waters, and also discusses the effects of temperature and pressure on equilibrium constants.

4.1 The Effect of Temperature on Acid-Base Equilibria

The relationship describing the temperature dependence of any equilibrium constant is

$$\frac{d \ln K}{dT} = \frac{\Delta H^{\varnothing}}{RT^2} \qquad [4.1]$$

where T is the absolute (Kelvin) temperature and R is the gas constant. This equation allows values for the standard enthalpy change $\Delta H^{\varnothing}$ to be calculated from data on the temperature dependence of K and *vice-versa*. Moreover, differentiation of [4.1] allows the calculation of the standard heat capacity at constant pressure $\Delta C_p^{\varnothing}$ (and *vice-versa*)

$$\Delta C_p^{\varnothing} = \frac{d(\Delta H^{\varnothing})}{dT} = \frac{d}{dT}\left(RT^2 \frac{d \ln K}{dT} \right) \qquad [4.2]$$

It has been found that reliable thermodynamic values of K can be derived from integrated versions of [4.1] having the general form

$$\log K = A + \frac{B}{T} + C \ln T + DT + ET^2 .... \qquad [4.3]$$

Usually, only some of the terms in [4.3] are necessary to provide an adequate fit to experimental data. A common example of this approach uses only the first, second and fourth terms:

$$\log K = \frac{a}{T} + b + cT \qquad [4.4]$$

where *a*, *b*, and *c* are constants. For the self dissociation of water, this semi-empirical equation is

$$\log K = -\frac{4470.99}{T} + 6.0875 - 0.01706\,T \qquad [4.5]$$

Equation [4.5] satisfactorily reproduces the experimental data for water over the temperature range 0–50°C for dilute solutions. Table 4.1 lists experimentally derived values of the parameters *a, b, c* for a selection of common weak acids.

Equation [4.5] predicts that there will be a temperature T_{max} at which the dissociation constant assumes a maximum value and ΔH is zero. This, and the equilibrium constant K_{max} at this temperature, are readily obtained by simple calculus

$$T_{max} = \sqrt{\frac{a}{c}} \qquad [4.6]$$

$$\log K_{max} = b - 2\sqrt{ac}$$

Table 2.2 also shows the T_{max} values calculated for the acids listed. For most weak acids, T_{max} is within the normal temperature range of liquid water. The homologous series of carboxylic acids

listed (methanoic through n-butanoic acid) all have T_{max} values near room temperature, decreasing up the series. Only for water itself and NH_4^+ is T_{max} above the normal boiling point, meaning that the dissociation constants for both of these substances increase strictly with temperature.

Table 4.1 *Dissociation constants for weak acids in aqueous solution at 25°C and their temperature dependence parameters for equation [4.3]. The final column shows the temperature of maximum log K_a, T_{max}. Infinitely dilute solution convention, molality scale.*

Acid	pK_a	–a	b	–c	T_{max} (K)
H_2O	13.997	4470.99	6.0875	0.01706	511.9
HCOOH	3.752	1342.85	5.2743	0.015168	297.5
CH_3COOH	4.756	1170.48	3.1649	0.013399	295.6
C_2H_5COOH	4.874	1213.26	3.3860	0.014055	293.8
n-C_3H_7COOH	4.820	1033.39	2.6215	0.013334	278.4
NH_4^+	9.245	2835.76	0.6322	0.001225	1521.0
H_3BO_3	9.234	2237.94	3.305	0.01765	356.1
H_2CO_3	6.352	3403.71	14.8435	0.032786	322.2
HCO_3	10.329	2902.39	6.4980	0.02379	349.3
H_3PO_4	2.148	799.31	4.5535	0.013486	243.5
H_2PO_4	7.198	1979.5	5.3541	0.019840	315.9

Another approach adopted by several authors, and used particularly by Millero for seawater equilibria, includes only the first three terms of [4.3] and is found to be satisfactory for most acid dissociation equilibria in the range 0 to 50°C.

$$\ln K = A + \frac{B}{T} + C \ln T \qquad [4.7]$$

Differentiation of this equation along the lines of [4.1] gives the following simple expression for the standard enthalpy change $\Delta H^{\varnothing}$

$$\Delta H^{\varnothing} = RT^2 \frac{d \ln K}{dT} = R(CT - B) \qquad [4.8]$$

while a second differentiation (following [4.2]) allows calculation of the standard heat capacity at constant pressure:

$$\Delta C_p^{\varnothing} = \frac{d \Delta H^{\varnothing}}{dT} = RCT \qquad [4.9]$$

In general, the agreement between $\Delta H^{\varnothing}$ and $\Delta C_p^{\varnothing}$ measured directly and estimated from the temperature dependence of acid dissociation constants is quite good.

Temperature Dependence of Activity Coefficients

The temperature dependence of the mean ionic activity coefficient of an electrolyte is related its partial molal enthalpy. For a simple 1:1 electrolyte MX, the partial molal enthalpy in solution is given by

$$\overline{H} = -T^2 \frac{\partial (\frac{\mu}{T})_{m,p}}{\partial T} \qquad [4.10]$$

The chemical potential μ of MX is related to the mean ionic activity coefficient as described in Chapter 3

$$\begin{aligned} \mu &= \mu^{\varnothing} + RT \ln a_{MX} \\ &= \mu^{\varnothing} + RT \ln [MX] + RT \ln \gamma_{\pm} \end{aligned} \qquad [4.11]$$

Combining [4.10] and [4.11] and carrying out the partial differentiation at constant composition and pressure, we obtain

$$\frac{\partial \ln \gamma_{\pm}}{\partial T} = -\frac{(\overline{H} - \overline{H}^{\varnothing})}{RT^2} \qquad [4.12]$$

For many electrolytes, the difference between $\overline{H}$ and $\overline{H}^{\varnothing}$ becomes appreciable at concentrations greater than 0.1 mol kg^{-1}. Thus in natural electrolytes such as seawater, activity coefficients in the infinitely dilute solution convention are measurably affected by temperature. Normal temperatures range in the ocean range approximately from 0°C in deep water to over 30°C in some equatorial surface waters.

Generally $\overline{H}$ can be expressed as a linear function of T over reasonable temperature ranges. Integrating [4.12] under these conditions yields an expression of the form

$$\log \gamma_{\pm} = -\frac{A_1}{T} + A_2 + A_3 \log T \qquad [4.13]$$

where A_1, A_2 and A_3 are positive constants characteristic of the electrolyte at a particular pressure and concentration.

Very few measurements of the temperature dependence of $\gamma_{\pm}$ have been made to test the validity of [4.13] and evaluate its parameters. Table 2.3 shows data for NaCl at a series of

temperatures. These results show that equation [4.14] reproduces the experimental variations in $\gamma_{\pm}$ with temperature quite well for this electrolyte.

$$\log\gamma_{\pm} = -\frac{535.45}{T} + 11.4326 - 3.9679\log T \qquad [4.14]$$

Table 4.2 *Measured mean ionic activity coefficient of 1 mol L^{-1} NaCl solution at various temperatures compared to values calculated from equation [4.8]*

T	$\gamma_{\pm}$ (meas)	$\gamma_{\pm}$ (calc)
0	0.638	0.638
15	0.654	0.653
25	0.658	0.658
40	0.655	0.660
60	0.655	0.654
70	0.648	0.648
80	0.641	0.640
90	0.632	0.631
100	0.622	0.621

4.2 Effects of Pressure on Acid-Base Equilibria

The effects of pressure on acid-base equilibria are often not actively considered because reactions are usually studied in the laboratory at atmospheric pressures. However pressure dependence is a significant factor in natural waters, particularly the ocean. Pressure changes by approximately 1 atm 100 kPa for each 10 m depth interval in a column of water. Thus even in moderately deep lakes (100-500 m depth), significant pressure changes are exerted on chemical equilibria. Over the mean depth range of the ocean (3500 m), absolute pressure increases almost 400 times over that at the surface level.

The variation in chemical potential of a solute with change in pressure is given by its partial molal volume

$$\left(\frac{\partial\mu}{\partial p}\right)_{n,T} = \overline{V} \qquad [4.15]$$

Thus for a chemical reaction involving solutes, we obtain $\Delta G^{\varnothing}$ from the chemical potential difference between reactants and products in the usual way and form the partial derivative according to [4.15]

$$\left(\frac{\partial\Delta G}{\partial p}\right)_{n,T} = \Delta\overline{V} \qquad [4.16]$$

More than one convention has been used for solution systems to define the conditions of the standard state with respect to pressure. If the standard state is taken to be one of fixed pressure at

all temperatures, then the partial derivative in [4.16] is zero and the equilibrium constant is independent of pressure. In this convention, pressure effects on equilibria are described by variations in the activity of the reference state with pressure.

More frequently, a variable-pressure standard state convention is used, so that μ is a function of pressure. In this case, both [4.15] and [4.16] may be applied to the standard state to obtain the pressure dependence of the equilibrium constant K in terms of the standard partial molal volume change $\Delta\overline{V}^{\varnothing}$.

$$\left(\frac{\partial \Delta G^{\varnothing}}{\partial p}\right)_{n,T} = -RT\left(\frac{\partial \ln K}{\partial p}\right)_{n,T} = \Delta\overline{V}^{\varnothing} \qquad [4.17]$$

Hence we obtain

$$\left(\frac{\partial \ln K}{\partial p}\right)_{n,T} = -\frac{\Delta\overline{V}^{\varnothing}}{RT} \qquad [4.18]$$

Equation [4.17] applies to any consistent convention for thereference state, and has been used to calculate the pressure dependence of equilibrium constants in both the infinitely dilute solution convention and the constant ionic medium convention.

If the standard partial molal volume change $\Delta\overline{V}^{\varnothing}$ is independent of pressure, [4.18] integrates to the simpler form

$$\ln\frac{K_p}{K_0} = -\frac{\Delta\overline{V}^{\varnothing}(p - p^{\varnothing})}{RT} \qquad [4.19]$$

where K_o is the equilibrium constant at the standard pressure $p^{\varnothing}$ = 101.3 kPa and K_p is its value at a pressure p.

More commonly, $\Delta\overline{V}^{\varnothing}$ is a linear function of pressure, in which case a second term involving the standard partial molal compressibility change $\Delta\overline{K}^{\varnothing}$ must be introduced

$$\ln\frac{K_p}{K_0} = -\frac{\Delta\overline{V}^{\varnothing}(p - p^{\varnothing})}{RT} + \tfrac{1}{2}\Delta\overline{K}^{\varnothing}\frac{(p - p^{\varnothing})^2}{RT} \qquad [4.20]$$

$$\text{where } \Delta\overline{K}^{\varnothing} = \left(\frac{\partial \Delta\overline{V}^{\varnothing}}{\partial p}\right)_T$$

The volume change for most weak acid dissociation reactions is negative, so that the effect of increasing pressure is to increase the value of the acid dissociation constant. Table 4.3 shows the effect of pressure on the dissociation constant of pure water at several temperatures.

Table 4.3 *Ratios of self-dissociation of water K_w at different pressures to the reference value at 100 kPa at three temperatures.*

p (kPa)	5°C	25 °C	45 °C
100	1	1	1

$2x10^4$	1.24	1.20	1.16
10^5	2.8	2.36	2.0

At 25°C in dilute aqueous solution, the equilibrium constant for dissociation of acetic acid increases by 40% in magnitude when pressure is increased 1000-fold over normal atmospheric pressure, while both the first and second dissociation constants for CO_2(aq) increase by a factor of approximately 3. While these changes are small in magnitude compared to the effects of temperature, the pressure dependence of acid-base equilibria over the depth range of the ocean is experimentally significant using modern analytical techniques. Later in this book we will see that the pressure dependence of the solubility equilibrium of calcium carbonate in the ocean has interesting consequences.

For seawater electrolytes, the partial molal volume change and partial molal compressibility change terms in [4.20] are expressed as polynomials in temperature:

$$\Delta\overline{V}^{\varnothing} = a_0 + a_1 t + a_2 t^2$$
$$\Delta\overline{K}^{\varnothing} = \frac{\partial \Delta\overline{V}^{\varnothing}}{\partial p} = b_0 + b_1 t + b_2 t^2 \qquad [4.21]$$

where t is the Celsius temperature.

Table 4.4 shows coefficients for use with [4.20] and [4.21] for a number of weak acids of interest to seawater chemistry given by Millero.

Table 4.4 *Coefficients for calculating the pressure dependence of acid dissociation constants using equations [4.20] and [4.21] (from Millero, 1995).*

Acid	a_0	a_1	a_2	b_0	b_1
H_2O	–25.6	0.2324	–0.0036246	–5.13	0.0794
H_2CO_3*	–25.5	0.1271	0	–3.08	0.0877
HCO_3^-	–15.82	–0.0219	0	1.13	–0.1475
HF	–9.78	–0.0090	–0.000942	–3.91	0.054
$B(OH)_3$	–29.48	–0.1622	0.002608	–2.84	0
HSO_4^-	–18.03	0.0466	0.000316	–4.53	0.0900
H_3PO_4	–14.51	0.1211	–0.000321	–2.67	0.0427
$H_2PO_4^-$	–23.12	0.1758	–0.002647	–5.15	0.09
HPO_4^{2-}	–26.57	0.2020	–0.003042	–4.08	0.0714
H_2S	–14.80	0.0020	–0.000400	–2.89	0.054
NH_4^+	–26.43	0.0889	–0.000905	–5.03	0.0814
K_s (calcite)	–48.76	–0.5304	0	–11.76	–0.3692
K_s (aragonite)	–35.00	–0.5304	0	–11.76	–0.3692

The pressure dependence of the mean ionic activity coefficient of an electrolyte follows naturally from [4.15] after expanding the expression for the chemical μ as we did for temperature

$$\frac{\partial \ln \gamma_{\pm}}{\partial p} = \frac{\overline{V} - \overline{V}^{\varnothing}}{RT} \qquad [4.22]$$

Unfortunately, few experimental data are available describing the pressure dependence of electrolyte activity coefficients to test the validity of this equation.

4.3 The Self-Dissociation of Water

The self-dissociation of water is fundamental to all acid-base equilibria in aqueous solution.

$$H_2O \quad H^+ + OH^- \qquad [4.23]$$

The thermodynamic equilibrium constant for this reaction has the complete definition

$$K_w = \frac{a_H a_{OH}}{a_{H_2O}} \qquad [4.24]$$

Generally, the activity of water in the denominator is so constant in dilute solutions that its value is subsumed into the equilibrium constant, i.e. unit activity is assumed. This approximation is generally not useful in concentrated electrolytes.

$$K_w = a_H a_{OH} \qquad (a_{H_2O} \approx 1) \qquad [4.25]$$

For pure water at 25°C, pK_w = 13.997 in the infinitely dilute solution convention and molality concentration scale. Often the rounded figure of pK_w = 14.0 is used in simple calculations, particularly if non-ideal behaviour is ignored.

The temperature and pressure dependence of K_w for pure water was discussed in Sections 4.1 and 4.2 above. The dissociation reaction [4.23] is exothermic, so following [4.1] its value increases with temperature (i.e. pK_w decreases). At 0°C, pK_w =14.93, while at 50°C, pK_w has decreased to 13.26. These changes mean that the pH of a neutral solution also depends on temperature, a fact that is often forgotten when dealing with natural waters having temperatures different from the laboratory standard of 25°C.

The following equation, based on [4.7], describes the temperature dependence of K_w for pure water

$$\ln K = 148.96502 - \frac{13847.26}{T} - 23.6521 \ln T \qquad [4.26]$$

Millero extended this equation to seawater electrolytes using an expression of the form

$$\ln K'_w - \ln K_w = (a_0 + \frac{a_1}{T} + a_2 \ln T) S^{1/2} + b_0 S \quad [4.27]$$

where K'_w is the value of K_w in seawater of salinity S and temperature T, and K_w is the pure water value calculated using [4.26]. For the total proton scale, the coefficients in [4.27] are

$$a_0 = -5.977 \quad a_1 = 118.67 \quad a_2 = 1.0495 \quad b_0 = -0.01615 \quad [4.28]$$

These values are based on a combination of experimental measurements, all of which are in good agreement. It is important to note that as with most examples of seawater-specific equilibrium constants, these values refer to the seawater concentration scale, i.e. mol per kg of seawater (unlike molality, which is mol per kg of solvent). Refer to Section 2.1 for information on converting to and from this concentration scale.

4.4 Acid-Base Reactions of CO_2

In the absence of water, CO_2 exists in the gas phase at normal environmental temperatures. Its mole fraction in normal atmospheric air is approximately 3.5×10^{-4}, making it only a minor atmospheric component. The equilibrium established between gaseous CO_2 and an aqueous solution with which it is in contact

$$CO_2(g) \quad CO_2(aq) \quad [4.29]$$

is described by Henry's Law of gas solubility

$$K_H = \frac{a_{CO_2}}{f_{CO_2}} \quad [4.30]$$

where the Henry's Law coefficient K_H is the equilibrium constant for reaction [4.29] and f_{CO2} is the fugacity of $CO_2(g)$. In many cases, the fugacity may be approximated by the partial pressure of CO_2 in the air. Exact conversion between these two quantities requires use of the virial equation of state for CO_2 in air.

Because of this phase equilibrium, one may speak of the fugacity (or partial pressure) of $CO_2(g)$ in equilibrium with a solution containing CO_2 species (whether the solution actually is in equilibrium with a gas phase or not). This quantity, usually termed the f_{CO2} (or p_{CO2}) of the solution, is useful in determining the degree of undersaturation or oversaturation of natural water with respect to gaseous CO_2. It may be calculated using an equilibrium model of CO_2 in the water, and also may be measured directly by equilibrating the solution with a small volume of air and subsequently measuring the gas-phase CO_2 concentration by gas chromatography or infrared spectroscopy.

The hydration of $CO_2(aq)$ proceeds by a complex mechanism outlined below to form a small amount of *carbonic acid* H_2CO_3 in solution

$$CO_2(aq) + H_2O \quad H_2CO_3 \quad [4.31]$$

The equilibrium constant for this reaction is rather small. Reported values for 25°C range from 1×10^{-3} to 2.9×10^{-3}. Thus very little CO_2 is actually present in the form of carbonic acid. Because of this, it has become conventional not to distinguish between the two undissociated forms by using a combined variable H_2CO_3* to symbolise both CO_2 species. Thus

$$[H_2CO_3^*] = [CO_2(aq)] + [H_2CO_3] \qquad [4.32]$$

The quantity $[H_2CO_3^*]$ corresponds to the total analytical concentration of undissociated CO_2 that would be determined by some chemical method, e.g. an acid-base titration.

For similar reasons, Henry's Law in [4.30] is more usually expressed in terms of the activity (or concentration) of $H_2CO_3^*$

$$K'_H = \frac{[H_2CO_3^*]}{f_{CO_2}} \qquad [4.33]$$

The following equation was given by Weiss for the calculation of K_H for seawater as a function of salinity S and temperature T; fugacity is expressed in atmospheres and $[H_2CO_3^*]$ on the seawater concentration scale:

$$\ln K'_H = a_1 + \frac{a_2}{t} + a_3 \ln t + S(b_1 + b_2 t + b_3 t^2) \qquad (t = \frac{T}{100}) \qquad [4.34]$$

where the coefficient values are

$a_1 = -60.2409$ $a_2 = 93.4517$ $a_3 = 23.3585$

$b_1 = 0.023517$ $b_2 = -0.023656$ $b_3 = 0.0047036$ [4.35]

Table 4.4 shows values of the Henry's Law constant calculated using equation [4.34] at various temperatures. The results show that like all gases, CO_2 is more soluble in cold water than it is in hot water.

The salinity dependence is less marked. At 25°C and a salinity of 30, pK_H decreases from its S = 35 value of 1.5468 to 1.5355, which corresponds to a 2.6% *increase* in the magnitude of K_H. Note that increasing the salinity decreases CO_2 solubility in seawater, indicating that like many neutral solutes, CO_2 is "salted out".

Table 4.4 *Values of the Henry's Law constant for CO_2 in seawater of salinity 35 at various temperatures (seawater concentration scale, CO_2 fugacity).*

T (°C)	pK_H
0.00	1.2016
5.00	1.2829
10.00	1.3577
15.00	1.4264
20.00	1.4894
25.00	1.5468
30.00	1.5991
35.00	1.6465

Mechanism of CO_2(aq) hydration

The mechanism of CO_2(aq) hydration and its subsequent dissociation to form the bicarbonate ions is relatively complex. One pathway involves initial formation of carbonic acid

$$CO_2 + H_2O \underset{k_{21}}{\overset{k_{12}}{\rightleftharpoons}} H_2CO_3 \qquad [4.36a]$$

followed by dissociation to bicarbonate ion

$$H_2CO_3 \underset{k_{32}}{\overset{k_{23}}{\rightleftharpoons}} HCO_3^- \qquad [4.36b]$$

The other pathway involves a Lewis acid-base reaction with water to yield bicarbonate ion directly

$$CO_2 + H_2O \underset{k_{31}}{\overset{k_{13}}{\rightleftharpoons}} HCO_3^- + H^+ \qquad [4.36c]$$

Reported values for the rate constants for equilibrium [4.36b] at 25°C show that it is very fast: i.e. $k_{32} \approx 5 \times 10^{10}$ L mol^{-1} s^{-1} and $k_{23} \approx 9 \times 10^6$ s^{-1}. Therefore [4.36b] can be considered instantaneously at equilibrium relative to the speeds of reactions [4.36a] and [4.36c]. The equilibrium constant derived from the forward and backward rates of [4.36b] is the intrinsic dissociation constant of carbonic acid itself, and has a thermodynamic value at 25°C of pK_a = 3.75.

Individual rate constants for [4.36a] and [4.36c] are not known, but their general magnitude can be deduced from the experimental rate law for the removal of CO_2(aq)

$$-\frac{d[CO_2]}{dt} = k_A[CO_2] - k_B[HCO_3^-][H^+] \qquad [4.37]$$

where $k_A \approx 0.03$ s^{-1} and $k_B \approx 10^5$ L mol^{-1} s^{-1} at 25°C. The first rate constant k_A can be identified with the two forward reactions in [4.36a] and [4.36c], so that neither k_{12} nor k_{13} is likely to be larger than 0.03 s^{-1}, and thus significantly smaller than k_{23}. Similar arguments apply to the rate of dehydration.

The overall mechanism may be summarised as follows

$$CO_2 + H_2O \overset{\text{slow}}{\rightleftharpoons} H_2CO_3 \overset{\text{fast}}{\rightleftharpoons} HCO_3^- + H^+ \qquad [4.38]$$

Because of the slow kinetics of the hydration step, the dissociation of CO_2(aq) to its conjugate base HCO_3^- is an unusually slow acid-base reaction. The pseudo-first order half time for the reaction is

$$t_{1/2} = \frac{\ln 2}{k_A} = \frac{0.6931}{0.031} \approx 20\,\text{sec} \qquad [4.39]$$

By contrast, most hydrogen ion transfer reactions in aqueous solution proceed to equilibrium on time scales of milliseconds or less. Thus acid-base titrations involving CO_2 species must be carried out slowly to preserve equilibrium.

Kinetic studies have also identified an alternative pathway to HCO_3^- involving reaction with OH^- ions that becomes important at high pH

$$CO_2 + OH^- \underset{k_{41}}{\overset{k_{14}}{}} HCO_3^- \qquad [4.40]$$

Reported values of the rate constants are $k_{14} \approx 8.5 \times 10^3$ L mol^{-1} s^{-1} and $k_{41} \approx 2 \times 10^{-4}$ s^{-1} at 25°C. The factor $k_{14}[OH^-]$ exceeds k_A for the low pH mechanism [4.36] when $[OH^-]$ is greater than about 4×10^{-6} mol L^{-1}, or pH ≈ 9. Above this pH, reaction [4.40] dominates the hydration reaction.

Acid dissociation of CO_2(aq)

Like the Henry's Law equilibrium [4.33], the first dissociation equilibrium of CO_2(aq) is normally expressed in terms of the "combined" species H_2CO_3*

$$H_2CO_3^* \quad HCO_3^- + H^+ \qquad [4.41]$$

while the second dissociation equilibrium of CO_2 is

$$HCO_3^- \quad CO_3^{2-} + H^+ \qquad [4.42]$$

The corresponding thermodynamic equilibrium constant K_1 and K_2 are

$$K_1 = \frac{a_H\, a_{HCO_3}}{a_{H_2CO_3}} \qquad K_2 = \frac{a_H\, a_{CO_3}}{a_{HCO_3}} \qquad [4.43]$$

In most practical situations, conditional values of these constants will be used, defined in terms of the concentrations of the H_2CO_3*, HCO_3^- and CO_3^{2-} and a suitable pH scale:

$$K_1' = 10^{-pH} \frac{[HCO_3^-]}{[H_2CO_3^*]} \qquad K_2' = 10^{-pH} \frac{[CO_3^{2-}]}{[HCO_3^-]} \qquad [4.44]$$

Representative thermodynamic values of pK_1 and pK_2 at various temperatures for the infinitely dilute solution convention and molality scale are given in Table 4.5.

Table 4.5 *Thermodynamic values of pK_1 and pK_2 for CO_2 in water at various temperatures (molality scale).*

T (°C)	pK_1	pK_2
0	6.579	10.625

5	6.517	10.557
10	6.464	10.490
15	6.419	10.430
20	6.381	10.377
25	6.352	10.329
30	6.327	10.290
35	6.309	10.250

Conditional values of pK_1 and pK_2 have been determined for seawater by several authors because of the importance of CO_2 equilibria in the ocean. One of the first sets was published by Mehrbach *et al.* whose measurements were based on the IUPAC Practical pH scale and used real seawater as the electrolyte:

$$\begin{aligned} pK_1' &= 17.788 - 0.073104T + 0.00011463T^2 - 0.0051087S \\ pK_2' &= 20.919 - 0.064209T + 0.000087313T^2 - 0.011887S \end{aligned} \qquad [4.45]$$

At about the same time, Hansson reported measurements using the total hydrogen ion pH scale, with a medium comprising artificial seawater containing sulfate but not fluoride.

$$\begin{aligned} pK_1' &= \frac{841.2}{T} + 3.2762 - 0.010382\,S + 0.00010287\,S^2 \\ pK_2' &= \frac{1376.4}{T} + 4.8256 - 0.018232\,S + 0.00011839\,S^2 \end{aligned} \qquad [4.46]$$

Some time later, Goyet and Poisson reported measurements made on the seawater pH scale, i.e. using a synthetic seawater medium containing both sulfate and fluoride:

$$\begin{aligned} pK_1' &= \frac{812.2}{T} + 3.356 - 0.0171\,S\ln T + 0.000091\,S^2 \\ pK_2' &= \frac{1450.87}{T} + 4.604 - 0.00385\,S\ln T + 0.000182\,S^2 \end{aligned} \qquad [4.47]$$

Finally the most recent set of measurements made by Roy*et al.* also used the total proton pH scale and the molality concentration scale:

$$\ln K_{1,2}' = a_1 + \frac{a_2}{T} + a_3 \ln T + (b_1 + \frac{b_2}{T})S^{1/2} + cS + d\,S^{3/2} \qquad [4.48]$$

where for pK_1 the constants are

a1 = 2.83655 a2 = –2307.1266 a3 = –1.5529413
b1 = –0.20760841 b2 = –4.0484
c = 0.08468345 d = –0.00654208 [4.49a]

and for pK_2 they are

a1 = –9.226508 a2 = –3351.6106 a3 = –0.2005743

b1 = –0.106901773 b2 = –23.9722

c = 0.1130822 d = –0.00846934 [4.49b]

Since these 4 sets of data do not use common concentration and pH scales, they must be converted to a common basis for comparison. Table 4.6 shows values of the 4 different measurement sets at a salinity of 35 and various temperatures using the total proton scale. The results are also compared graphically in Figure 4.1, which plots the differences for the first three data sets from those of the most recent measurements by Roy *et al.*

For pK_1, the agreement between the 4 data sets is within ± 0.01, which is quite good. The worst departure from this mutual agreement occurs with the Mehrbach *et al.* results, originally made using the NBS pH scale. For pK_2, the agreement is worse for the earlier measurements by Mehrbach *et al.* and Hansson. The more recent data sets by Goyet and Poisson and Roy *et al.* agree with each other very well.

Table 4.6 *Comparison of the conditional values of pK_1 and pK_2 for CO_2 in seawater at of salinity 35 at various temperatures (total proton pH scale, seawater concentration scale).*

T (^oC)	Roy *et al.*	Goyet &Poisson	Hansson	Merhbach *et al.*
0	6.1080	6.1088	6.1185	6.1132
5	6.0536	6.0551	6.0631	6.0499
10	6.0014	6.0034	6.0096	5.9920
15	5.9512	5.9534	5.9580	5.9390
20	5.9028	5.9051	5.9081	5.8908
25	5.8563	5.8584	5.8599	5.8469
30	5.8115	5.8132	5.8133	5.8072
0	9.3830	9.3948	9.3448	9.3905
5	9.2848	9.2949	9.2721	9.2993
10	9.1900	9.1986	9.1961	9.2113
15	9.0985	9.1055	9.1172	9.1264
20	9.0102	9.0155	9.0356	9.0444
25	8.9249	8.9285	8.9516	8.9651
30	8.8424	8.8444	8.8653	8.8884

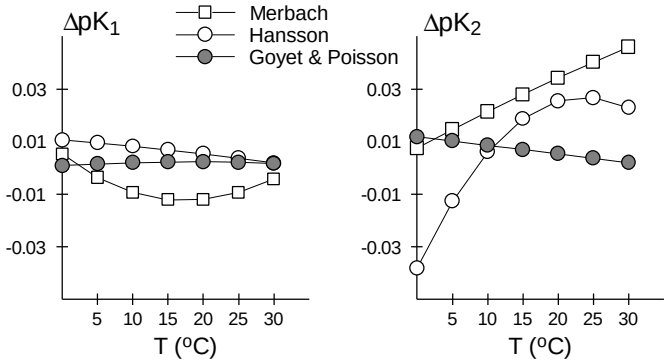

Figure 4.1 *Differences between pK_1 and pK_2 values measured by Goyet and Poisson (solid circles), Hansson (open circles) and Mehrbach, Hansson (open circles) and Mehrbach et al. (open squares) from those measured by Roy et al. (total proton pH scale, data taken from Table 4.6).*

Figure 4.2 shows the composition-pH diagram for CO_2 in seawater calculated using the constants of Roy *et al.* at a total carbon dioxide concentration of 2.1 mmol kg^{-1} as a function of pH (total proton scale). This diagram covers a much larger range in pH than is normally observed in seawater (pH = 7.7 – 8.3), so it is of interest only in the context of compositional changes that would occur on the addition of acid or base to the seawater in the laboratory.

The diagram shows the features expected of this dibasic acid. The curves for H_2CO_3* and HCO_3^- cross each other at pH = pK_1 = 5.8563, while those for HCO_3^- and CO_3^{2-} cross at pH = pK_2 = 8.9249. At normal seawater pH, HCO_3^- is the dominant species, followed by CO_3^{2-} and then H_2CO_3* as the least important.

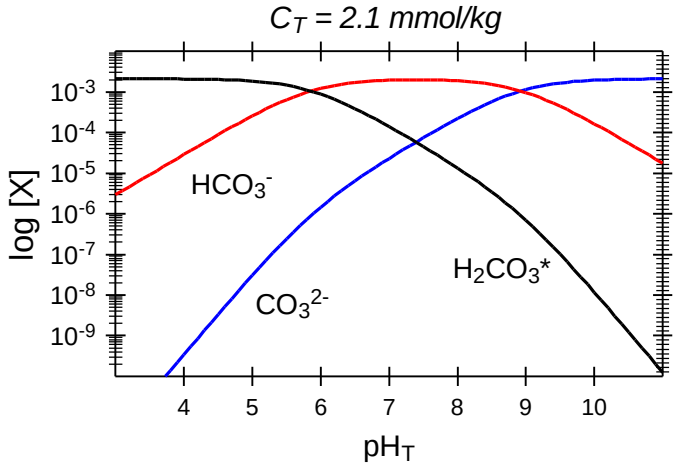

Figure 4.2 *Composition-pH diagram for carbon dioxide in seawater of salinity 35, total CO_2 = 2.1 mmol kg^{-1} and temperature 25°C as a function of pH (total proton scale) calculated using the constants of Roy et al.*

4.5 Boric acid

The anion of boric acid, H_3BO_3, is the second most abundant base species in seawater next to the various forms of CO_2(aq). Its total analytical concentration in seawater of salinity 35 is 4.16×10^{-4} mol kg^{-1} and at may be calculated from salinity using the relation

$$B_T = 0.000416 \frac{S}{35.000} \qquad [4.50]$$

This concentration is sufficient for the borate anion of boric acid to make a measurable contribution to the total alkalinity of seawater.

The dissociation equilibrium for boric acid may be written in the form

$$H_3BO_3 + H_2O \quad H^+ + B(OH)_4^- \qquad [4.51]$$

A thermodynamic value for this acid dissociation constant, normally symbolised pK_B, at 25°C of 9.24 has been reported. Because of this large value, further dissociation of $B(OH)_4^-$ is not significant in most aqueous solutions. In seawater media on the total proton pH scale, the following formula may be used to calculate the conditional value for pK_B (seawater concentration scale)

$$\ln K'_B = a_1 + a_2 S^{1/2} + a_3 S + \frac{b_1 + b_2 S^{1/2} + b_3 S + b_4 S^{3/2} + b_5 S^2}{T} + (c_1 + c_2 S^{1/2} + c_3 S) \ln T + d_1 S^{1/2} T \qquad [4.52]$$

where the coefficient values are

$a_1 = 148.0248$ $a_2 = 137.1942$ $a_3 = 1.62142$

$b_1 = -8966.90$ $b_2 = -2890.53$ $b_3 = -77.942$

$b_4 = 1.728$ $b_5 = -0.0996$

$c_1 = -24.4344$ $c_2 = -25.085$ $c_3 = -0.2474$

$d_1 = 0.053105$ [4.53]

Since boric acid effectively functions as a monoprotic acid, its composition-pH diagram is straightforward and similar to the examples presented in Chapter 2.

4.6 Hydrofluoric acid

Hydrofluoric acid is the only halo-hydrogen acid that is a weak acid in aqueous solution. The acids HCl, HBr and HI all dissociate completely in aqueous solution. The thermodynamic dissociation constant for HF has a value of 6.7×10^{-4} (molality scale) at 25°C. In solution, HF and F^- exhibit a tendency to associate with each other

$$HF + F^- \quad HF_2^- \qquad [4.54]$$

This reaction has an equilibrium constant of 3.9 (molality scale) at 25°C. This association behaviour leads to unusually low values for the activity coefficient of HF solutions as the concentration increases. For example, at [HF] = 0.001 mol kg^{-1}, $\gamma = 0.544$ whereas at 0.1 mol kg^{-1} it is only 0.077.

Seawater of salinity 35 contains 6.84×10^{-5} mol kg^{-1} of total fluoride. Thus HF makes a small but experimentally significant contribution to the total concentration of hydrogen ions in seawater. The dissociation constant in seawater can be calculated using the relation derived from measurements made by Dickson and Riley (molality, free proton pH scales)

$$\ln K_F = \frac{1590.2}{T} - 12.641 + 1.525 I^{1/2} \qquad [4.55]$$

where I is the ionic strength.

In 'normal' seawater (salinity 35, temperature 25°C), $pK_F = 2.4953$ and $F_T = 6.833 \times 10^{-5}$ mol kg^{-1}, so that for a nominal free proton pH = 8.00, the proportion α_o presented as undissociated HF is given by

$$\alpha_0 = \frac{[H^+]}{[H^+] + K_F} \approx \frac{[H^+]}{K_F} = \frac{1 \times 10^{-8}}{10^{-2.4953}} = 3.13 \times 10^{-6} \qquad [4.56]$$

Thus the fraction of undissociated HF is negligible, and will remain so until very low pH values. Nonetheless, this small fraction is not negligible compared to the total H^+ concentration:

$$\frac{[HF]}{[H^+]} = \frac{3.13 \times 10^{-6} \times 6.833 \times 10^{-5}}{1.0 \times 10^{-8}} = 0.0214 \qquad [4.57]$$

Thus only about 2% of the hydrogen ions are present in the form of HF at most reasonable pH values, a fraction which is nevertheless of significance in the precise work. As already mentioned, the species HF is implicitly part of the pH_{SWS} (seawater) scale, but in the total proton and free proton pH scales its presence must be explicitly considered.

Hydrofluoric acid is of practical use in many industrial processes, particularly the etching of glass and the manufacture of the fluorine-based chemicals such as Freons (chlorofluorocarbons) and polymers such as Teflon. It arises as an environmental pollutant from two main sources superphosphate manufacture, where it is a minor constituent of the phosphate minerals used, and aluminium smelting where it is a major component of the cryolite electrolyte.

4.7 Sulfuric acid

Sulfuric acid is a very important commercial acid-base substance. It is manufactured in enormous quantities from elemental sulfur using catalytic oxidation to SO_3. It is an important industrial chemical feedstock, especially in the fertiliser industry. Sulfuric acid is also an important constituent of acid rain, where is derives from the oxidation of sulfur-containing fuels such as coal.

Sulfuric acid, H_2SO_4, is a strong acid so far as its first dissociation to HSO_4^- is concerned. However HSO_4^- itself is a weak acid

$$HSO_4^- \quad H^+ + SO_4^{2-} \qquad [4.58]$$

This reaction is important in seawater, where a significant proportion of hydrogen ions are bound as bisulfate ion. Seawater of salinity 35 contains a total sulfate concentration of 0.02825 mol kg^{-1}, allowing calculation of the total sulfate concentration S_T from salinity in the same way as total boron

$$S_T = 0.02825 \frac{S}{35.000} \qquad [4.59]$$

The most recent measurements of the dissociation constant for [4.48] in seawater were reported by Dickson (molality, free proton scale):

$$\ln K'_S = a_1 + \frac{a_2}{T} + a_3 \ln T + (b_1 + \frac{b_2}{T} + b_3 \ln T) I^{1/2} + (c_1 + \frac{c_2}{T} + c_3 \ln T) I + d_1 \frac{I^{3/2}}{T} + d_2 \frac{I^2}{T} \qquad [4.60]$$

where the coefficients are

$a_1 = 141.328$	$a_2 = 4276.1$	$a_3 = -23.093$
$b_1 = 324.57$	$b_2 = -13856$	$b_3 = -47.986$
$c_1 = -771.54$	$c_2 = 35474$	$c_3 = 114.723$
$d_1 = -2698$	$d_2 = 1776$	[4.61]

In 'normal' seawater (salinity 35, temperature 25°C), $pK_S = 0.9987$ and $S_T = 0.02825$ mol kg^{-1}, so that for a nominal free proton pH = 8.00, the proportion α_o presented as undissociated HSO_4^- ions is given by

$$\alpha_0 = \frac{[H^+]}{[H^+] + K_S} \approx \frac{[H^+]}{K_S} = \frac{1 \times 10^{-8}}{10^{-0.9987}} = 9.97 \times 10^{-8} \qquad [4.62]$$

Thus only at very low pH values does a significant fraction of the sulfate become protonated (see also equation [3.44]). However, the small fraction that does is quite large in relation to the free H^+ concentration.

$$[HSO_4^-] = \alpha_0 S_T = 9.97 \times 10^{-8} \times 0.02825 = 2.82 \times 10^{-9} \ \text{mol kg}^{-1} \qquad [4.63]$$

Comparing this to the free H^+ concentration

$$\frac{[HSO_4^-]}{[HSO_4^-] + [H^+]} = \frac{2.82 \times 10^{-9}}{2.82 \times 10^{-9} + 10.0 \times 10^{-9}} = 0.22 \qquad [4.64]$$

This means that about 78% of the hydrogen ions are free in solution and 22% are bound by sulfate (ignoring the small effect of fluoride).

4.8 Silicic acid

Silicic acid is a very important nutrient species in seawater. It is required by planktonic organisms that manufacture their exoskeleton by precipitating *opal*, a pure mineral form SiO_2. The main examples of organisms requiring silicic acid are diatoms and radiolaria. Silicic acid is a growth-limiting nutrient over large parts of the ocean, having very low concentrations (< 1 μmol kg^{-1}) in most surface waters. Accordingly, its effect on the acid-base properties of surface waters can normally be neglected, even in the most precise work. However, because of the dissolution of opal exoskeleta of dead organisms in the deep waters of the ocean, total silicic acid

concentrations there are much higher (up to 300μmol kg^{-1}). Thus in deep ocean waters, silicic acid must be explicitly considered when examining the acid-base chemistry and pH.

Relatively speaking, silicic acid is a much more important component of fresh waters of the Earth (rivers and lakes). Concentrations in these waters are quite variable, and are typically in the range 0–300 μmol kg^{-1}. It is generated through the dissolution of silicate-containing minerals by water and atmospheric CO_2 in a process known as *weathering*. An archetypal example of a weathering reaction is

$$2NaAlSi_3O_8 + 2CO_2 + 9H_2O \rightarrow 2Na^+ + 2HCO_3^- + Al_2Si_2O_7 + 4Si(OH)_4 \qquad [4.65]$$

Because of the involvement of CO_2, the global silicic acid and carbon cycles are closely linked together.

The thermodynamic dissociation constant for silicic acid is pK_{Si} = 9.8312 at 25°C (molality scale), which means that the conjugate base form, silicate ion, is only the dominant species in natural waters of rather high pH (pH > 10). A similar situation was found for boric acid. Thus, further proton dissociation of silicate is not considered.

In seawater, the dissociation constant pK_{Si} = 9.3838 at 25°C and salinity 35 (seawater concentration scale, total proton pH scale). Thus at normal seawater pH, less than 10 % of the silicic acid is present as the conjugate base.

The value of pK_{Si} in seawater may be calculated using the following equation which is a shortened form of that used for boric acid (molality, total proton scale):

$$\ln K'_S = a_1 + \frac{a_2}{T} + a_3 \ln T + (b_1 + \frac{b_2}{T}) I^{1/2} + (c_1 + \frac{c_2}{T}) I + d_1 \frac{I^{3/2}}{T} + d_2 \frac{I^2}{T} \qquad [4.66]$$

The coefficients in [4.66] are as follows

a1 = 117.385	a2 = –8904.2	a3 = –19.334
b1 = 3.5913	b2 = –458.79	
c1 = –1.5998	c2 = 188.74	
d1 = 0.07871	d2 = –12.1652	[4.67]

4.9 Phosphoric acid

Phosphoric acid is also a very important nutrient species in seawater. It is required by all planktonic organisms, primarily as a key component of the ADP-ATP energy transfer enzyme system. Throughout much of the global ocean, phosphate is regarded as a key growth-limiting nutrient, along with nitrate. Accordingly, surface water concentrations of phosphate are normally quite small (< 0.1 μmol kg^{-1}), and the impact of phosphoric acid species on acid-base equilibria in most surface seawaters is minimal. However, somewhat like silicic acid, because of the remineralization of dead phytoplankton tissue in deep parts of the ocean, much higher concentrations are found in deep waters. In addition, polar regions and other areas where deep

waters upwell to the surface contain phosphate concentrations that are significant for acid-base chemistry.

Phosphoric acid is triprotic and has three thermodynamic dissociation constants: pK_{1P} = 2.155, pK_{2P} = 7.2063 and pK_{3P} = 12.3515 at 25°C (molality scale). In seawater of salinity 35 the corresponding values are pK_{1P} = 1.6119, pK_{2P} = 5.9618 and pK_{3P} = 8.7893 at the same temperature (total proton scale, seawater concentration scale). When these values are compared to the nominal pH 8 of normal seawater, it is clear that the major species is HPO_4^{2-}. This is confirmed by inspection of the dissociation-pH diagram for phosphoric acid in seawater shown in Figure 4.3.

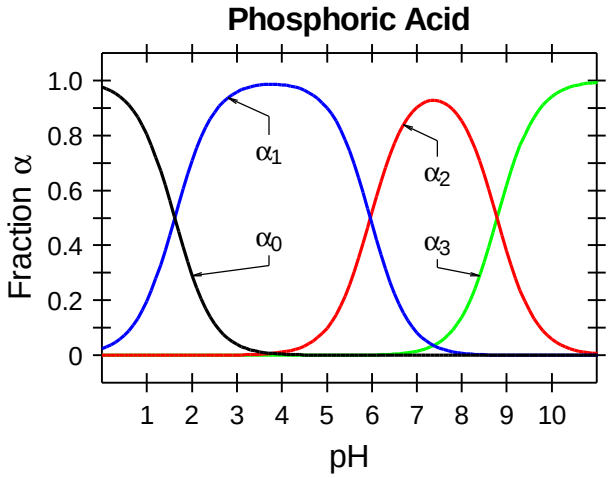

Figure 4.3 *Dissociation -pH diagram for phosphoric acid in seawater of salinity 35, temperature 25°C (total proton scale).*

The three dissociation constants for H_3PO_4 in seawater may be calculated using the equation (total proton pH scale, seawater concentration scale)

$$\ln K'_{nP} = a_1 + \frac{a_2}{T} + a_3 \ln T + (b_1 + \frac{b_2}{T}) S^{1/2} + (c_1 + \frac{c_2}{T}) S \qquad [4.68]$$

For K_{1P}, the coefficients are

a1 = 115.525 a2 = –4576.752 a3 = –18.453
b1 = 0.69171 b2 = –106.736
c1 = –0.01844 c2 = –0.6543 [4.69a]

For K_{2P}

a1 = 172.0883 a2 = –8814.715 a3 = –27.927
b1 = 1.3566 b2 = –160.340
c1 = –0.05778 c2 = 0.37335 [4.69b]

and for K_{3P}

a1 = –18.141 a2 = –3070.750 a3 = 0
b1 = 2.81197 b2 = 17.27039
c1 = –0.09984 c2 = –44.99486 [4.69c]

Further Reading

A.G. Dickson and F.J. Millero (1987). A comparison of the equilibrium constants for the dissociation of carbonic acid in seawater media , *Deep-Sea Research* 34, 1733-1743.

C. Goyet and A. Poisson (1989). New determination of carbonic acid dissociation constants in seawater as a function of temperature and salinity. *Deep-sea Research* 36: 1635-1654.

I. Hansson (1973). A new set of acidity constants for carbonic acid and boric acid in seawater. *Deep-sea Research* 20: 461-478.

C. Mehrbach, C.H. Culberson, J.E. Hawley and R.M. Pytkowicz (1973). Measurement of the apparent dissociation constants of carbonic acid in seawater at atmospheric pressure. *Limnology and Oceanography* 18: 897-907.

F.J. Millero (1979). The thermodynamics of the carbonate system in seawater, *Geochimica et Cosmochimica Acta* 43, 1651-1661.

F.J. Millero (1995). Thermodynamics of the carbon dioxide system in the oceans, *Geochimica et Cosmochimica Acta* 59, 661-677.

R.N. Roy, L.N. Roy, K.M. Vogel, C.P. Moore, T. Pearson, C.E. Good and Millero, F.J. (1993) The dissociation constants for carbonic acid in seawater at salinities 5 to 45 and temperatures 0 to 45^{o}C, *Marine Chemistry* 44, 249-267.

R.F. Weiss (1974). Carbon dioxide in water and seawater : the solubility of a non-ideal gas. , *Marine Chemistry* 2, 203-215.

Chapter 5 Calculations involving Acid-base Equilibria

This chapter discusses methods for computing the composition of solutions influenced by acid-base equilibria, with particular reference to the speciation of CO_2 in natural waters.

In most undergraduate chemistry courses, techniques for making calculations of this type are almost always based on the use of simplifying assumptions about the composition of a solution that allow it to be approximated using simple hand calculations. While this approach has some practical merit, the author has found that most students take a long time to develop the degree of experience needed to be confident with this approach, and usually become quite confused when faced with a problem involving more than 2 or 3 species. Furthermore, computer programs that solve the composition of even complex equilibrium systems have become quite minor applications on today's desktop computer.

Therefore, this chapter adopts exclusively a more general approach to multi-component equilibria that hopefully facilitates understanding of the principles involved.

5.1 A General Approach to Acid-base Equilibrium Calculations

Our starting point for considering the speciation of solutions affected by acid-base equilibria is to recognize the importance of pH as a controlling variable. We shall see that now matter how complex the composition of a solution, once the pH has been calculated all other concentration parameters can be derived from it in a straightforward manner.

A second guiding principle is that in general, the pH of any solution can be adjusted to almost any reasonable value by the addition of strong acid (e.g. HCl) or strong base (e.g. NaOH). Along with this goes the more subtle concept that *any* solution having acid-base properties can be prepared by adding to water appropriate quantities of one or more weak electrolytes, plus some strong acid and/or some strong base. This arises because whatever form a weak electrolyte happens to be in at the start, the addition of either strong acid or strong base (as the case may be) will convert it to its conjugate form. In some cases, the quantities of one or more of the latter three (weak electrolyte, strong acid, strong base) may be zero, but this is only a special case.

We now set out the general approach using simple examples.

5.2 Strong Electrolytes Only

We start with the simplest case, a solution not containing any weak electrolytes except for the solvent water. This example will be developed in some detail because it allows many of the critical concepts needed for more complex systems to be dealt with.

Suppose that the concentration (known) of strong acid added to form the final solution is c_A, and that the concentration of strong base (known) also added is c_B. Such a solution has 4 composition parameters to be calculated:

- the concentrations of H^+ and OH^-,
- the concentration of the strong acid anion, e.g. Cl^-, and
- the concentration of the strong base cation, e.g. Na^+

The last two are easy to calculate. Since a strong acid is completely dissociated into its constituent ions in solution, by definition, its conjugate base has *zero* tendency to react with protons. Therefore, on the grounds of *mass-balance*, its concentration must be the same as that of the strong acid:

$$[Cl^-] = c_A \qquad [5.1]$$

By exactly the same reasoning, we can equate the concentration of the strong base cation with its known concentration

$$[Na^+] = c_B \qquad [5.2]$$

Note that both [5.1] and [5.2] remain true even when strong acid, or strong base, has not been added (zero concentration).

We now have 2 remaining unknown parameters, $[H^+]$ and $[OH^-]$. By the law of algebra, we need to find 2 corresponding equations to solve for the composition. The first such equation is the Law of Chemical Equilibrium as applied to the self-dissociation of water, which allows us to link together our two remaining parameters. In its most general form, this is

$$K_w = \frac{a_H \, a_{OH}}{a_{H_2O}} \qquad [5.3]$$

Note that this introduces a 5th parameter, the activity of H_2O. However, in most aqueous solutions, it is conventional to take a_{H2O} as constant and absorb it into the value of K_w. At the same time, we would also adopt a conditional value for K_w so that it is expressed in terms of the hydroxide ion *concentration* and a suitable pH scale:

$$\begin{aligned} K_w &= 10^{-pH}[OH^-] \\ &= h[OH^-] \end{aligned} \qquad [5.4]$$

where the simplification h has been used for the antilogarithm term 10^{-pH}. We should note that any of the pH scales discussed in Chapter 3 would be suitable for the above use. The conditional value of K_w could be obtained by direct measurement in the solution of interest, or it could be estimated from the thermodynamic value by calculation of the required activity coefficients.

The other equation that can always be applied to an aqueous solution is the *charge-balance condition*, which expresses the notion that the solution is always electrically neutral, i.e. it has no excess of either negative or positive charge. The charge balance condition equates the sum of all charges on cations *i* with that on all anions *j*:

$$\sum_i |z_i| c_i = \sum_j |z_j| c_j \qquad [5.5]$$

For the solution under consideration, the charge balance condition is

$$[Na^+] + [H^+] = [Cl^-] + [OH^-] \qquad [5.6]$$

which, using [5.1], [5.2] and [5.4] simplifies to

$$c_B + [H^+] = c_A + \frac{K_w}{h} \qquad [5.7]$$

However, this still contains 2 unknown parameters, $[H^+]$ and h. The first, $[H^+]$ is the free proton concentration in the solution[2], while h is identified with the chosen pH scale. The relationship between the two is a familiar one:

$$\frac{h}{[H^+]} = \gamma_H \qquad [5.8]$$

This shows that in order to solve for the composition, we must know the relationship between hydrogen ion activity and concentration in the solution of interest. For dilute solutions using the NBS pH scale, γ_H could be reliably estimated using the Davies equation or equivalent. For a more concentrated electrolyte, we must use a concentration-based pH scale, i.e. one based on the constant ionic medium convention. In the latter case, the activity coefficient is unity and we can equate h and $[H^+]$. In either case, the general equation becomes

$$c_B + \frac{h}{\gamma_H} = c_A + \frac{K_w}{h} \qquad [5.9]$$

This is a quadratic equation in a single variable h that is easily solved using the general quadratic formula. However, arriving at an exact algebraic solution to [5.9] is academic, since for any more complex equilibrium system, the equivalent to [5.9] will be more complicated and will not have such an algebraic solution. Therefore, for the general case, we need to find a robust *numerical* method for solving [5.9] and its more complex equivalents. This can be done by rearranging the equation so that the unknown terms involving h are on the right-hand side:

$$c_A - c_B = \frac{h}{\gamma_H} - \frac{K_w}{h} \qquad [5.10]$$

In [5.10], the left-hand side corresponds to the known stoichiometric excess of strong acid over strong base, and in general this quantity could be positive, negative or zero. Finding the solution (i.e. the correct value if h) is made simple once we note that the right-hand side is a monotonic increasing function of h, i.e. as h increases, its value also increases and *vice-versa*. This behaviour is illustrated in Figure 5.1, which shows values of [5.1] calculated at various pH values. In the figure we see that when h is too large, i.e. pH is too small, the calculated value of [5.10] is larger than the known value of $c_A - c_B$, and *vice-versa*. This suggests a robust method of finding the solution:

1 Guess a value of h, and calculate the right-hand side of [5.10].

2 If it is larger than the known value of $c_A - c_B$ then keep choosing smaller values of h until it becomes smaller than $c_A - c_B$, otherwise choose larger values until it becomes greater.

---

[2] More correctly, it is the total proton concentration taking account of any weak bases combined with H^+ we have chosen to be part of the constant ionic medium. See Chapter 3.

3 Now that we have two estimates of *h*, one too large and one too small, keep on bisecting the difference between them until the new, middle *h* value is close enough to the required result within some acceptable margin of error.

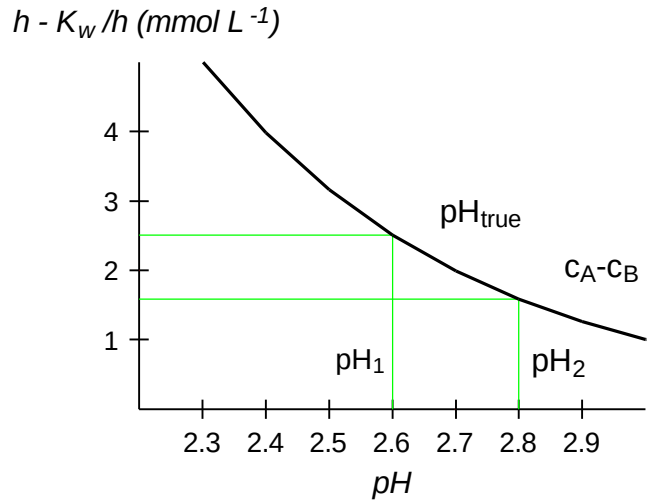

Figure 5.1: Calculated values of equation [5.10] for a hypothetical system in which the value of $c_A - c_B$ is 2 mmol L^{-1} and γ_H = 1.000. The results of estimating the solution at pH values of 2.60 and 2.80 are shown; the true value is pH = 2.699.

In fact, more efficient mathematical methods for finding the solution than step 3 in the scheme outlined above do exist, and are the ones that are generally used in multi-component equilibria computer algorithms. However, these details are not important, in chemical terms, to an understanding how the solution can be found.

5.3 A Single, Monoprotic Weak Electrolyte

We now extend the scheme just considered by introducing into the system a single, monoprotic weak electrolyte. We will assume, for the sake of discussion, that this is a neutral weak acid HA and its conjugate base A^-, with a total analytical concentration of c_{HA}. Our strong acid and strong base are still part of the system. This will cover any acidic or basic possibilities involving the weak electrolyte. For example, a solution of the pure weak acid HA will have both strong electrolyte concentrations c_A and c_B zero, whereas a solution of the pure weak base form Na^+A^- is one in which c_A is zero and $c_B = c_{HA}$.

Introduction of the weak electrolyte has added 2 further composition parameters that must be calculated. Therefore, to guarantee a solution, we require 2 new equations independent of those already considered. Fortunately, for any such case, this is always possible. The first equation is the *mass-balance condition* for the weak electrolyte

$$c_{HA} = [HA] + [A^-] \qquad [5.11]$$

Mass-balance conditions are particularly important because they are an example of what is termed a *conservative capacity factor*. This is a quantity that is invariant both to changes in temperature and pressure in the solution[3], and to mixing of two or more different solutions. For example, if two solutions containing the weak electrolyte HA are mixed together, the total concentration of the mixture c_{HA} is readily calculated from the values for the two separate solutions, taken in proportion to the quantity of each used to make the mixture. This is not true of the *individual species* that contribute to c_{HA}, i.e. [HA] and [A^-], because these will generally change through shifts in the dissociation equilibrium. Only in the trivial case where the two solutions have exactly the same composition would such shifts in the position of the dissociation equilibrium not take place.

The second equation is the dissociation equilibrium for the weak acid

$$K_a = h\frac{[A^-]}{[HA]} \qquad [5.12]$$

where it has been implicitly assumed, as with K_w earlier, that the dissociation constant K_a is a suitable conditional value measured using an appropriate pH scale.

Combining [5.11]and [5.12] in a manner similar to the derivation of the degree of dissociation (Chapter 2) leads readily to the relations

$$[HA] = \alpha_0\, c_{HA} = c_{HA}\frac{h}{h+K_a}$$
$$[A^-] = \alpha_1\, c_{HA} = c_{HA}\frac{K_a}{h+K_a} \qquad [5.13$$

Recall that both α_o and α_1 are functions of *h* and therefore can be used in our treatment. It remains to insert, in this case, the expression for the conjugate base concentration into the charge balance equation [5.6]

$$[Na^+] + [H^+] = [Cl^-] + [OH^-]\ [A^-] \qquad [5.14]$$

which, combined with [5.13]

$$c_B + [H^+] = c_A + \frac{K_w}{h} + c_{HA}\,\alpha_1 \qquad [5.15]$$

As before, we rearrange this to put all the terms involving*h* on the right-hand side:

$$c_A - c_B = \frac{h}{\gamma_H} - \frac{K_w}{h} - c_{HA}\,\alpha_1 \qquad [5.16]$$

---

[3] Strictly speaking, this is only true in the molality and seawater concentration scales. However, small changes in solution volume take place through T and p effects, which have a measurable effect on the molarity of solutes.

When this result is compared with [5.10] for the case of strong electrolytes only, it is seen that the addition of the weak electrolyte has introduced a single new term on the right-hand side that represents, in this case, the concentration of the conjugate base. More importantly, because this new term involves the *subtraction* of a quantity (α_1) *inversely* related to h, it preserves the property we used to find the solution numerically, i.e. that [5.16] increases as h increases.

Therefore, the numerical method outlined previously for the simple case of strong electrolytes will work equally well for this more complex example!

In deriving [5.16], we made the assumption that the weak acid was a *neutral* species, so that only its univalent conjugate base contributes to the charge balance equation. This will not always be the case, of course. For example, the base species NH_3 is neutral and its conjugate base is the cation NH_4^+. It turns out that this factor does not remove the generality of [5.16]. In this second case, where the base is neutral (A) and conjugate acid enters the charge balance equation as HA^+, we would proceed as follows

$$[Na^+] + [H^+] + [HA^+] = [Cl^-] + [OH^-] \qquad [5.17]$$

Again making use of [5.13], we can replace $[HA^+]$

$$c_B + [H^+] + c_{HA}\,\alpha_0 = c_A + \frac{K_w}{h} \qquad [5.18]$$

Thus the new equation for estimating h to replace [5.16] is

$$\begin{aligned} c_A - c_B &= \frac{h}{\gamma_H} - \frac{K_w}{h} + c_{HA}\,\alpha_0 \\ c_A - c_B - c_{HA} &= \frac{h}{\gamma_H} - \frac{K_w}{h} - c_{HA}\alpha_1 \end{aligned} \qquad [5.19]$$

The right-hand side of this equation is identical to the previous case [5.16]. However, now the left-hand side has the additional term $-c_{HA}$. Surprisingly, this only makes the equation *apparently* different from [5.16], as becomes clear if we compare the two under comparable conditions. Suppose, in both cases, we are interested in the specific solution prepared by adding the conjugate acid to water. In the case of a neutral weak acid HA, this means that both c_A and c_B in [5.16] will be zero:

$$0 = \frac{h}{\gamma_H} - \frac{K_w}{h} - c_{HA}\,\alpha_1 \qquad [5.20]$$

For a positively charged conjugate acid, it is not possible to add *only* the acid form since a balancing anion must also be included. This anion is supplied, in effect by an equivalent concentration of strong acid. Thus in [5.19], c_B is zero and c_A and c_{HA} are equal to each other

$$\begin{aligned} c_A - c_{HA} &= \frac{h}{\gamma_H} - \frac{K_w}{h} - c_{HA}\alpha_1 \\ &= 0 \end{aligned} \qquad [5.21]$$

which is identical to [5.20]. Thus, when these two different cases are examined under *comparable conditions*, the governing equations are the same in each case.

There are other possibilities in which *both* acid and conjugate base form bear a charge and are both present in the charge balance condition (note that*at least one* of them must appear since the acid and its conjugate base must always differ in charge by a single proton charge). It is simple to show that the equivalent of [5.16] for the situation where the charge on the conjugate acid form is z_{HA} is as follows

$$c_A - c_B = \frac{h}{\gamma_H} - \frac{K_w}{h} + c_{HA}(z_{HA} - \alpha_1) \qquad [5.22]$$

5.4 Polyprotic Weak Electrolytes

The preceding discussion is easily extended to polyprotic acids. Consider carbon dioxide, whose acid-base equilibria were introduced in Section 2.5. We formulate the mass-balance condition by defining the quantity C_T, termed *total carbon dioxide* (in some texts this is symbolized ΣCO_2):

$$C_T = [H_2CO_3^*] + [HCO_3^-] + [CO_3^{2-}] \qquad [5.23]$$

The charge-balance condition in the general case becomes

$$[Na^+] + [H^+] = [Cl^-] + [OH^-] + [HCO_3^-] + 2[CO_3^{2-}] \qquad [5.24]$$

Note the factor of 2 that precedes the carbonate ion concentration. This is because of its double negative charge.

The concentrations of bicarbonate and carbonate ions may be expressed in terms of the mass balance condition as follows (see equations [2.43] to [2.49])

$$[HCO_3^-] = C_T \alpha_1$$
$$[CO_3^{2-}] = C_T \alpha_2 \qquad [5.25]$$

which, after substitution into the charge-balance equation [5.24] leads to

$$c_A - c_B = \frac{h}{\gamma_H} - \frac{K_w}{h} - C_T(\alpha_1 + 2\alpha_2) \qquad [5.26]$$

Once again, the right-hand side is a monotonic increasing function of h that can be readily solved using the numerical scheme outlined in Section [5.2].

The case of a triprotic acid, e.g. H_3PO_4 is a logical extension of this approach (see Section 2.6)

$$c_A - c_B = \frac{h}{\gamma_H} - \frac{K_w}{h} - \Sigma PO_4(\alpha_1 + 2\alpha_2 + 3\alpha_3) \qquad [5.27]$$

where ΣPO_4 is the total concentration of phosphoric acid species.

5.5 Summary of Principles

The examples presented in the previous sections illustrate several important principles:

Firstly, each time a new weak electrolyte is added to the system, there will be at least one new term in the charge balance equation (one for each of the*charged* conjugate forms), a single new mass-balance condition for the new electrolyte and an acid dissociation equilibrium for each conjugate acid-base pair. The addition of these new equations guarantees that a solution to the combined equations always exists, at least in principle.

Secondly, the addition of a new weak electrolyte always leads to a final equation that can be cast in the form of a monotonic increasing function of hydrogen ion activity, whose general form can be written

$$c_A - c_B = \frac{h}{\gamma_H} - \frac{K_w}{h} + f(c_{HA}, h) \qquad [5.28]$$

where f is a function of the H^+ activity h and the concentration of the weak electrolyte c_{HA}. This provides a general numerical scheme for finding the solution, as outlined in Section 5.2.

The development of this equation involves no simplifying assumptions, and it therefore remain valid under general conditions, i.e. in the presence of arbitrary amounts of strong acid (c_A) and/or strong base (c_B). Thus it can be used for calculating the composition of single solutions, or titration curves in which c_A and/or c_B vary from point to point.

Finally, the most important point to make concerns the chemical significance of the characteristic equation [5.28]. The left-hand side, $c_A - c_B$, is a conservative capacity parameter because it contains only terms that are themselves of this type. Thus, $c_A - c_B$ is independent of any changes in temperature and pressure, and has a value that is conserved during the mixing of different solutions. Most importantly, it is *experimentally accessible* through an acid-base titration. To illustrate this, consider the simple example of the titration of a weak acid HA with strong base. The version of the general equation that covers this case is [5.16] with the strong acid concentration set to zero

$$-c_B = \frac{h}{\gamma_H} - \frac{K_w}{h} - c_{HA}\,\alpha_1 \qquad [5.29]$$

which rearranges readily to

$$c_B = c_{HA}\,\alpha_1 - \frac{h}{\gamma_H} + \frac{K_w}{h} \qquad [5.30]$$

Equation [5.30] can be used to compute the titration curve, pH as a function of strong base concentration, as discussed in Section 5.7 below. Consider the particular case of the start of the titration where c_B is zero.

$$0 = c_{HA}\,\alpha_1 - \frac{h}{\gamma_H} + \frac{K_w}{h} \qquad [5.31]$$

This represents a solution obtained by adding only the neutral weak electrolyte HA to water. The unique pH of this solution can be obtained by solving [5.31] for h. This in turn means that the general form [5.30] represents the concentration of strong base that would be needed to bring the solution to any higher pH value.

It may also be viewed in reverse: [5.30] equally represents the concentration of *strong acid* that would be need to be added to convert the solution to one having the same pH as the weak acid-only solution, i.e. where [5.30] has a zero value. Seen in this light, [5.30] is a measure of how well the solution is able to neutralize strong acid compared to a solution containing only the weak acid HA.

5.6 Acid and Base Neutralizing Capacities

The preceding discussion shows that the conservative capacity factor represented by [5.30] is one that measures the *acid neutralizing capacity* (ANC) of the solution. This definition of ANC always implies a *reference point*, which in this case corresponds to the pure weak electrolyte (HA) solution. Such a reference point is often termed a *reference proton condition*: in reality it is a unique solution pH defined by some variant of the charge balance condition for the solution.

We now generalize [5.30] for the case where a strong acid might be present to give

$$\mathrm{ANC(HA)} = c_{\mathrm{B}} - c_{\mathrm{A}} = c_{\mathrm{HA}}\,\alpha_1 - \frac{h}{\gamma_{\mathrm{H}}} + \frac{\mathrm{K_w}}{h} \qquad [5.32]$$

where the terminology ANC(HA) implies an acid neutralizing capacity relative to a solution of HA as the reference proton condition.

Experimentally, ANC(HA) corresponds to the concentration of strong acid titrant required to bring the solution (mixture of HA and NaOH) to the equivalence point for the reaction

$$\mathrm{H^+ + A^- \rightarrow HA} \qquad [5.33]$$

Therefore, it can be measured by means of a titration in which the chosen indicating method is properly set up to record the arrival at this equivalence point. This is readily achieved by means of a potentiometric titration, as discussed in Chapter 6.

Experimentally, ANC(HA) will only be a positive quantity if the pH of the original solution is *higher* than that of the reference proton condition (in which case it would have to have contained some strong base).

One can also consider the converse of ANC, namely the hypothetical concentration of strong base needed to bring the solution to the same pH, which is a *base neutralizing capacity* (BNC):

$$\mathrm{BNC(HA)} = c_{\mathrm{A}} - c_{\mathrm{B}} = \frac{h}{\gamma_{\mathrm{H}}} - \frac{\mathrm{K_w}}{h} - c_{\mathrm{HA}}\,\alpha_1 \qquad [5.34]$$

Obviously, BNC(HA) would be a negative quantity unless the pH of the original solution was *less than* that of the reference proton condition (in which case it would have to have contained some strong acid).

The two capacities are trivially related to each other

$$\mathrm{ANC(HA) + BNC(HA)} = 1 \qquad [5.35]$$

from which it is obvious that only one of them can be positive.

For a weak electrolyte, it makes more sense to consider the BNC with respect to a different proton condition, namely the solution containing only the weak base Na^+A^-. This corresponds to the solution where $c_B = c_{HA}$

$$\begin{aligned} c_B &= c_{HA}\,\alpha_1 - \frac{h}{\gamma_H} + \frac{K_w}{h} \\ &= c_{HA} \end{aligned} \qquad [5.36]$$

which is easily rearranged to

$$\begin{aligned} 0 &= c_{HA}\,(\alpha_1 - 1) - \frac{h}{\gamma_H} + \frac{K_w}{h} \\ &= -c_{HA}\,\alpha_0 - \frac{h}{\gamma_H} + \frac{K_w}{h} \end{aligned} \qquad [5.37]$$

Therefore, BNC for this proton condition corresponds to the excess of strong acid over the value given by [5.37]

$$BNC(Na^+A^-) = c_A - c_B = c_{HA}\alpha_0 + \frac{h}{\gamma_H} - \frac{K_w}{h} \qquad [5.38]$$

Experimentally, this BNC corresponds to the quantity of strong base needed to titrate the solution to the equivalence point for the reaction

$$HA + OH^- \rightarrow A^- \qquad [5.39]$$

Obviously [5.38] also has a corresponding, and less useful, ANC value that will be a negative quantity unless the pH is higher than that of the reference condition.

The ANC for the HA proton condition and the BNC for the Na^+A^- proton condition are not independent of each other since they are both derived from the charge balance equation. This is shown by forming the sum of the two

$$\begin{aligned} ANC(HA) + BNC(Na^+A^-) &= c_{HA}\alpha_1 - \frac{h}{\gamma_H} + \frac{K_w}{h} + c_{HA}\alpha_0 + \frac{h}{\gamma_H} - \frac{K_w}{h} \\ &= c_{HA}(\alpha_1 + \alpha_0) \\ &= c_{HA} \end{aligned} \qquad [5.40]$$

Thus, these two neutralizing capacities are, in effect, a restatement of the charge balance and mass balance conditions for this system. More importantly, however, both are experimentally accessible, and therefore provide an experimental entry point into defining the composition of aqueous solutions. We shall see in the next section that this is particularly important for CO_2 species in water.

5.7 Acidity and Alkalinity

The concepts of ANC and BNC were originally developed for understanding the acid-base chemistry of CO_2 in water. The general equation for this system was presented earlier as [5.26]. If we write down the negative of [5.26], we obtain

$$c_B - c_A = \frac{K_w}{h} + C_T(\alpha_1 + 2\alpha_2) - \frac{h}{\gamma_H} \qquad [5.41]$$

Following the concepts developed in the previous section, this equation can be viewed as defining an ANC with respect to a solution prepared by dissolving the neutral weak electrolyte $CO_2(aq)$ in water. Equation [5.41] is termed the *alkalinity* of an aqueous solution, and as expected from its definition, it represents the stoichiometric concentration of strong acid needed to titrate the solution to the equivalence point for the reaction

$$HCO_3^- + H^+ \rightarrow H_2CO_3 \qquad [5.42]$$

Thus equation [5.42] represents the equivalent concentration of bases in solution stronger than, and including HCO_3^- (the conjugate base of H_2CO_3), *minus* the equivalent concentration of acids stronger than H_2CO_3 (in this case, H^+). The reference proton condition is a solution of H_2CO_3 in water. In Chapter 7 we shall see that in seawater, which contains weak electrolytes other than those of CO_2, the definition of alkalinity must be extended to include those other species. However, [5.41] serves as a definition of alkalinity in waters containing only CO_2 and H_2O as weak electrolytes.

In the context of this definition, alkalinity is measured by titrating the aqueous solution of interest with standard HCl to an end-point corresponding to [5.42]. In simple work, this is usually achieved using the indicator methyl orange, which has a pK_a value of about 4.3 in dilute solution, corresponding closely to the pH of the equivalence point. Another method is to add excess HCl, boil to expel CO_2 and then back-titrate the excess HCl with standard alkali. More complex methods for seawater are discussed in Chapter 7.

In terms of the individual ions contributing to alkalinity (assuming ideal behaviour), equation [5.41] may be expressed

$$Alk = [OH^-] + [HCO_3^-] + 2[CO_3^{2-}] - [H^+] \qquad [5.43]$$

Often, the alkalinity contributed by carbon dioxide species alone, the so-called *carbonate alkalinity* CA, is also calculated as

$$CA = [HCO_3^-] + 2[CO_3^{2-}] \qquad [5.44]$$

In most freshwater systems, the main contributors to alkalinity are HCO_3^- and, to a lesser extent, CO_3^{2-} and the terms in $[H^+]$ and $[OH^-]$ may be conveniently neglected.

One of the useful properties of alkalinity is the fact that since it is defined as the ANC in excess of the proton condition comprising a solution of $H_2CO_3 = CO_2$ in water, then exchange of CO_2 with an aqueous solution does not affect the alkalinity. In the natural environment, such changes might arise through changing solubility of $CO_2(g)$ with temperature. These may therefore

be treated theoretically as an equilibrium system at constant alkalinity. More will be made use of this important characteristic in seawater systems in Chapter 7.

Another neutralizing capacity factor for natural water systems is the property known as *acidity*. This is defined as the BNC of a solution with respect to the reference proton condition comprising a solution prepared from a solution of a carbonate salt, e.g. Na_2CO_3. The formal definition of acidity is

$$\text{Acy} = [H^+] + 2[H_2CO_3] + [HCO_3^-] - [OH^-] \qquad [5.45]$$

This quantity represents the stoichiometric concentration of strong base needed to titrate the water to a reference proton condition equivalent to a solution of Na_2CO_3 having the same C_T. As with alkalinity, the link between the definition and the experimental method used to measure acidity is reasonably obvious. Acidity corresponds to the equivalence point for the reaction

$$HCO_3^- + OH^- \rightarrow CO_3^{2-} + H_2O \qquad [5.46]$$

In simple work, the indicator phenolphthalein is often used to detect this equivalence point. Acidity can be represented in similar terms to [5.38]

$$\text{Acy} = \text{BNC}(CO_3^{2-}) = c_A - c_B = \Sigma CO_2(2\alpha_0 + \alpha_1) + \frac{h}{\gamma_H} - \frac{K_w}{h} \qquad [5.47]$$

Just as alkalinity is independent of changes caused by addition or removal of CO_2 to the system, so acidity is itself independent of any addition or removal of its reference proton species, CO_3^{2-}, to the system. This is of particular significance with respect to the dissolution or precipitation of $CaCO_3$, the most common insoluble CO_2 species in natural waters. Such changes may therefore be treated as systems operating at constant acidity.

As expected from the general case discussed in the previous section, alkalinity and acidity are not independent of each other. Taking the sum of [5.43] and [5.45], we eventually obtain

$$\text{Alk} + \text{Acy} \rightarrow 2\,C_T \qquad [5.48]$$

showing that both are linked through the mass-balance condition for CO_2.

Most natural waters have a pH intermediate between the proton conditions defining alkalinity (pH 4) and acidity (pH 9). However, although it is both possible and convenient to independently measure both parameters by means of acid-base titrations, this dual determination is not commonly carried out. Rather, it is most common to determine alkalinity by titration and the mass-balance parameter C_T, either by separate methods, as outlined in Chapter 7, or as part of the alkalinity determination by potentiometric methods, as outlined in Chapter 6.

Figure 5.2 illustrates the concepts of alkalinity and acidity in the context of the titration of Na_2CO_3 solution with standard HCl. The horizontal axis is presented in terms of the net concentration $c_A - c_B$ of the original solution, as defined in [5.26]. At –100 mmol L^{-1}, the solution contains pure CO_3^{2-} corresponding to the reference proton condition for acidity. At this point, the solution has zero acidity (by definition) and an alkalinity equal to twice the total CO_2 concentration of the solution (2x0.050 = 0.100 mmol L^{-1}).

Similarly at the reference proton condition for H_2CO_3, corresponding to $c_A - c_B$ equal to zero, the alkalinity is zero (by definition) and the acidity is now twice C_T.

An interesting point is halfway between these two reference proton conditions (at −50 mmol L^{-1}), which corresponds to a solution of the intermediate species, HCO_3^-. At this point, both acidity and alkalinity are equal to C_T. Thus a solution of $Na^+HCO_3^-$ is one that has, at the same time, maximum alkalinity and acidity for a given C_T.

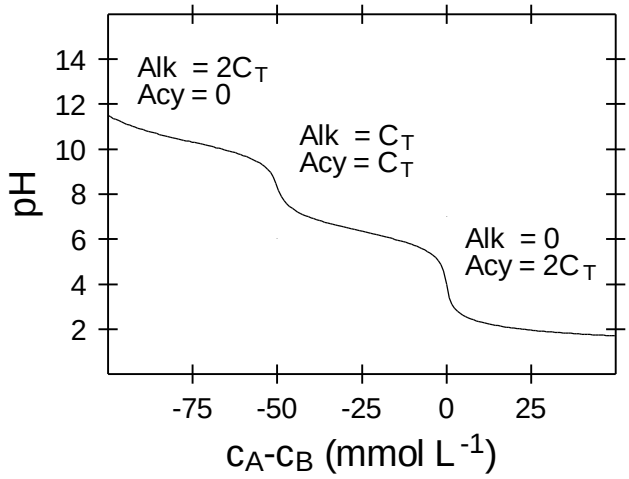

Figure 5.2: Calculated titration curve for 0.05M Na_2CO_3 solution titrated with HCl or NaOH relative to the reference proton condition of H_2CO_3 in water.

Figure 5.3 shows the variation with pH of alkalinity and acidity in water at 25°C containing 1 mmol L^{-1} of C_T. It shows that in the intermediate pH region common to many natural waters, 6 < pH < 9, the variation with pH of both parameters is rather small, and both are of similar magnitude. At very low pH, acidity becomes larger than the theoretical maximum of 2 C_T because of the effect of mineral acidity (see below). Conversely at high pH, caustic alkalinity (see below) makes alkalinity large.

Figure 5.4 shows the speciation of CO_2 as a function of pH in a closed system having C_T = 1 mmol L^{-1} that corresponds to Figure 5.3. Detailed comparison of the two figures reveals which species contribute to the alkalinity and acidity parameters. For example, maximum alkalinity and acidity together occurs near the crossing point for CO_3^{2-} and H_2CO_3* at pH 8.2: this corresponds to a solution prepared by adding pure $NaHCO_3$ to water.

In the pH range of most natural waters, the bicarbonate ion dominates the CO_2 speciation, with carbonate being somewhat less abundant and H_2CO_3* usually the least.

Other CO_2 Neutralizing Capacities

The example presented in Figure 5.2 shows that the CO_2 system has 4 other neutralizing capacities that could be defined, all of which are largely of historical interest only.

The converse of alkalinity, which corresponds to the strong base concentration needed to titrate the water to the reference proton condition of H_2CO_3, is termed *mineral acidity*, and is

normally a negative quantity. Mineral acidity is positive only in solutions containing excess strong acid (i.e. mineral acid).

Similarly, the converse of acidity, which corresponds to the strong acid concentration needed to titrate the water to the reference proton condition of CO_3^{2-}, is termed *caustic alkalinity*, and is also normally a negative quantity. Caustic alkalinity is positive only in solutions containing excess strong base (i.e. caustic alkali).

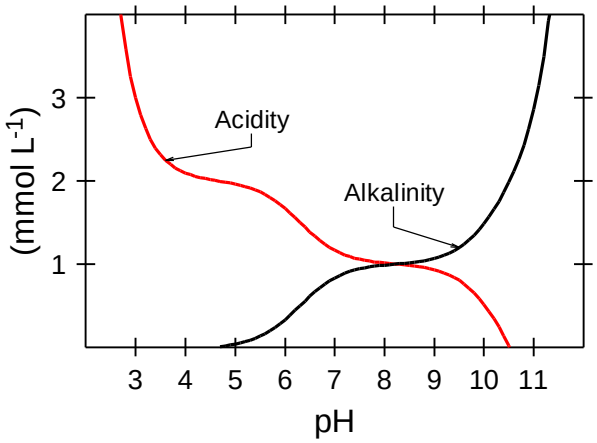

Figure 5.3: Calculated pH dependence of alkalinity and acidity for water at 25°C containing 1 mmol L^{-1} of C_T.

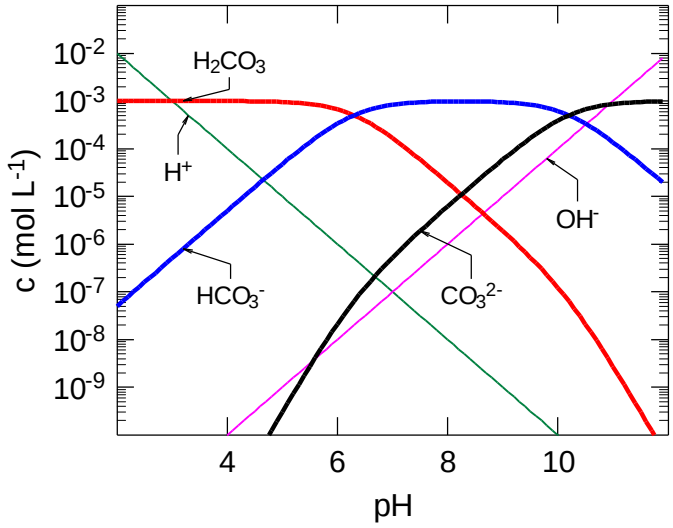

Figure 5.4: Calculated speciation of CO_2 as a function of pH in water at 25°C with total carbon dioxide C_T = 1 mmol L^{-1}.

The equivalence point in Figure 5.2 corresponding to a solution of the bicarbonate ion HCO_3^- provides, as expected, two neutralizing capacity parameters. The quantity of strong acid

needed to titrate the solution to this point is termed the *p-alkalinity*, while the converse concentration of strong base needed to reach the same proton condition is termed the *p-acidity*. Consistent with earlier arguments, none of these quantities is independent of each other, and each is derived from C_T. and the charge balance equation.

CO_2 Speciation in Open Systems

The discussion of CO_2 speciation in a closed system of constant C_T. just presented is relevant to situations where natural waters are out of contact with the atmosphere. In many situations, the system is open to the atmosphere and exchange of CO_2 is able to take place with the gas phase. At the global level, where one considers the entire atmosphere and the entire ocean phases, this equilibrium is complex and is discussed in detail in Chapter 7.

On a smaller scale, one can consider the gas phase to be essentially infinitely large, so that the solution maintains equilibrium with it according to the Henry's Law equilibrium for CO_2 dissolution that was discussed in Chapter 4, equation [5.49].

$$K_H = \frac{a_{CO_2}}{f_{CO_2}} \qquad [5.49]$$

This means that $[H_2CO_3^*]$ in an open system will be constant at a value determined by the gas exchange equilibrium. Under these conditions, calculation of the speciation as a function of pH is relatively simple:

$$[HCO_3^-] = \frac{K_1}{[H^+]}[H_2CO_3^*]$$
$$[HCO_3^-] = \frac{K_1K_2}{[H^+]^2}[H_2CO_3^*] \qquad [5.50]$$

Figure 5.5 shows the speciation of CO_2 calculated for an open system in equilibrium with air containing 350 ppm by volume of CO_2, which is a typical modern-day value for normal air (in the 1990's).

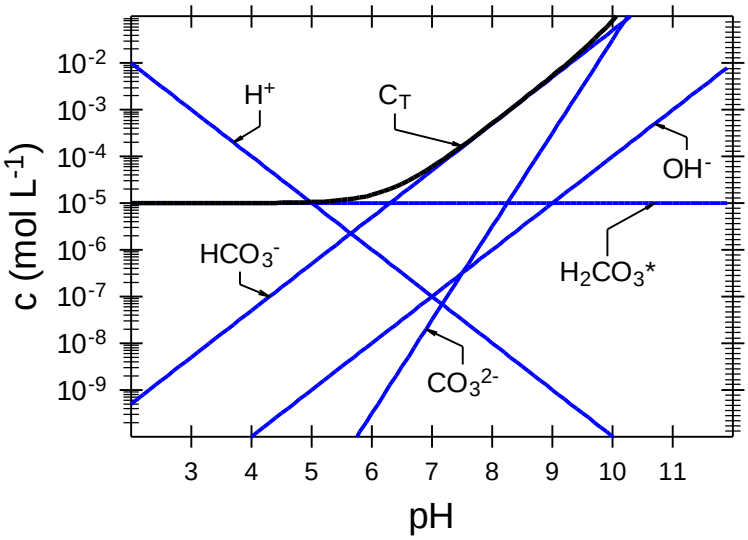

Figure 5.5: Calculated speciation of CO_2 as a function of pH in water at 25°C in an open system in equilibrium with air containing 350 ppmv of CO_2.

Comparison of Figures 5.4 and 5.5 shows considerable differences between the open and closed systems. The important reference point is the pH attained by pure water in equilibrium with air. This corresponds to the crossing point for H^+ and HCO_3^- on the diagram, since in pure water the dissociation of carbonic acid controls the pH

$$H_2CO_3^* \quad HCO_3^- + H^+ \qquad [5.51]$$

The pH at this point is 5.65, corresponding to a solution of zero alkalinity. At all pH values below this, the speciation remains dominated by $H_2CO_3^*$ and C_T. is constant. On the other hand, at higher pH, the importance of first HCO_3^- and then CO_3^{2-} increases progressively and C_T. increases. As expected from the equilibria involved, HCO_3^- dominates when pH > pK_1, except where pH > pK_2 when CO_3^{2-} is dominant.

Further Reading

W. Stumm and J.J. Morgan (1981). *Aquatic Chemistry: An Introduction Emphasizing Chemical Equilibria in Natural Waters.* Wiley and Sons, New York, Chapters 3 and 4.

Ingri, N., W. Kakoeowicz, L.G. Sillen, and B. Warnquist, High-speed computers as a supplement to graphical methods - V. Haltafall, a general program for calculating the composition of equilibrium mixtures , *Talanta, 14*, 1261-1286, 1967.

Chapter 6 Potentiometric Titrations of Acids & Bases

This chapter discusses the use of potentiometric titration methods for measuring neutralizing capacities of solutions such as alkalinity or acidity, and for the determination of acid-dissociation constants.

6.1 Introduction

In the previous chapter we saw that the pH of an aqueous solution containing a weak electrolyte could be calculated using an equation of the general form

$$c_A - c_B = \frac{h}{\gamma_H} - \frac{K_w}{h} + f(c_{HA}, h) \qquad [6.1]$$

We saw that the function f comprises terms containing the concentration of the weak electrolyte c_{HA} and one or more degree of dissociation terms α_i. The latter are themselves functions of the solution pH and the dissociation constant(s) for the weak electrolyte.

Experimentally, there is considerable interest in performing the reverse procedure. In other words, if measurements of the solution pH as a function of net added strong acid (or strong base) are made, is it possible to invert [6.1] so as to obtain experimental measurements of the weak electrolyte concentration c_{HA} or its dissociation constant(s)? The answer to this question is yes, provided a satisfactory method is available for measurement of pH. Generally this involves the use of a galvanic cell containing a H^+-sensitive glass electrode whose potential is measured during the titration. Such methods, termed potentiometric titrations, represent a powerful method for the determination of both concentrations (i.e. neutralizing capacities) and acid-dissociation constants.

We begin the analysis of this approach by looking at a theoretical titration curve for a simple monoprotic weak electrolyte.

6.2 Calculated pH Titration Curve for a Monoprotic Acid

As already mentioned, the general pH calculation technique introduced in Chapter 5 is ideal for the calculation of pH during an acid-base titration. Consider the example of a simple neutral weak acid electrolyte HA, for which the specific form of [6.1] is as follows

$$c_A - c_B = \frac{h}{\gamma_H} - \frac{K_w}{h} - c_{HA}\,\alpha_1 \qquad [6.2]$$

In the particular case of the titration of a solution of HA with standard alkali, c_A is zero as [6.2] can be expressed more conveniently as

$$c_B = c_{HA}\,\alpha_1 - \frac{h}{\gamma_H} + \frac{K_w}{h} \qquad [6.3]$$

In a titration, we are generally interested in the fraction f (where $f = c_B/c_{HA}$) of the analyte HA that has been titrated at each point. Recasting [6.3] in these terms, we obtain

$$f = \alpha_1 - \frac{h}{\gamma_H c_{HA}} + \frac{K_w}{h c_{HA}} \qquad [6.4]$$

This equation may be used to calculate the titration curve, pH as a function of *f*. Generally, experimental titration curves are represented in the form of pH *versus* volume, or amount, of the titrant. These are easily related to the parameters used in [6.3] and [6.4]. If v_o is the volume of the analyte (HA) solution, then after addition of a volume v of base, the concentration c_B in the combined analyte + titrant solution is

$$c_B = \frac{v}{v_0 + v} [\text{NaOH}] \qquad [6.5]$$

Calculation of *f* follows naturally once the analyte concentration c_{HA} is known (usually, this is one of the targets of the titration analysis). Figure 6.1 shows the calculated curve for 0.100 M acetic acid (pK_a = 4.76 at 25°C) titrated with NaOH of the same concentration. The curve shows the familiar appearance, with a sharp increase in pH at the equivalence point *f* = 1.

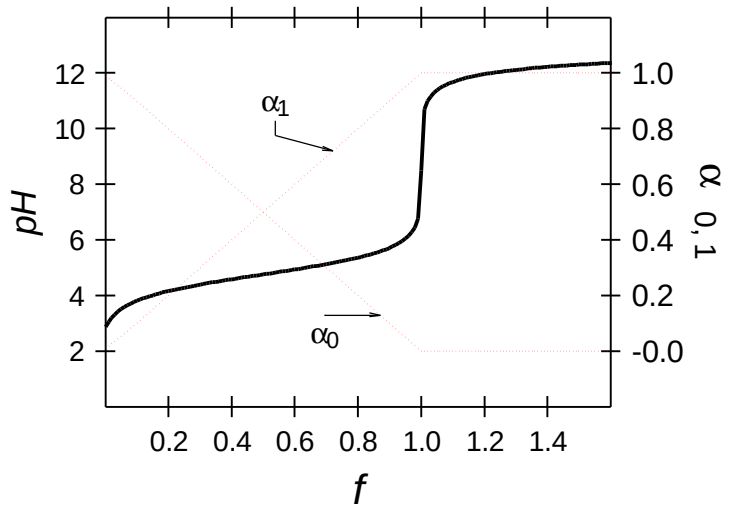

Figure 6.1: Calculated titration curve for 0.100 M acetic acid solution titrated with 0.100 M NaOH; also showing how the degrees of dissociation a_0 and a_1 (right vertical axis) depend on the fraction titrated.

The plots for the degrees of dissociation α_0 and α_1 in this example are almost linear, showing that the titration reaction

$$HOAc + OH^- \rightarrow OAc^- + H_2O \qquad [6.6]$$

proceeds more or less to completion after the addition of each aliquot of NaOH, with negligible "back-dissociation" of the conjugate base. Detailed examination shows some curvature very close to *f* = 1. We shall observe later that this linearity can be put to good use in determining the position of the equivalence point from experimental data.

6.3 Technique of Potentiometric Titration

The experimental technique used for potentiometric titration is fairly straightforward. Generally, the solution pH is measured using a cell of the type containing an H^+-responsive glass electrode with a suitable reference electrode:

$$\text{Ag, AgCl} \mid \text{KCl (sat)}, H^+ \text{ (ref)} \mid \text{glass} \mid H^+ \text{ (test)} \parallel \text{KCL (sat)} \mid \text{AgCl, Ag} \qquad [6.7]$$

If this cell is used in dilute solution and calibrated with NBS standard buffers, its response follows the Nernst-like equation

$$E = E_o - k\, pH_{NBS} \qquad [6.8]$$

Commonly, for the measurement of equilibrium constants, the test solution contains an excess of inert electrolyte to buffer changes in activity coefficients, and a concentration-based pH scale can be established:

$$E = E_o + k \log [H^+] \qquad [6.9]$$

where the $[H^+]$ term may refer to the free H^+ concentration, or a related scale such as total H^+ or the seawater scale (see Chapter 3). In some situations, it is useful to include in [6.9] a term representing the residual liquid junction potential ΔE_j.

As noted later, if the primary purpose of the titration is to determinethe concentration of the analyte, it is not always necessary to calibrate the electrode system in terms of a sensible pH scale, but rather to rely only on the changes in cell potential that take place.

The process of repeatedly adding aliquots of titrantto the analyte solution and recording the equilibrium cell potential is tedious, but is particularly easy to automate through the use of a small computer. Accordingly, *automatic titrators* have become quite commonplace in many laboratories. Both commercial models and those that have been custom-built for specific purposes, such as the alkalinity titration of seawater, are available.

6.4 Methods for Equivalence-Point Determination

In classical potentiometric titration analysis, the titration end-point is determined by one technique or other that is based on the rapid change in pH (or potential) that takes place at that point, as seen in Figure 6.1. A common approach is to calculate, by difference methods, the slope at each titre point and then determine the titre volume at which the slope ismaximum. Other techniques are based on the shape of the titration curve. While many of these classical methods are simple in nature, they are not particularly reliable and all suffer from some degree of systematic bias. They are difficult to apply in dilute solutions where the pH changes are small. In addition, they are difficult to automate, which is a shortcoming where the titration itself is under the control of a computer.

In the 1950's, the Swedish chemist Gran devebped the first systematic technique for location of equivalence points. His method is based on a simplified model for the changes taking place in the solution equilibria as titrant is added. While both powerful and useful, Gran's method languished in obscurity for several decades because it was difficult to apply conveniently before the advent of cheap electronic calculators in the 1970's followed by cheap personal computers about a decade later.

Gran's method is based on the assumption that a titration curve can be divided into characteristic regions, within each of which a single process can be assumed to dominate the control of solution pH. The basis for this is already clear in Figure 6.1, which shows that when f is less than unity, the degree of dissociation parameters change linearly with the amount of added base titrant. This is consistent with the view that reaction [6.6] dominates in this region. Similarly, when f exceeds unity, essentially all of the weak acid has been titrated and the solution pH is dominated by the buildup of unreacted hydroxide ions from the excess of NaOH added.

This view of events during the titration is confirmed by Figure 6.2 which shows the *amounts* of the various species as a function of the titrant volume. The amounts, rather than concentrations, of the species are used in the diagram to remove the effects of the dilution that occurs as the titrant volume increases, which is just a side issue.

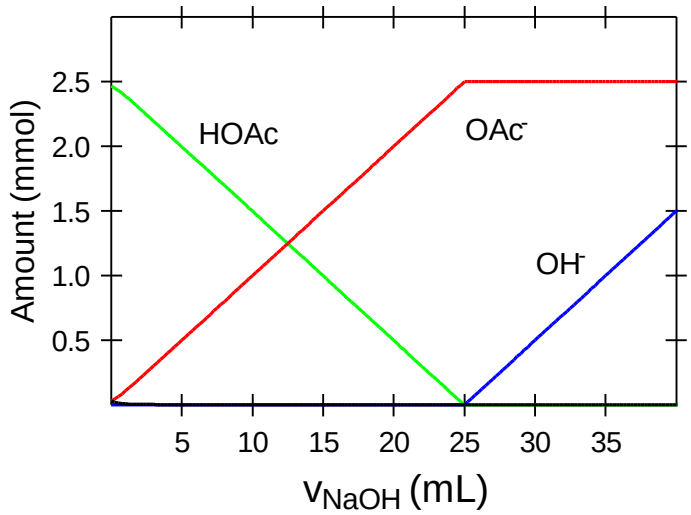

Figure 6.2: Calculated speciation for the titration of 25.00 mL of 0.100 M acetic acid solution with 0.100 M NaOH.

Figure 6.2 shows that when the titrant volume v is less than that required for equivalence v_e, the amount of analyte HA decreases linearly with volume while that of the conjugate base increases. On the other hand, when $v > v_e$, the amount of conjugate base remains constant (no more can form) and that of hydroxide ion begins to increase linearly.

The linear plots for both hydroxide ion and the weak acid are attractive, because they both cross the volume axis baseline at the equivalence point volume. This suggests that if we could use the experimental data to calculate the amounts of each species, we would obtain two independent methods for finding the value of the equivalence point volume.

In the case of the hydroxide ion, it is relatively simple to calculate the amount of OH^- from the experimental titration data by inverting the Nernst equation [6.9] as follows:

$$n_{OH} = [OH^-](v + v_0) = \frac{K_w}{[H^+]}(v + v_0)$$

$$[H^+] = 10^{+\frac{E-E_0}{k}} \qquad [6.10]$$

$$n_{OH} = K_w (v + v_0) 10^{-\frac{E-E_0}{k}}$$

As noted from Figure 6.2, the quantity n_{OH} should be a linear function of v in the post-equivalence point region $v > v_e$, and should extrapolate to a zero value on the horizontal volume axis at $v = v_e$. In fact, the situation is even simpler than this. Since we are interested only in where this straight line crosses the horizontal volume axis, we can remove any multiplying or dividing constants from [6.10], since these serve only to change the slope of the line, not its zero intercept. This is particularly convenient since it saves the bother of calibrating the glass electrode to measure pH.

Using this principle, [6.10] can be simplified by removing the terms in K_w and the cell constant E_o to give a *Gran function F* that is linearly related to volume:

$$F = (v + v_0) 10^{-E/k} \propto (v - v_e) \qquad [6.11]$$

In Gran's scheme, this function is based on the assumption that all of the hydroxide ions in the region $v > v_e$ derive from the stoichiometric excess of NaOH. Generally, this assumption is a good one, except very close to the equivalence point when hydroxide ions produced by the dissociation of the weak conjugate base need to be taken into account.

In the acidic region of the titration curve, reaction [6.6] is assumed to dominate the pH control of the solution. This assumption can be used to develop another Gran function, this time based on the amount of unreacted HA which also extrapolates to zero at the equivalence volume (Figure 6.2):

The amount of conjugate base produced at any titre volume v is

$$n_A = v\,[NaOH] \qquad [6.12]$$

At the equivalence volume, the amount of added NaOH is equivalent to the amount of weak acid in the original solution

$$v_e\,[NaOH] = v_o\,c_{HA} \qquad [6.13]$$

Thus the unreacted HA at any titre volume is

$$n_{HA} = v_o\,c_{HA} - n_A = [NaOH](v_e - v) \qquad [6.14]$$

Inserting these into the expression for the dissociation constant, we obtain

$$K_a = [H^+]\frac{n_A}{n_{HA}} = [H^+]\frac{v}{v_e - v} \qquad [6.15]$$

which easily rearranges to the linear form required

$$v\frac{[H^+]}{K_a} = (v_e - v) \qquad [6.16]$$

As with the previous example, we replace [H^+] by the inverted Nernst equation and drop out the multiplying constants to get the required Gran function

$$F = v10^{+E/k} \propto (v_e - v) \qquad [6.17]$$

Figure 6.3 shows a plot of both Gran functions for an experimental titration of acetic acid with NaOH superimposed on the original titration curve. Since the slope of the Gran functions is not important, each has been multiplied by an arbitrary constant to scale the data to a suitable range for the graph. It can be seen that for most of the volume range, the linear character expected of the two Gran functions is indeed found.

The two Gran functions do not cross the volume axis at exactly the same point, but show a small gap between them that is often interpreted as being due to the presence of impurities in the supporting electrolyte and/or NaOH solution. However, such a gap can also arise as an artifact because of non-linearity in the Nernstian response of the glass electrode.

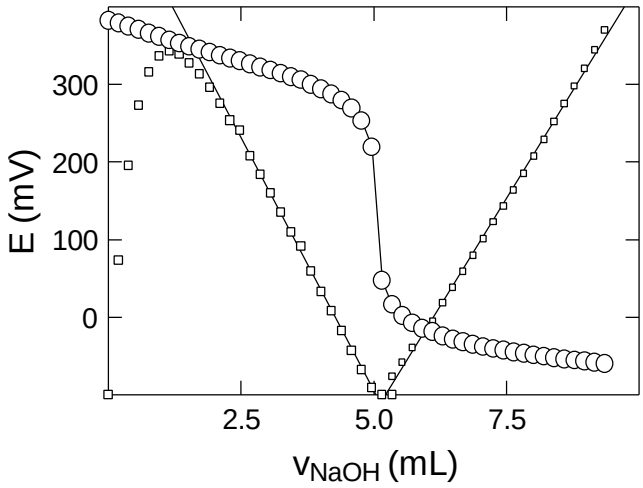

Figure 6.3: Experimental potentiometric titration curve for titration of 204.6 mL of 2.422 mM acetic acid solution with 0.09751 M KOH at 25°C in 0.7 M KCl supporting electrolyte; also shown are the two Gran functions calculated as described in the text. Drawn using data collected by Dr Lay Choo Chong.

Determination of the Dissociation Constant

The introductory treatment of Gran functions makes it clear how this approach can be generalized to also produce estimates of the acid dissociation constant. For the example in Figure 6.3, a separate calibration of the glass electrode used was carried out and the experimental parameters for the Nernst equation [6.9] were found to be as follows:

$$E_o = 596.29 \text{ mV}, \quad k = 59.162 \text{ mV} \qquad [6.18]$$

These values were then used, along with the measured cell potential E in the acidic region of the titration curve, to calculate $[H^+]$ by inverting the Nernst equation

$$[H^+] = 10^{+\frac{E-E_0}{k}} \qquad [6.19]$$

Values of the degree of acetic acid dissociation α_1 were calculated for the same titration points by assuming that in this region, all of the added NaOH is consumed by reaction with the weak acid, as suggested by Figure 6.1. Thus for any titre volume v

$$\alpha_1 = \frac{v}{v_e} \qquad [6.20]$$

where v_e is the equivalence point volume determined using the Gran function [6.17]. Finally, the $[H^+]$ and α_1 values are combined to calculate K_a

$$K_a = [H^+] \frac{\alpha_1}{1-\alpha_1} \qquad [6.21]$$

Figure 6.4 shows the calculated pK_a values as a function of titrant volume v calculated in this manner for the results in Figure 6.3. When the titre volume is less than 1 mL, corresponding to about 20% of the acetic acid titrated, the calculated pK_a values are not particularly constant, but become so in the range $1 < v < 5$ mL. Ignoring the first 6 points, the calculated pK_a has a standard error of only 0.1%, which is very good.

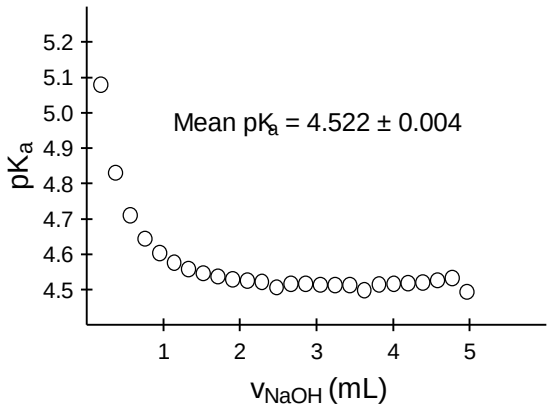

Figure 6.4: Experimental pK_a values for acetic acid at various titre volumes calculated using the data in Figure 6.3.

6.5 Determination of K_w for water

The self-dissociation constant for water can be conveniently determined by means of a potentiometric titration involving a strong acid (e.g. HCl) and a strong base (e.g. NaOH). Usually, the measurements are made in the presence of a large excess of inert supporting

electrolyte that minimizes changes in the activity coefficients. In this situation, the constant ionic medium convention can be used and the glass electrode system calibrated in terms of hydrogen ion concentration in the acidic region of the titration where the concentration of H^+ is known. Once the electrode is calibrated, it may be used to determine $[H^+]$ indirectly, from the cell potential, in the alkaline region of the titration curve. This value, combined with the concentration of OH^-, which is known from the amount of excess NaOH added, finally yields the measurement of K_w.

We now follow this brief outline of the method in more detail using some actual data. Figure 6.4 shows the titration data, cell potential E as a function of titrant volume v, for titration of 75.591 mL of NaOH solution in 0.7 M NaCl supporting electrolyte using 0.1000 M standard HCl as the titrant. The titration curve shows the expected shape, with a sharp increase in potential at the equivalence point.

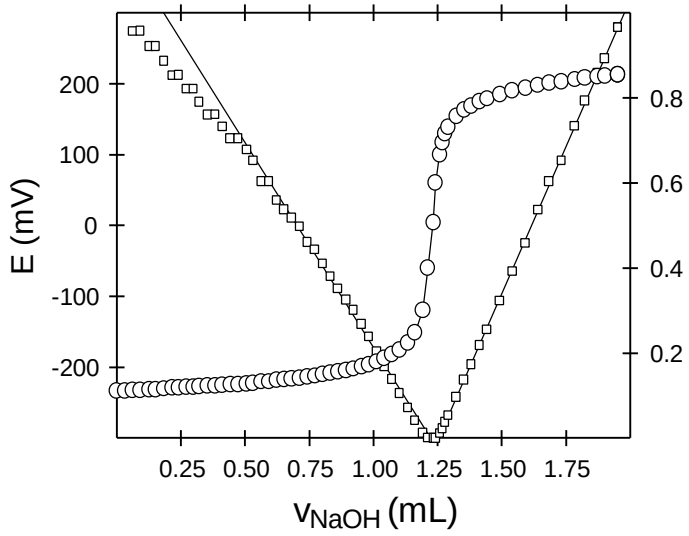

Figure 6.4: Experimental potentiometric titration curve for NaOH in 0.7 M NaCl solution (v_0 = 75.591 mL) titrated with 0.100 M HCl at 25°C; also shows the two Gran functions calculated as described in the text. Drawn using data collected by Dr Lay Choo Chong.

Locating the Equivalence Points using Gran Functions

The first step in analyzing these results is to determine the equivalence point volume using Gran functions. This follows the treatment outlined in the previous section. In the right-hand part of the curve, where excess HCl is present, we make the assumption that thepH of the analyte solution is dominated by the stoichiometric excess of HCl. Thus, the amount of H^+ should vary linearly with titrant volume v and extrapolate to zero at the equivalence point volume v_e

$$n_{\mathrm{H}} = [\mathrm{H}^+](v + v_0) \propto (v - v_e) \qquad [6.22]$$

Applying the inverted Nernst equation and dropping out multiplying constants, we obtain the Gran function

$$F = (v + v_0)10^{+E/k} \propto (v - v_e) \quad [6.23]$$

Note that this is the same as [6.11] for excess NaOH in the acetic acid titration, except for sign of the exponential term.

This Gran function is superimposed on Figure 6.4 to the right of the diagram. Fitting a least-squares regression line through the data gives the following value for the equivalent volume (symbolized v_2):

$$v_2 = 1.254 \pm 0.008 \text{ mL} \quad [6.24]$$

In the first part of the titration curve, the NaOH analyte is present in excess. Thus for this region, we make the assumption that the excess OH^- controls the solution pH. Accordingly, the Gran function for this region is proportional to the amount of excess OH^- and extrapolates to zero at the equivalence volume

$$F = (v + v_0)10^{-E/k} \propto (v_e - v) \quad [6.25]$$

Figure 6.4 also shows this Gran function superimposed on the left of the titration curve. Its linearity is rather worse that the excess acid Gran function [6.23], but a satisfactory straight line can still be drawn through the later points to estimate the equivalence volume v_1

$$v_1 = 1.221 \pm 0.023 \text{ mL} \quad [6.26]$$

Notice that the two estimates of the equivalence volume do not coincide, but that v_1 (excess base) is slightly less that v_2 (excess acid). This difference is usually ascribed to the presence of impurities in the NaOH and NaCl electrolyte. The concentration of the impurity can be calculated from the difference between the two volumes:

$$\begin{aligned} c_{\text{IMP}} &= \frac{v_2 - v_1}{v_0}[\text{HCl}] \\ &= \frac{1.254 - 1.221}{75.591} \times 0.1000 \\ &= 0.044 \pm 0.043 \text{ mmol L}^{-1} \end{aligned} \quad [6.27]$$

The error in this estimate is rather large because it is the difference between two quantities of similar magnitude.

Calibrating the Glass Electrode

Next, we use the equivalence volume v_2, after which all bases have reacted, to calculate the stoichiometric excess of H^+ in the solution. For any titrant volume $v > v_2$

$$[H^+] = \frac{(v - v_2)}{(v + v_0)}[\text{HCl}] \quad [6.28]$$

These values are then used to construct a graph of cell potential E *versus* –log $[H^+]$ according to equation [6.9] to estimate the constant terms E_o and k of the Nernst equation. This is illustrated in the left graph of Figure 6.5 below.

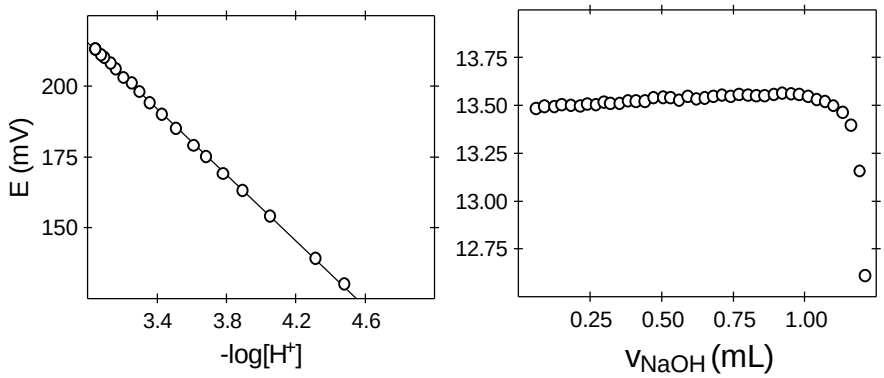

Figure 6.5: The left graph shows a plot of the Nernst equation for points taken from the acidic region ($v > v_2$) of the titration curve in Figure 6.4. The right graph shows values of pK_w calculated from points in the alkaline region of the curve, $v < v_1$.

The least-squares regression line fitted through these results gives the following estimates for the Nernst equation parameters

$$E_o = 390.40 \pm 0.85 \text{ mV}$$
$$k = 58.34 \pm 0.24 \text{ mV} \qquad [6.29]$$

Calculating $[H^+]$, $[OH^-]$ and K_w

The values for E_o and k calculated in [6.29] may now be used to calculate $[H^+]$ in the alkaline region of the curve $v < v_1$ directly from the measured E values:

$$[H^+] = 10^{+\frac{E-E_0}{k}} \qquad [6.30]$$

At the same time, $[OH^-]$ can be estimated from the stoichiometric excess of NaOH in this region of the curve:

$$[OH^-] = \frac{(v_1 - v)}{(v + v_0)}[HCl] \qquad [6.31]$$

Finally, the independent estimates for $[H^+]$ and $[OH^-]$ for each point in the alkaline region are multiplied together to obtain K_w

$$K_w = [H^+][OH^-] \qquad [6.32]$$

The right-hand graph in Figure 6.5 shows the point-by-point values obtained for pK_w using this method. There is a slight drift towards higher pK_w as the volume increases, which suggests that the Nernst equation calibration is probably not exactly right. Near v_1 the calculated value of pK_w drops sharply as the impurity is being titrated. The final result, ignoring the few points near v_1, is obtained by averaging the point-by-point results:

$$pK_w = 13.5221 \pm 0.0054 \qquad [6.33]$$

This particular potentiometric titration technique has been widely used for the determination of pK_w for seawater media.

6.6 Determination of K_1 and K_2 for Carbon Dioxide

The acid dissociation constants K_1 and K_2 for this diprotic acid (see Chapter 3) can be readily determined using a titration of Na_2CO_3 with standard HCl as titrant.

$$K_1 = [H^+]\frac{[HCO_3^-]}{[H_2CO_3^*]} = [H^+]\frac{\alpha_1}{\alpha_0}$$
$$K_2 = [H^+]\frac{[CO_3^{2-}]}{[HCO_3^-]} = [H^+]\frac{\alpha_2}{\alpha_1} \qquad [6.34]$$

Since the CO_2 partial pressure becomes quite large near the end of this titration, as the solution becomes acidic, CO_2 gas is likely to escape from the titration solution. Therefore for the best work, it is important to use a sealed titration vessel to avoid CO_2 loss.

The principles of this technique are similar to the K_w example already discussed, except that impurities are usually ignored. Gran functions are used to locate the two equivalence points corresponding to the titration reactions:

$$CO_3^{2-} + H^+ \rightarrow HCO_3^- \quad (v_1) \qquad [6.35a]$$
$$HCO_3^- + H^+ \rightarrow H_2CO_3^* \quad (v_2) \qquad [6.35b]$$

Next, the known stoichiometric excess of HCl in the acidic region $v > v_2$ is used to calibrate the glass electrode system, after which $[H^+]$ for the other regions of the curve $v < v_2$ can be calculated from the measured potential E using the Nernst equation. This provides the $[H^+]$ values in [6.34. Finally, the degrees of dissociation α_0, α_1 and α_2 are calculated from the equivalence point volumes derived earlier.

Figure 6.6 shows an experimental titration curve for this system, with the two Gran functions superimposed. The Gran function for excess acid $v > v_2$ is identical in form to that used in the K_w experiment

$$F_2 = (v + v_0)10^{+E/k} \propto (v - v_2) \qquad [6.36]$$

This plot, on the right of Figure 6.6, is reasonably linear except near to v_2 itself. Using least-squares linear regression, a result of v_2 = 0.3321 ± 0.0045 mL was calculated.

Two possibilities exist for locating the other equivalence volume v_1. The method shown in Figure 6.6 is derived from the assumption that in the intermediate region $v_1 < v < v_2$ the main process consuming the titrant HCl is reaction [6.35b]. In this case, the amount of $H_2CO_3^*$ generated at any titre volume v is proportional to the amount of HCl added in excess of that required to reach the first equivalence volume, i.e. that used for reaction [6.35a].

$$n_{H_2CO_3} = (v - v_1)[HCl] \qquad [6.37]$$

Conversely, the amount of unreacted HCO_3^- is proportional to the HCl still required to complete reaction [6.35b], i.e. the volume required to reach v_2

$$n_{HCO_3} = (v_2 - v)[HCl] \qquad [6.38]$$

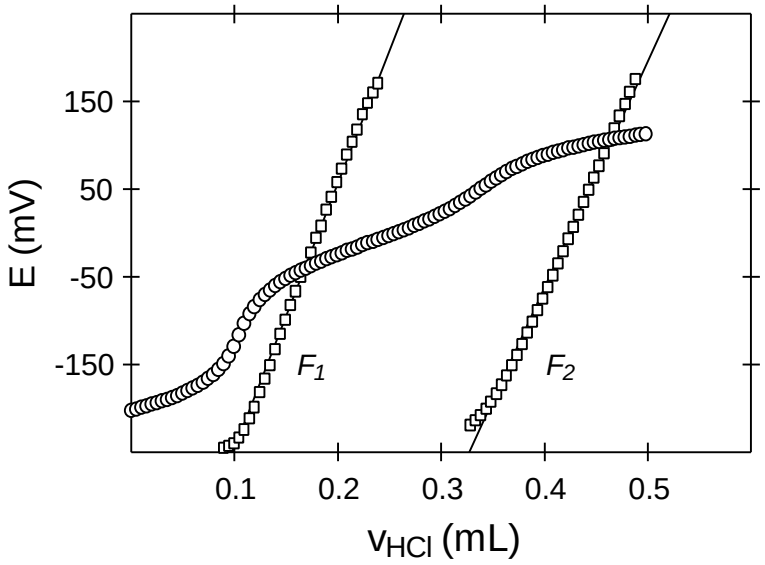

Figure 6.6: Experimental titration curve for the titration of 120.00 mL of Na_2CO_3 solution containing 0.7 M NaCl supporting electrolyte with 0.1000 M standard HCl. The two Gran functions discussed in the text. Drawn using data collected by students in the Chemistry 336 class, University of Otago.

Inserting both of these into the expression for the first dissociation constant, we obtain

$$K_1 = [H^+]\frac{[HCO_3^-]}{[H_2CO_3^*]} = [H^+]\frac{(v_2 - v)}{(v - v_1)} \qquad [6.39]$$

This is readily rearranged, after dropping out multiplying constants, to the required Gran function for estimating v_1

$$F_1 = (v_2 - v)10^{+E/k} \propto (v - v_1) \qquad [6.40]$$

Note that the previously obtained value for v_2 is required to calculate the Gran function. The plot of F_1 shown on the left of Figure 6.6, is reasonably linear except near to v_1 itself. Using least-squares linear regression, a result of $v_1 = 0.1019 \pm 0.0013$ mL was calculated.

Once v_1 is obtained, equation [6.39] then allows calculation of K_1 from the titration points in the same region $v_1 < v < v_2$. Equivalently, one may calculate the relevant α_i terms directly and then use these to calculate K_1.

$$\alpha_0 = \frac{(v - v_1)}{(v_2 - v_1)} \qquad \alpha_1 = \frac{(v_2 - v)}{(v_2 - v_1)} \qquad [6.41]$$

The results of this calculation are shown in the left-hand graph of Figure 6.7 below. Except near the extremes of the region concerned, i.e. near v_1 and v_2, the calculated pK_1 values agree very well at different volumes. A final result of $pK_1 = 6.039 \pm 0.005$ was obtained.

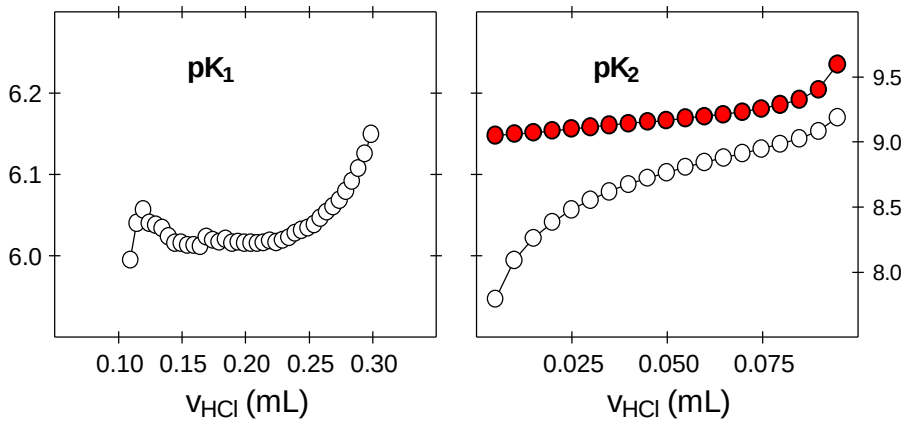

Figure 6.7: The left-hand graph shows values of pK_1 calculated from the experimental titration data in Figure 6.6 for the region $v_1 < v < v_2$. The open circles in the right-hand graph show the corresponding values calculated in the region $v < v1$ for pK_2 using equation [6.44], while the solid circles show pK_2 values corrected for the presence of hydroxide ion.

In the region $v < v_1$ we assume that reaction [6.35a] is now dominant. In this case, we can equate the amount of HCO_3^- formed to the amount of added HCl

$$n_{HCO_3} = v[HCl] \qquad [6.42]$$

and the amount of unreacted CO_3^{2-} to the quantity of HCl needed to reach v_1

$$n_{CO_3} = (v_1 - v)[HCl] \qquad [6.43]$$

These two are then inserted into the expression for K_2 in a similar way to K_1

$$K_2 = [H^+]\frac{[CO_3^{2-}]}{[HCO_3^-]} = [H^+]\frac{v}{(v_1 - v)} \qquad [6.44]$$

In terms of the α's

$$\alpha_1 = \frac{v}{v_1} \qquad \alpha_2 = \frac{(v_1 - v)}{v_1} \qquad [6.45]$$

The right graph in Figure 6.7 shows the values of pK_2 calculated using [6.44] as open circle symbols, Unlike with pK_1 earlier, these results do not look very good. There is a consistent increase in the apparent pK_2 value with volume of more than +1 log unit (factor of 10) across the volume range.

The reason for this discrepancy is the assumption that the single reaction [6.35a] dominates the consumption of the HCl titrant is unrealistic. This can be seen by using the results of a theoretical calculation of the speciation during this titration. The calculation method required was outlined in Section 5.4 and makes use of equation [5.26]. The results are shown in Figure 6.8 below.

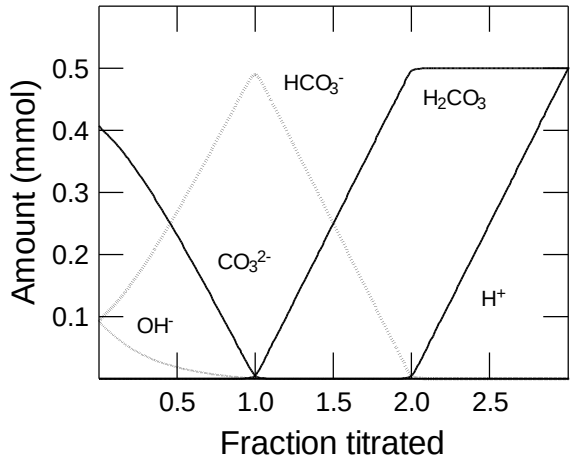

Figure 6.8: Calculated speciation for the titration of 0.5 mmol of Na_2CO_3 with HCl.

The calculated results show that reaction [6.35a] between CO_3^{2-} and the added HCl is not the only reaction consuming H^+ ions. In fact, substantial amounts of OH^- are also reacting. This OH^- is generated by the dissociation of the carbonate ion

$$CO_3^{2-} + H_2O \rightarrow HCO_3^- + OH^- \qquad [6.46]$$

Accordingly, the assumptions used to derive [6.42] and [6.43] are incorrect. The true bicarbonate ion concentration will be *higher* than that predicted by [6.42], and the corresponding carbonate ion concentration will be *lower* than that predicted by [6.43]. In this situation, the calculated value of K_2 will be made too low (pK_2 too high) by both factors. Notice that in the vicinity of the second equivalence point, the simple assumptions used to derive K_1 look to be quite valid.

The observations made from Figure 6.8 suggest a strategy for modifying the equations used to derive K_2. Firstly, [6.42] is modified so that the concentration of bicarbonate is now the sum of that produced by the titration reaction [6.35a] and that produced by the dissociation reaction [6.46]. The latter can be equated to $[OH^-]$, which is calculated from $[H^+]$ and the K_w value for this electrolyte, as reported in Section 6.5 ($pK_w = 13.522$).

$$[HCO_3^-] = \frac{v}{v_0 + v}[HCl] + \frac{K_w}{[H^+]} \qquad [6.47]$$

Similarly, equation [6.43] for the amount of unreacted CO_3^{2-} needs to be modified to include the carbonate ion lost by dissociation

$$[CO_3^{2-}] = \frac{v_1 - v}{v_0 + v}[HCl] - \frac{K_w}{[H^+]} \qquad [6.48]$$

The solid circle symbols in Figure 6.7 show the values of pK_2 calculated using these modified equations. The variation in the corrected values is comparable to that seen for pK_1, and can be regarded as acceptable. A final result of $pK_2 = 9.199 \pm 0.031$ was obtained. Later in this chapter we will look at a more sophisticated method for deriving the equilibrium constants, and

other data, from such titration curves that does not involve the simple assumptions used in the Gran function approach.

This example also illustrates the value of simple calculation methods for assessing how to interpret experimental titration data.

6.7 The Alkalinity of Fresh Waters

As mentioned in Section 5.6, pure water in equilibrium with air at 25°C has a pH of about 5.6 and zero alkalinity. Rain water in remote areas often has a CO_2 composition close to this, although less remote rain also contains other acidic materials, especially nitric and sulfuric acids. However, most surface fresh waters (rivers, lakes and ponds) have a substantially higher pH and alkalinity, while ground waters can be very alkaline.

This alkalinity arises from acid-base reactions between CO_2-containing water and basic minerals such as limestone

$$CaCO_3 + H_2O + CO_2 \rightarrow Ca^{2+} + 2\ HCO_3^- \qquad [6.49]$$

and aluminosilicate

$$NaAlSi_3O_8 + CO_2 + 6.5H_2O \rightarrow Na^+ + 2HCO_3^- + 2H_4SiO_4 + \tfrac{1}{2}Al_2Si_2O_5(OH)_4$$

(albite) *(kaolinite)* [6.50]

Reaction [6.49] follows the stoichiometry indicated, but occurs both for pure $CaCO_3$ limestone and for magnesium containing analogues such as magnesian calcite and dolomite.

Reaction [6.50] is *archetypal*, i.e. it is meant to represent the kind of reaction involved in aluminosilicate weathering. Other mineral compositions, and cations other than Na^+, are involved.

These weathering reactions are responsible for both the alkalinity and the cationcontent of most natural waters. The latter follows both from the role of cations in the weathering reactions written above, and from the fact that these ions balance the negative charge of the carbonate and bicarbonate anions in the charge balance equation. For a typical natural water, this charge balance condition would be expressed as

$$\Sigma+ = [Na^+] + [K^+] + 2[Mg^{2+}] + [Ca^{2+}] + [H^+] + \ldots \quad \text{(total cation charge)}$$

$$\Sigma- = [Cl^-] + 2[SO_4^{2-}] + [HCO_3^-] + 2[CO_3^{2-}] + [OH^-] + \ldots \quad \text{(total cation charge)}$$

In most river and lake waters, the carbonate and bicarbonate terms dominate the total anion charge, in other words that alkalinity is close to the total anion charge in magnitude. In this situation, the alkalinity is also close to the total charge contributed by cations derived from weathering. The anion charge in seawater, on the other hand, is dominated by the first two ions listed, chloride and sulfate, both of which are derived from volcanic gases (HCl, SO_2). The cations that balance their charge are therefore not directly involved in the weathering reactions shown in [6.49] and [6.50].

The alkalinity of fresh waters is normally measured by titration with standard acid, and potentiometric methods using Gran functions offer very good precision and accuracy. The low ionic strength of most river and lake waters means that in an untreated water sample, substantial changes in the activity coefficients of the ions involved in the titration reactions will normally take

place, and this can confuse the use of Gran functions by causing substantial curvature. Therefore, it is useful to add some inert electrolyte, e.g. KCl, to buffer the ionic strength of the sample before carrying out the titration. Provide that care is taken to ensure that the inert electrolyte is free of acidic or basic impurities, its addition to the sample will not change either the alkalinity of the C_T. It will, however, change the pH, so initial pH measurements should be made on the original water sample before addition of the electrolyte.

The Gran functions used to locate the equivalence points in the alkalinity titration are identical to those discussed in the previous section for titration of Na_2CO_3 solution by HCl. There are 2 equivalence points. The first corresponds to the conversion of CO_3^{2-} to HCO_3^- (denoted v_1), and has the Gran function given earlier as [6.40]

$$F_1 = (v_2 - v)10^{+E/k} \propto (v - v_1) \qquad [6.51]$$

The second, denoted v_2, corresponds to the complete reaction of HCO_3^- to form H_2CO_3 and has the Gran function seen several times before

$$F_2 = (v + v_0)10^{+E/k} \propto (v - v_2) \qquad [6.52]$$

This equivalence point corresponds, of course, to the alkalinity, which may therefore be calculated from the v_2 value obtained using [6.52], the known concentration of the HCl and the volume v_0 of water sample taken for titration:

$$\text{Alk} = \frac{v_2}{v_0}[\text{HCl}] \qquad [6.53]$$

The first equivalence point v_1 is often very close to zero and difficult to measure reliably. In many cases, especially with water samples that have been left open to the atmosphere, the value of v_1 is actually *negative*. What this means is that the carbonate ions in the water have undergone reaction with CO_2, and possibly other acidic materials, so that the sample has been effectively "titrated" past the first equivalence point when it is subjected to the alkalinity titration.

In the case where the sample contains sufficient carbonate that v_1 is positive and can be measured, we can identify it with the original $[CO_3^{2-}]$:

$$[CO_3^{2-}] = \frac{v_1}{v_0}[\text{HCl}] \qquad (v_1 > 0) \qquad [6.54]$$

If we assume that the contributions of $[H^+]$ and $[OH^-]$ to the measured alkalinity can be neglected, which is usually reasonable, we can use this result to calculate the bicarbonate ion concentration

$$\begin{aligned}[HCO_3^-] &\approx \text{Alk} - 2[CO_3^{2-}] \\ &= \frac{v_2 - 2v_1}{v_0}[\text{HCl}]\end{aligned} \qquad [6.55]$$

The remaining composition parameters $[H_2CO_3^*]$ and C_T can then be estimated from these values and the pH of the water using an appropriate value of the dissociation constant for carbonic acid K_1.

In the case where v_1 is negative, its value can be used to estimate [H_2CO_3*]

$$[H_2CO_3^*] = \frac{-v_1}{v_0}[HCl] \qquad (v_1 < 0) \qquad [6.56]$$

Moreover, since in this case the water contains negligible carbonate, the alkalinity may be directly identified with [HCO_3^-].

Figure 6.9 shows an example of an alkalinity titration of a lake water sample with the two Gran functions superimposed.

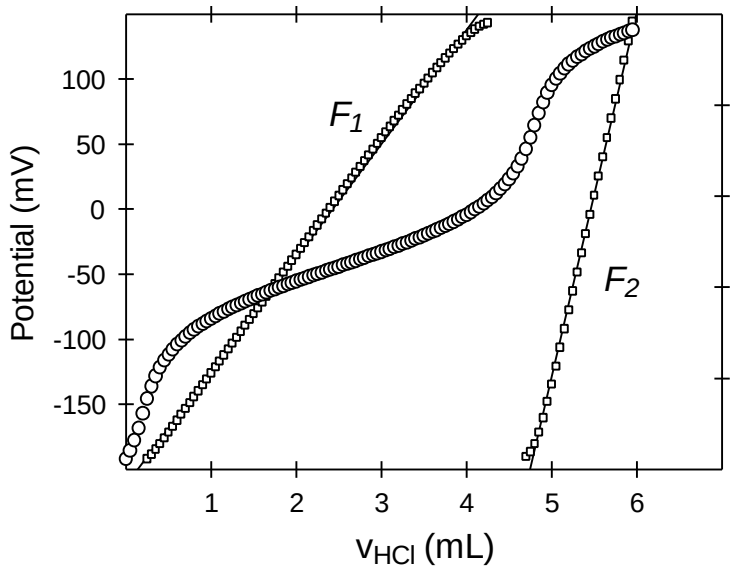

Figure 6.9: Alkalinity titration of 200 mL of lake water with 0.100 M HCl at 25°C after addition of 10 mM KCl as inert electrolyte recorded using an automatic titrator. Also shown are the Gran functions F_1 and F_2 corresponding to equations [6.51] and [6.52]. Drawn using data collected by the author.

From a least-squares regression analysis of the two Gran functions, the following values were calculated for the equivalence volumes:

v_1 = 0.1744 ± 0.0025 mL

v_2 = 4.757 ± 0.086 mL [6.57]

From these, the composition parameter values are obtained:

Alk = 2.378 ± 0.043 mM

CO_3^{2-} = 0.0872 ± 0.0012 mM

HCO_3^- = 2.204 ± 0.040 [6.58]

6.8 The Alkalinity of Sea Water

The simple scheme based on Gran functions for the evaluation of alkalinity does not work very well for seawater because this medium contains a number of other weak electrolytes that contribute measurably to the alkalinity.

Figure 6.9 shows the results of an alkalinity titration of sea water made under similar conditions to that if the lake water in Figure 6.8, except that because the ionic strength of sea water is naturally quite high, a supporting electrolyte does not need to be added.

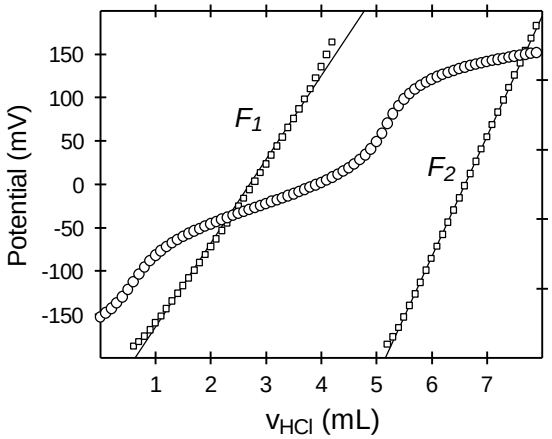

Figure 6.9: Alkalinity titration of 200 mL of seawater with 0.100 M HCl at 25°C recorded using an automatic titrator. Also shown are the Gran functions F_1 and F_2 corresponding to equations [6.51] and [6.52]. Drawn using data collected by the author.

The Gran function F_2 on the right of the diagram corresponding to excess HCl in equation [6.52] is reasonably linear, but shows some curvature near the corresponding equivalence point. Although some of the first points can be ignored in fitting the best-fit line, this procedure is not very systematic. Moreover, detailed examination of cases like this shows considerable variation in the results depending on the choice of points that are included. While it is not very obvious from the diagram, the Gran function is noticeably curved.

The Gran function F_1 on the left of the diagram corresponding to equation [6.51] is markedly curved throughout its valid volume range, and it is difficult to see how a reliable estimate of the equivalence point can be obtained.

These problems arise because seawater contains other acids and bases that participate in the titration reactions. Many of these were mentioned in this context in Chapter 4.They include the weak base borate, and the acidic species bisulfate and hydrofluoric acid. As mentioned in Chapter 4, phosphate and silicate can also contribute, although the water sample examined in the present example contains very low concentrations of both these species.

We recall that alkalinity is defined as the ANC of the water with respect to the reference proton condition of pure H_2CO_3. In this situation, the full definition of the alkalinity for seawater must include the abovenamed species. The following definition, which achieves this aim, was suggested by Dr Andrew Dickson:

$$A_T = [HCO_3^-] + 2[CO_3^{2-}] + [OH^-] - [H^+] + [B(OH)_4^-] + [HPO_4^{2-}] + 2[PO_4^{3-}] + [SiO(OH)_3^-] - [HSO_4^-] - [HF] - [H_3PO_4] \quad [6.59]$$

The first line contains the usual alkalinity components seen in earlier definitions. The second line contains the bases specific to seawater that are stronger than HCO_3^-, while the third line contains the corresponding acids stronger than H_2CO_3. Two additional species could also be included, NH_3 and HS^-, but these are normally not significant in most seawaters.

Equation [6.59] defines what is termed the *total alkalinity* A_T of seawater. The effect of these minor constituents can be examined by using this equation, together with the relevant equilibrium constants and mass-balance conditions, to calculate the speciation of the seawater system during the titration. For this, zero concentration of phosphate and silicate were assumed, while the concentrations of the other minor species in [6.59] were calculated using the information presented in Chapter 4.

Figure 6.10 shows the calculated seawater speciation near the first equivalence point v_1 obtained by this method.

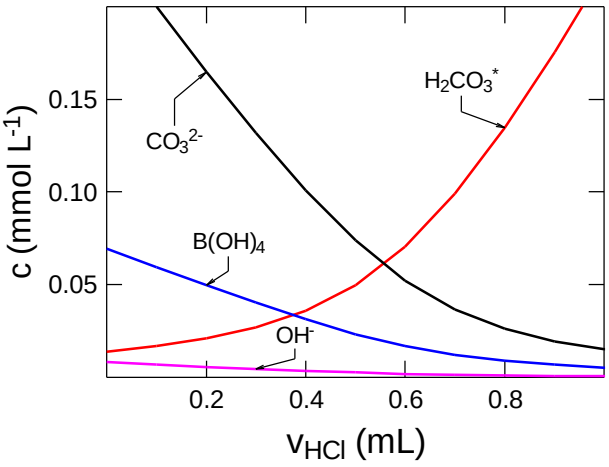

Figure 6.10: Calculated seawater speciation near the first equivalence point v_1 for the alkalinity titration of sea water, as shown in Figure 6.9.

In interpreting Figure 6.10, we recall that the simple assumption of the Gran function for locating v_1 is that for $v < v_1$ the added HCl is consumed through reaction with carbonate ions, which are all titrated at exactly $v = v_1$.

$$CO_3^{2-} + H^+ \rightarrow HCO_3^- \quad (v_1) \quad [6.60a]$$

After this ($v > v_1$), the added HCl reacts only with bicarbonate ions to form H_2CO_3*

$$HCO_3^- + H^+ \rightarrow H_2CO_3^* \quad (v_2) \quad [6.60b]$$

Therefore, this idealized situation should see the amount of CO_3^{2-} decrease linearly to zero at $v = v_1$, after which the amount of H_2CO_3* should increase linearly from zero. Inspection of Figure 5.10 shows that this is far from the case[4]. CO_3^{2-} continue to be titrated well after $v = v_1$, and H_2CO_3* is produced well before, i.e. HCO_3^- begins to be titrated *before* all of the CO_3^{2-} has reacted[5].

In addition to these features, which arise from the properties of the CO_2 species, it is apparent that both the borate ion and, to a lesser extent, free OH^- are also measurably titrated in the region $v < v_1$. For most of this region, about 1/3 of the HCl is consumed by reaction with borate ion.

It follows that the derivation ofthe Gran function F_1 in [6.51] is not valid in seawater media and will not give reliable results.

Figure 6.11 shows the calculated seawater speciation near the second equivalence pointv_2 obtained by the same calculation method as Figure 6.11.

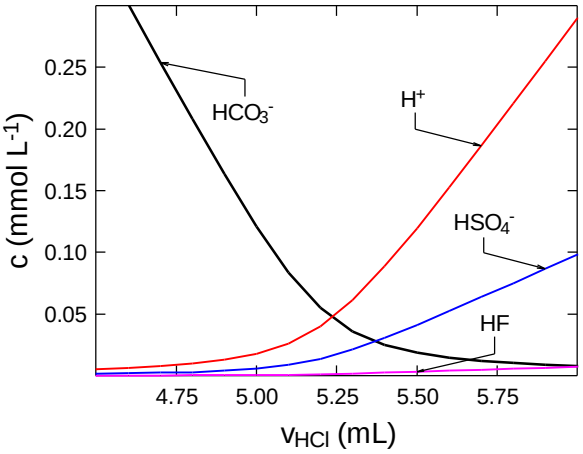

Figure 6.11: Calculated seawater speciation near the second equivalence point v_2 for the alkalinity titration of sea water, as shown in Figure 6.9.

In deriving the Gran function F_2 for this equivalence point, equation [6.52], the simplifying assumption was made that reaction [6.30b] continues to completion at $v = v_2$, after which all bases have reacted and excess free H^+ builds up in solution. Thus, the amount of HCO_3^- should decrease linearly to reach zero at $v = v_2$, after which the amount of free H^+ should increase linearly from zero.

---

[4] Although Figure 6.10 uses *concentration*, rather than amount, and is therefore affected by dilution as the titrant is added, the volume changes are very small because of the large sample volume (200 mL).

[5] This problem is common to all diprotic acids. The two reactions overlap measurably unless the pK_a values differ by more than about 4 log units.

Reference to the Figure shows that this is far from the case. HCO_3^- ions continue to be titrated well after $v = v_2$ and free H^+ ions appear in the solution well before. In addition, a significant quantity of HSO_4^- is formed near $v = v_2$, and lesser amount of HF, showing that the bases sulfate and fluoride ion are also reacting with the titrant.

Accordingly, the assumptions involved in deriving the second Gran function F_2 are also invalid. Comparison of the two speciation curves suggests that the discrepancies are rather less severe in the case of the Gran function for v_2 than they are for that required to calculate v_1. This is in agreement with the curvature seen in the experimental titration curve, Figure 6.9.

6.9 Multi-Parameter Methods

The shortcomings of the simple Gran functions method seen in the previous section for the seawater alkalinity titration is only one example of the limitations that this approach has in solutions containing more than one or two components. Its primary weakness is the necessity to assume that in each region of the titration curve, a single process is responsible for control of solution pH. In this context, the Gran function method is the analogue of the simple methods used to calculate the composition of an equilibrium system. Neither is generally applicable.

We have already seen, in Chapter 5, that it is possible to set up a simple general procedure for calculating the pH, and other composition parameters, for any acid-base equilibrium system using an equation of the type

$$c_A - c_B = \frac{h}{\gamma_H} - \frac{K_w}{h} + f(c_{HA}, h) \qquad [6.61]$$

A general approach to analyzing potentiometric titration data would involve *inverting* this equation, i.e. taking measured values of the hydrogen ion activity h (or equivalently, the potential of the H^+-sensitive electrode system) and using them to calculate the equilibrium constants and component concentrations that would normally be used as input parameters in [6.61]. This general approach is made possible by the ready availability of personal computers, which make it simple and convenient to carry out the extensive numerical fitting required. Because these methods involve estimation of more than one parameter at a time, they are often termed *multi-parameter methods.*

The multi-parameter approach will be illustrated using the example of the titration used to determine K_w in Section 6.5. In this case, the applicable version of [6.61] is

$$c_A - c_B = \frac{h}{\gamma_H} - \frac{K_w}{h} + c_{INP}\alpha_1^{INP} \qquad [6.62]$$

in which allowance has been made for the presence of an unknown impurity INP whose total concentration is c_{INP}. Both this concentration and the dissociation constant K_{INP} will be regarded as unknown parameters that need to be evaluated. The example presented in Section 6.5 uses the constant ionic medium, so that γ_H is unity and h can be identified with the free H^+ concentration:

$$c_A - c_B = [H^+] - \frac{K_w}{[H^+]} + c_{INP}\frac{K_{INP}}{K_{INP} + [H^+]} \qquad [6.63]$$

where α_1 has been expanded to its full form.

The values of $[H^+]$ at each titre point will be linked to the potential measurements using the Nernst equation presented earlier as [6.9]. In the general case, the residual liquid junction potential ΔE_j is included in these calculations in the form of a term proportional to $[H^+]$

$$E = E_o + k \log [H^+] + j_H [H^+] \qquad [6.64]$$

Where the constants E_o, k and j_H in this equation will be assumed unknown, so they must also be evaluated by our procedure (this was also the case with the Gran function method).

Finally, as with the Gran function method, we shall regard the concentration of NaOH in the original solution and K_w also as unknown parameters.

We should also note that for each titre volume *v*, the concentrations of strong acid and strong base in the solution must be calculated by accounting for dilution

$$c_A = \frac{v}{v + v_0} [HCl]$$
$$c_B = \frac{v_0}{v + v_0} [NaOH] \qquad [6.65]$$

where v_0 is the original volume of NaOH solution taken for titration.

Calculation Procedures

There are a number of different ways for calculating the required unknown parameters. One general procedure is as follows:

1 Estimate reasonable starting values for the unknown parameters: [NaOH], K_w, c_{INP}, K_{INP} and the Nernst constants E_0 and k.

2 For each titre point *v*, use these values to solve [6.63] for the pH of the solution at that point.

3 Use the calculated pH value to calculate an estimate of the potential E_{calc} using the Nernst equation [6.64].

4 Over all the titration points, form the sum of squared deviations SSQ of the calculated E values from the corresponding experimental values

$$SSQ = \sum_i (E_{calc} - E_{expt})^2 \qquad [6.66]$$

5 *Systematically vary the values of the unknown parameters until the value of SSQ reaches a minimum.*

A wide variety of mathematical techniques is available for carrying out this last step, a mathematical technique known as *non-linear optimization*. However, the details of the procedures are not important to an understanding of how the method is used in chemistry. Therefore, they will not be further considered in this book.

The final set of parameter values obtained by this method will represent the "best" fit to the experimental data. Because the method used is not unique, the concept of a "best fit" is a little

vague. The procedure outlined above is an obvious and robust one, but is rather slow to carry out for complex systems. An alternative approach, which is much faster to perform, is as follows:

1. Estimate reasonable starting values for the unknown parameters: [NaOH], K_w, c_{INP}, K_{INP} and the Nernst constants E_0 and k.
2. For each titre point *v*, use the Nernst equation to calculate the pH of the solution at that point, and then use [6.63] to calculate the concentrations of all other species.
3. Use these values to calculate the net charge-balance CB of the solution.

$$CB = [Na^+] + [H^+] - [OH^-] - [Cl^-] - [INP^-] \qquad [6.67]$$

4. Over all the titration points, form the sum of squared CB values

$$SSQ = \sum_i CB^2 \qquad [6.68]$$

5 *Systematically vary the values of the unknown parameters until the value of SSQ reaches a minimum.*

The rationale of this method is that only the correct values of the unknown parameters will give the required zero charge balance at every titration point.

Figure 6.12 shows the results obtained by the first of these two methods for the titration data presented in Figure 6.4. In this particular calculation, the slope of the Nernst equation was held constant at the theoretical value for 25°C, 59.162 mV and the j_H term for the residual liquid junction potential was included in the calculations as a variable.

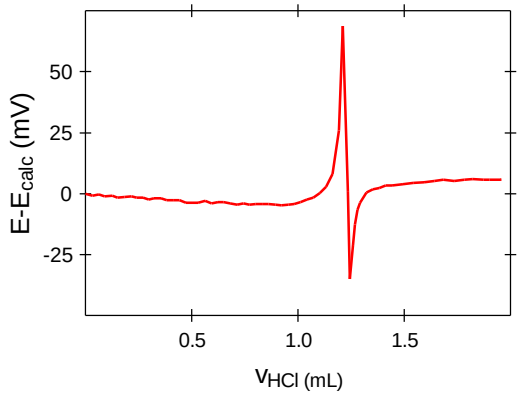

Figure 6.12: Deviation between measured and calculated cell potential using the multi-parameter method for the results in Figure 6.4 by minimizing the squared deviations of the calculated potential.

The values of the calculated parameters were as follows:

E0	386.644 mV
j_H	82.1178 mV L mol^{-1}
pK_w	13.2593
[NaOH]	1.6372 mM

[IMP]	0.00617 mM	
pK_{IMP}	2.834	[6.69]

The pK_w value differs from that estimated using the Gran method because a different pH model is being used.

Figure 6.12 shows that the worst points in the multi-parameter estimation are those affected by the impurity. This problem can be dealt with by eliminating points in this region from the data set and treating the remaining points in two steps. Points in the acidic region $v > v_e$ can be used for a multi-parameter determination of the electrode parameters E_0, j_H and k. Subsequently points in the alkaline region may be used for determination of [NaOH] and pK_w.

This type of approach helps to minimise the number of variable parameters used in the optimisation. One of the weaknesses of multi-parameter methods is that the more variable parameters are included, the better the resultant fit (lower value of SSQ). However this does not mean that a better solution has been found, because the optimised values of one or more parameters may not be realistic. For example, it is often possible to improve SSQ by allowing the Nernst electrode slope k to vary. However, quite silly values of k will often result from this approach.

6.10 The case of a Very Weak Acid - Glycine

Very weak acids or bases are very difficult to analyse by titration methods in aqueous solution because their limited degree of dissociation means that the pH change at the equivalence point is quite small. For example, it is easy to analyse a weak acid like acetic acid (pK_a =4.76) by titration with standard base, but it is next to impossible to analyse its conjugate base the acetate ion (pK_b = 9.24) by titration with standard acid. Needless to say, acid or base dissociation constants of such species are also difficult to measure by simple methods such as the Gran function approach detailed earlier . However, multi-parameter methods allow many such species to be treated successfully.

As an example, we will look at the acid dissociation reactions of the amino acid, *glycine*. In aqueous solutions, glycine exists mainly in a protonated form $CH_2(COOH)NH_3^+$ that undergoes dissociation to the neutral amino acid

$$CH_2(COOH)NH_3^+ \quad CH_2(COOH)NH_2 + H^+ \qquad [6.70]$$

For this dissociation, pK_{a1} has an approximate value of 12. The carboxylic acid functional group can also dissociate

$$CH_2(COOH)NH_2 \quad CH_2(COO^-)NH_2 + H^+ \qquad [6.71]$$

For this second dissociation, pK_{a2} is about 10.

The large values for both pK_{a1} and pK_{a2} mean that very little dissociation of the protonated species $CH_2(COOH)NH_3^+$ takes place except at very high pH, making it difficult to locate the equivalence points in a titration with standard base.

Figure 6.13 shows the potentiometric titration curve for titration of a solution containing HCl and glycine with standard NaOH.

Notice that the equivalence point for titration of the HCl initially present, theoretically expected at 5.00 mL, is clearly seen. However there is little indication of the reaction between glycine and NaOH at v > 5.00 mL. The theoretical equivalence point is approximately v = 20 mL, but there is no real evidence of curvature in this region.

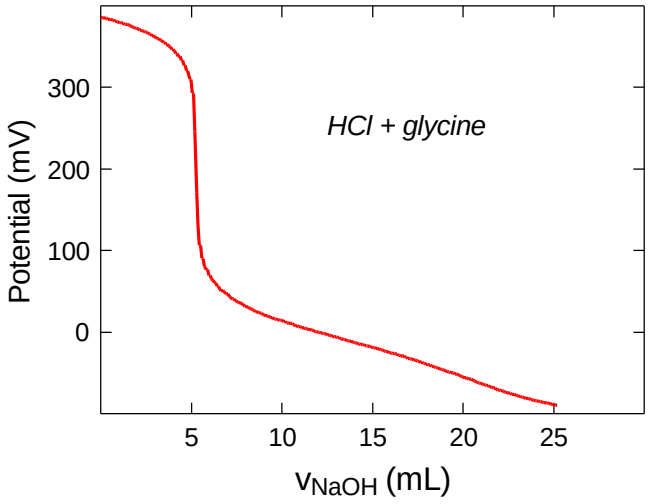

Figure 6.13: Experimental potentiometric titration curve for 204.59 mL of a mixture of 2.4822 mM HCl and 7.500 mM glycine with 0.10105 M NaOH solution in 1.0 M NaCl supporting electrolyte. This curve was generated by an automatic titrator. Drawn using data collected by Dr Lay Choo Chong.

The data shown in Figure 6.13 can be analysed by the multi-parameter method quite easily. For simplicity of notation, we will denote the glycinate ion $CH_2(COO^-)NH_2$ by L^-. The dissociation equilibria can then be written

$$K_{a1} = [H^+]\frac{[HL]}{[H_2L^+]}$$
$$K_{a2} = [H^+]\frac{[L^-]}{[HL]} \qquad [6.72]$$

The mass-balance relationship for glycine is

$$[L]_T = [H_2L^+] + [HL] + [L^-] \qquad [6.73]$$

Finally, the charge balance equation for the system is

$$[H^+] + [H_2L^+] + [Na^+] = [OH-] + [Cl^-] + [L^-] \qquad [6.74]$$

The combination of these three equations [6.72] through [6.74], together with the equilibrium for the self-dissociation of water, forms the basis of the multi-parameter method for this system.

At this point, one may ask what role the HCl plays in the analyte solution. This was added to allow for a calibration of the glass electrode. The calibration is carried out by selecting those

points in the excess acid region (in this case v < 5.00 mL) and carrying out a multi-parameter analysis in a similar way to that described in the previous section. Making the assumption that the analyte contains only HCl in this region of the titration curve is quite reasonable in view of the weakness of glycine as an acid.

This preliminary analysis gave suitable constant values for the following parameters

$$\begin{aligned} [HCl] &= 0.0024823 \text{ M} \\ [NaOH] &= 0.10105 \text{ M} \\ E_o &= 592.3 \text{ mV} \\ j_H &= 59.2 \text{ mV M}^{-1} \\ k &= 59.152 \text{ mV} \end{aligned} \qquad [6.75]$$

Next, multi-parameter analysis with $[L]_T$, K_{a1} and K_{a2} as the variable parameters gave the following final results

$$\begin{aligned} [L]_T &= 7.690 \text{ mM} \\ pK_{a1} &= 12.26 \\ pK_{a2} &= 9.67 \end{aligned} \qquad [6.76]$$

The plot of the difference between calculated and experimental potentials for this system is shown in Figure 6.14, from which it clear that a very reasonable agreement between calculated and experimental data is found.

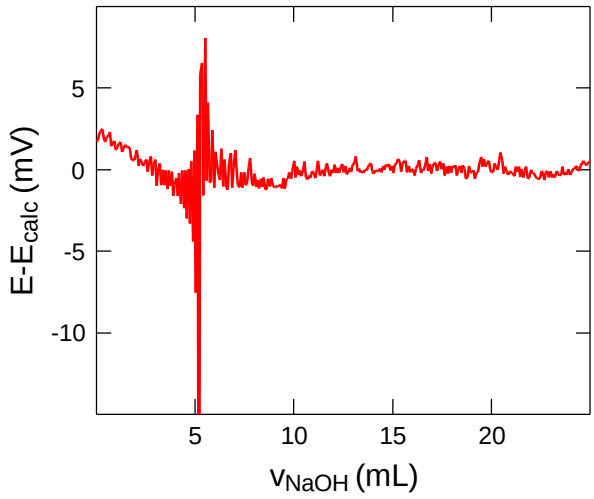

Figure 6.14: Deviation between measured and calculated cell potential using the multi-parameter method for the HCl+glycine results in Figure 6.13; determined by minimizing the squared deviations of the calculated potential.

The glycine example is a good one to illustrate the value of multi-parameter methods because this system is one that is commonly used to "calibrate" methods for the determination of equilibrium constants. By means of a variety of independent measurements, it has been agreed

that the equilibrium constants for acid dissociation of glycine in 1.0 M NaCl electrolyte at 25.0°C are

$$pK_{a1} = 12.07 \pm 0.26$$
$$pK_{a2} = 9.65 \pm 0.01 \quad [6.77]$$

The agreement between this range of values and the results presented here is, therefore, very good indeed!

6.11 Seawater Total Alkalinity Revisited

The multi-parameter method is particularly useful for computing total alkalinity from potentiometric titration data for seawater samples. In Section 6.5 it was found that the simple Gran function approach is not successful for analyzing thus type of data because of the presence of other protolytes such as borate, sulfate and fluoride. This situation is amenable to the multi-parameter treatment.

Figure 6.15 shows a typical set of high-quality titration data obtained for a seawater sample during the GEOSECS Program.

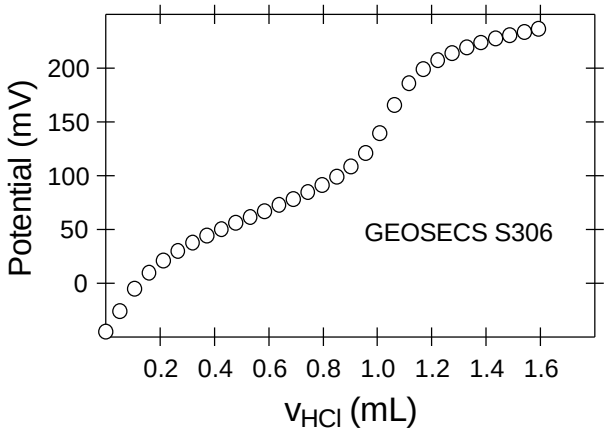

Figure 6.15: Experimental potentiometric titration curve for 110.74 mL of seawater titrated with standard HCl (0.24414 mol kg^{-1}) containing 1.64 mmol kg^{-1} phosphate and 21.3 mmol kg^{-1} phosphate, salinity 35.024. Drawn using data collected during the GEOSECS Program, Station S306, data published by Bradshaw et al., 1981.

The starting point for multi-parameter analysis of these results is the full definition of total alkalinity put forward in Section 6.8 as equation [6.59]

$$A_T = [HCO_3^-] + 2[CO_3^{2-}] + [OH^-] - [H^+]_{free} + [B(OH)_4^-] + [HPO_4^{2-}] + 2[PO_4^{3-}] + [SiO(OH)_3^-] - [HSO_4^-] - [HF] - [H_3PO_4] \quad [6.78]$$

Each of the terms in [6.78] may be calculated from a combination of mass-balance and equilibrium conditions using the information set out in detail in Chapter 4.

The terms in $[HCO_3^-]$ and $[CO_3^{2-}]$ are related to C_T , which is considered to be a variable parameter in the evaluation, as follows:

$$[HCO_3^-] = C_T \alpha_1$$
$$[CO_3^{2-}] = C_T \alpha_2 \qquad [6.79]$$

where the general definitions of α_1 and α_2 in terms of $[H^+]$, K_1 and K_2 were given in equations [2.44] and [2.45]. Values of the equilibrium constants relevant to seawater were given in Section 4.4.

$[H^+]_{free}$ is the free proton concentration, which is linked to [OH] through the self-dissociation equilibrium of water discussed in Section 4.3.

The terms involving borate, sulfate and fluoride use equilibrium data presented in Chapter 4, and the total concentrations of these species in the seawater are estimated from its salinity, as also discussed in that chapter.

The minor species phosphate and silicate have variable concentrations in seawater. For the current example, specific values derived from separate measurements were used as input data. As with the other species, equilibrium constant values presented in Chapter 4 were used. In all cases, the total proton pH scale was used.

Calculation of the results was made along lines very similar to the second general method presented in Section 6.9 where the charge imbalance was minimized. If the defining equation for total alkalinity [6.78] is inverted in sign, we obtain the total analytical concentration of hydrogen ions c_H relative to the reference proton condition of pure H_2CO_3:

$$\begin{aligned} c_H = {} & [H^+]_{free} + [HSO_4^-] + [HF] + [H_3PO_4] \\ & - [HCO_3^-] - 2\,[CO_3^{2-}] - [OH^-] \\ & - [B(OH)_4^-] - [HPO_4^{2-}] - 2[PO_4^{3-}] - [SiO(OH)_3^-] \end{aligned} \qquad [6.80]$$

The initial value of c_H before the titration starts is, obviously, the negative of the total alkalinity. At any point in the titration, after a mass m of HCl of concentration c_{HCl} has been added, the new value of c_H can be calculated as

$$c_H = \frac{m\,c_H - m_0 \mathrm{TA}}{m_0 + m} \qquad [6.81]$$

Note that in this formulation, sample mass is used rather than volume because it is normal to express concentrations on the seawater scale, mol kg^{-1} seawater.

As with the other multi-parameter methods, the Nernst equation is used to link the total proton concentrations $[H^+]$ at each point with the corresponding cell potential value E. The Nernst equation model adopted allowed the slope term k to very, and a residual liquid junction term j_H was not included.

The calculation method starts with reasonable assumed values for A_T and C_T, together with estimated constant values for the acid dissociation constants and the total concentrations of the minor species. These are used to evaluate c_H independently using both [6.80] and [6.81], minimizing the sum of squared differences between both estimates over all titration points.

Because the quantity c_H is based directly on the charge balance equation, this technique is essentially identical to the second general method outlined in section 6.9.

The final results of applying this method to the data presented in Figure 6.15 are:

A_T = 2307.0 μmol kg^{-1}

C_T = 2164.5 μmol kg^{-1}

E_0 = 408.38 mV

k = 58.880 mV [6.82]

Figure 6.16 shows how well the calculated results fit the experimental data by plotting the difference between the calculated and experimental values of c_H for each titre point

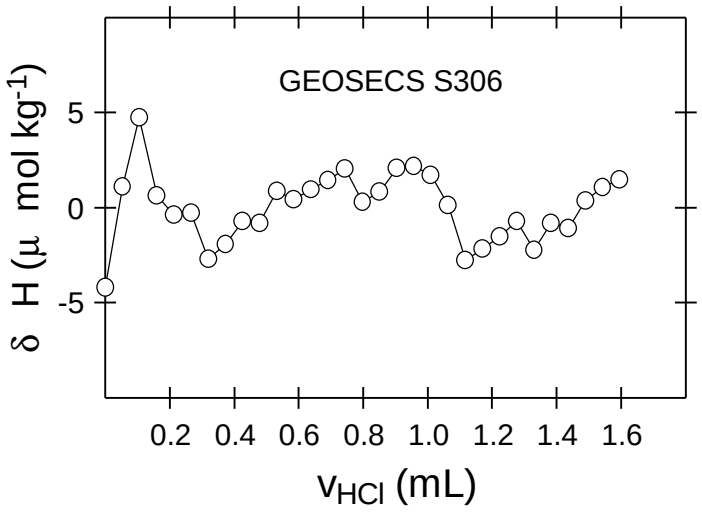

Figure 6.16: Plot of difference between experimental and calculated total proton concentration for the titration data in Figure 6.15, fitted using the multi-parameter method as outlined in the text.

The difference in c_H has a maximum magnitude of 5 μmol kg^{-1}, equivalent to 0.2 % error, while the average magnitude across the whole titration is 1.4 μmol kg^{-1}, equivalent to 0.06 % error in each point.

While this calculation procedure yields values for C_T in addition to A_T, the results obtained show a small discrepancy compared with direct measurements. As discussed in more detail in the next chapter, this is believed to result from non-linearity in the response of the glass electrode.

Further Reading

Ben-Yaakov, S., R. Raviv, H. Guterman, A. Dayan, and B. Lazar, Application of personal microcomputers in the analytical laboratory-I: Potentiometric analysis, *Talanta*, *29*, 267-274, 1982.

Bradshaw, A.L., and P.G. Brewer, High precision measurements of alkalinity and total carbon dioxide in seawater by potentiometric titration -1. Presence of unknown protolytes(s)?, *Marine Chemistry*, *23*, 69-86, 1988.

Bradshaw, A.L., and P.G. Brewer, High precision measurements of alkalinity and total carbon dioxide in seawater by potentiometric titration. 2. Measurements on standard solutions, *Marine Chemistry*, *24*, 155-162, 1988.

Bradshaw, A.L., P.G. Brewer, D.K. Shafer, and R.T. Williams, Measurements of total carbon dioxide and alkalinity by potentiometric titration in the GEOSECS program, *Earth and Planetary Science Letters*, *55*, 99-115, 1981.

Dickson, A.G., An exact definition of total alkalinity and a procedure for the estimation of alkalinity and total inorganic carbon from titration data, *Deep-Sea Research*, *28*, 609-623, 1981.

Dickson, A.G., The development of the alkalinity concept in marine chemistry, *Marine Chemistry*, *40*, 49-63, 1992.

Millero, F.J., J.-Z. Zhang, K. Lee, and D.M. Campbell, Titration alkalinity of seawater, *Marine Chemistry*, *44*, 153-165, 1993.

Chapter 7 CO_2 Equilibria in Seawater

This chapter brings together the information and knowledge of the preceding chapters in an overview of the CO_2 equilibrium system in the ocean. Many aspects of this system have been discussed in general terms in Chapters 2-4, with particular reference to calculation methods in Chapter 5 and measurement techniques for total alkalinity in Chapter 6. Here we look in detail at how the system is approached both conceptually and experimentally, thereby setting the scene for an examination of the geochemical behaviour of CO_2 in the next, and final, chapter.

7.1 Composition Parameters of the CO_2 System

The CO_2 system in seawater can be described by several important composition parameters. These include:

1. The constituent species H_2CO_3*, HCO_3^- and CO_3^{2-}
2. Total dissolved carbon dioxide, C_T
3. Total alkalinity A_T
4. pH (NBS, total, free, or seawater scales)
5. CO_2 fugacity $f(CO_2)$, or equivalently the CO_2 partial pressure $p(CO_2)$

Not all of these parameters are independent of each other. Indeed, it is sufficient to measure, or specify, only two of the parameters listed above in order to fix the system composition. The remaining parameters may then be estimated using the methods outlined in Chapters 4 and 5, and in Section 7.6 below.

The first three parameters are useful in understanding some features of CO_2 chemistry. However, they are not easily measured directly and are not conservative capacity parameters. Therefore, it is rare for the concentrations of any of the group H_2CO_3*, HCO_3^- and CO_3^{2-} to be obtained other than by calculation.

Both C_T and A_T are, from many points of view, an ideal choice as a starting point for defining the CO_2 system, e.g. by measurement. Firstly, both are conservative capacity parameters that are independent of changes in temperature and pressure. Since both of the latter parameters vary considerably throughout the ocean, it is particularly convenient to have a p, T-independent basis for examining how the CO_2 composition is affected by variation in T and p. Secondly, both quantities are readily measured, although for both the measurement techniques are rather slow (2-4 samples per hour) and can therefore be applied only to discrete samples.

CO_2 fugacity (or partial pressure) is directly important in the context of CO_2 gas exchange with the atmosphere. The equilibrium CO_2 fugacity of oceanic surface waters defines, in the long term, the atmospheric concentration of this important greenhouse gas. While this parameter can be calculated from measurements of, for example, C_T and A_T, it is considerably simpler and probably more accurate to make direct measurements. Moreover, reliable techniques now exist for making continuous measurements in surface waters, allowing 2-dimensional mapping of the surface water concentrations in real time. The same mapping abilities are provided by pH, which can be measured using relatively simple techniques.

Thus in modern marine chemistry, surface mapping of one or both of these parameters has become the base method for looking at details of the CO_2 system in surface waters. At the same time, it is common practice to measure at least one of A_T and C_T on regular discrete samples. The measurement of more than 2 system parameters effectively over-determines the system. This is considered useful because the equilibrium calculation methods are not yet accurate enough for there to be complete agreement between the measurement and indirect calculation of its parameters. As knowledge of the equilibrium system improves, particularly of the values of the equilibrium constants involved, this situation is likely to become unimportant.

We now consider briefly the various measurement methods used to study the CO_2 system. Much progress has been made over the last 10-15 years in the development of these techniques. This has been aimed largely at improving the accuracy and precision of the methods to a point where meaningful results can be obtained in terms of the increases in C_T expected to take place as a result of fossil fuel CO_2. To this end, various target accuracies and precisions have been specified, as set out in Table 7.1. The present-day accuracies are limited mainly by the availability of suitable reference standards. The target precisions refer to 1 standard deviation for the difference between laboratories, and between different oceanographic cruises. A better value of about half those listed should be achieved within a single laboratory or cruise.

Table 7.1 Target desired accuracy and between lab/cruise precision for measurement parameters of the CO_2 system in seawater.

Measurement	Accuracy	Precision
C_T	± 1 μmol kg^{-1}	± 4 μmol kg^{-1}
A_T	± 1 μmol kg^{-1}	± 1 μmol kg^{-1}
pH	± 0.002	± 0.001
$f(CO_2)$	± 0.5 μatm (± 0.05 Pa)	± 1 μatm (± 0.1 Pa)

7.2 Total Alkalinity

The basic concepts underlying the definition and measurement of total alkalinity in seawater were discussed in Chapter 6. The calculation of the results from the titration data is carried out in the manner described in that Chapter, and yields both A_T and an estimate of C_T as calculated results.

The recommended procedure for the best work involves a computer-controlled potentiometric titration in a closed cell. The cell is closed to avoid CO_2 loss to the atmosphere as the solution becomes acidified. However, many workers have reported that reliable A_T values can be obtained by titration in an open vessel. The closed cell is less convenient since it requires a piston arrangement to accommodate the increase in total solution volume as the titrant HCl is added.

Since A_T is defined in terms of the reference proton condition of pure H_2CO_3 in water, such CO_2 exchange should not, in principle, affect the alkalinity. It will, however, make the values of C_T derived from the calculation procedure unreliable.

The procedure can be calibrated in several ways. Standard samples of known alkalinity are available from Dr Andrew Dickson at Scripps Institution of Oceanography, California. These are particularly useful for ensuring that results are comparable to other laboratories. The HCl titrant may be calibrated using accurately weighed aliquots of pure Na_2CO_3 , a method that is adaptable for use at sea. Increasingly, it is common to calibrate the HCl directly by means of coulometry, in which OH^- is generated directly at a platinum electrode by reduction of water at a known constant current.

The primary shortcomings of the alkalinity method relate to the use of the glass electrode for pH measurement. As noted in Chapter 3, these electrodes suffer from measurement uncertainties arising from the liquid junction potential that are difficult to overcome. Non-linearity in the Nernst response of the electrode is considered to have little effect on the calculated A_T results, but does affect the accuracy of the C_T values also derived from the calculations. This discrepancy has been made obvious by independent measurements of C_T.

For example, during the GEOSECS Program[6] Bradshaw and Brewer noticed that C_T values derived from A_T titrations were consistently about 21 μmol kg^{-1} higher than those measured directly by gas extraction. They ascribed this difference to an unknown protolyte not included in their equilibrium model for CO_2. Some of this difference has since been removed by improvements in the reliability of equilibrium constants, but most still remains. More recently, Millero *et al.* (1993) appear to have resolved the problem. They showed that using the standard computational scheme for treating titration data (as presented in Chapter 6), in which the glass electrode calibration is incorporated into the calibrations, C_T calculated from the titration data were 20 μmol kg^{-1} higher than known values for standard samples. On the other hand, if standard seawater buffers were used to calibrate the electrodes (see Section 6.4), reliable values were obtained. They concluded that the non-Nernstian response of typical glass electrodes, compensated for by buffer calibration, gives results that masquerade as an unknown protolyte similar in chemical properties to HCO_3^- ion. Millero *et al.* suggest several practical ways to eliminate this problem.

Thus, while C_T derived from titration data are inherently less reliable than direct methods, this does offer a cheap alternative if care is taken with electrode calibration. In Section 6.4, alternatives for pH measurement involving spectrophotometric measurements of coloured pH indicators are discussed. These techniques do not suffer from the non-linear response problems of the glass electrode and have considerable potential as a substitute for the pH-monitoring component of the alkalinity titration. At least 3 research groups, including that of the present author, are exploring this possibility. Fibre-optics technology and compact charge-coupled diode array photometers make this approach very promising.

---

[6] The GEOSECS Program, acronym for **GEO**chemical **O**cean **SEC**tion **S**tudy, was a major international scientific study of the chemistry and physics of the global ocean conducted in the 1970's. It made a significant contribution to our present knowledge and set the pattern for later similar studies.

7.3 Total CO_2

The most reliable methods for measurement of C_T are direct. All involve acidification of the seawater sample with phosphoric acid and purging with CO_2-free gas to quantitatively purge the released CO_2, followed by one of several measurement techniques:

1. Gas chromatography
2. Infrared gas analysis
3. Coulometric titration of the isolated CO_2

Of these, the coulometric technique is the most commonly used. This involves trapping the CO_2 gas emitted after acidification in a solution containing ethanolamine, which forms hydroxyethyl carbamic acid

$$CO_2 + HO(CH_2)_2NH_2 \rightarrow HO(CH_2)_2NHCOO^- + H^+ \quad [7.1]$$

The equivalent amount of H^+ generated by this reaction is quantitatively determined by coulometry using electro-generated hydroxyl ions. The anode involves the dissolution of silver. The change in pH during the titration is monitored by spectrophotometry using thymolphthalein indicator present in the solution. The equipment used for the whole procedure can be automated under computer control, and has now reached a high degree of reliability.

It has been shown that the coulometric system is not 100 % efficient, and one or more side reactions occur during electrolysis. The overall efficiency is calibrated using known amounts of CO_2 gas, either from a source of standard CO_2 or using Na_2CO_3 standard solutions.

The gas chromatography detection method is only readily applicable to analysis of discrete samples since it involves an analysis time of at least 10 minutes. The usual technique is to reduce the CO_2 to methane using a palladium-hydrogen catalyst after chromatographic separation, allowing the use of a sensitive flame ionization detector. The main advantage of the GC method is that other carbon-containing gases can be analyzed at the same time, specifically CO and CH_4. The latter is also an important greenhouse gas. GC detection is also commonly used in the determination of CO_2 fugacity on discrete samples.

CO_2 efficiently absorbs infrared radiation, which is why it is a greenhouse gas. This property may also be used to measure CO_2 concentrations in air. The equipment involved is most commonly used for continuous, underway measurements of f (CO_2) and is discussed in more detail in Section 7.5. It is likely to have potential as part of a future technique for continuous measurement of C_T.

7.4 pH

As discussed in Chapter 3, several different pH scales are in common use in seawater. They include the NBS (IUPAC) Practical pH scale pH_{NBS}, the total proton scale pH_T, the seawater scale pH_{SWS} and the free proton pH scale pH_F. In the context of using a glass electrode, or any other galvanic cell, each is distinguished by the way in which the cell is calibrated to measure H^+ activity. Usually, but not always, this calibration is carried out with one or more pH buffer standard, a solution whose pH has been defined on one of these scales and normally has a value assigned on the basis of careful measurements using a hydrogen electrode. The same

consideration applies to the measurement of pH using indicators, for the use of these relies upon previously-determined values for the pK_a of the indicator, a measurement that will have been made according to one of the pH scales mentioned.

A potentially confusing issue that has already been mentioned in this book is that for any particular scale, there are three concentration scales in common use: molarity, molality and the seawater concentration scale. It goes without saying that the use of pH as a quantity must be done in a way that uses a consistent concentration scale as well. In the remainder of this chapter, unless otherwise stated, the seawater concentration scale will be assumed.

The different pH scales may related to each other in a straightforward way. The activity of H^+ on the NBS scale is related to the free proton concentration through a total activity coefficient f_H that also incorporates the effect of liquid junction potential changes between the standard buffer and seawater

$$a_H\,(\text{NBS}) = f_H\,[H^+]_F \qquad [7.2]$$

The three concentration-based pH scales are related to each other by

$$[H^+]_F = \frac{[H^+]_T}{1 + \dfrac{S_T}{K_S}} = \frac{[H^+]_{SWS}}{1 + \dfrac{S_T}{K_S} + \dfrac{F_T}{K_F}} \qquad [7.3]$$

where S_T and F_T are the total analytical concentrations of sulfate and fluoride and K_S, K_F are the acid dissociation constants of HSO_4^- and HF respectively.

Potentiometric pH measurements

With these three scales, it is important to be able to minimize the residual liquid junction potential ΔE_j. The best way to achieve this is to prepare standard buffers in seawater itself. The assignment of $[H^+]_X$ (free, total or SWS) to the standard buffer is based on measurements using the following type of cell

$$\text{Pt} \mid H_2\,(g, p^{\varnothing}) \mid \text{seawater medium + buffer} \mid \text{AgCl(s)} \mid \text{Ag (s)} \qquad [7.4]$$

where the seawater medium is a synthetic solution having the ionic composition required for the chosen pH scale.

A number of weak acid buffers have been used. The main requirement is that the weak acid form have a pK_a value reasonably close to the pH of normal seawater. Most are organic nitrogen bases:

2-amino-2-hydroxymethyl-1,3-propanediol ("Tris")

2-amino-2-methyl-1,3-propanediol ("Bis")

tetrahydro-1,4-isooxazine ("morpholine")

2-aminopyridine

Dr Andrew Dickson has presented equations for calculating the standard pH of these buffers in 0.04 mol kg^{-1} synthetic seawater solutions. Table 7.2 shows values for three of the buffers at different temperatures.

Table 7.2 pH of standard seawater buffers at various temperatures (total proton scale, molality) reported by Millero et al 1993.

T (^oC)	Tris	Bis	Morpholine
5	8.732	9.498	9.123
15	8.392	9.145	8.844
25	8.072	8.810	8.573
35	8.768	8.491	8.310
45	7.475	8.187	8.053

The pH of the tris buffer in seawater of a given salinity and temperature has been fitted to the following equation (total proton pH scale, seawater concentration scale)

$$pH_T = \frac{11997.0 + 3.7669\,S + 0.00178\,S^2}{T} - 381.3088 - 0.011634\,S + 67.63163\,\ln T - 0.121538\,T - \log(1 - 0.00106\,S) \quad [7.5]$$

The actual measurement of pH in seawater is normally carried out with a cell incorporating an H^+-responsive glass electrode of the following type:

glass electrode | seawater || KCl (sat) | reference electrode [7.6]

This cell can be calibrated with any of the seawater standard buffers mentioned above for potentiometric measurement of seawater pH to yield values that are consistent with the best available equilibrium description of the seawater CO_2 system. As already noted, without the use of the standard buffers, the non-linear response of the glass electrode near pH 8 gives rise to "phantom" protolytes in the alkalinity titration, making the derived C_T values unreliable.

Therefore, it is highly recommended that the slope response of the electrodes in use be checked using two different standard buffers. If the measured cell potentials using buffers with standardized values pH_1 and pH_2 are E_1 and E_2 then the slope term is calculated as

$$k = -\frac{E_1 - E_2}{pH_1 - pH_2} \quad [7.7]$$

If the slope term does not correspond to the theoretical value (2.303RT/F = 59.162 mV at 25°C) then the electrodes should be rejected.

After calibration with tris buffer, the pH of a seawater sample pH_X is calculated from the measured cell potential E_X using the equation

$$pH_X = pH_S + \frac{E_S - E_X}{k} \quad [7.8]$$

where E_S is the cell potential measured when the cell is filled with the tris buffer of pH_S. The expected precision of this measurement is ± 0.002 pH.

Spectrophotometric pH measurements

A recent alternative to the use of the glass electrode is photometry using a coloured acid-base indicator of suitable pK_a value. This method relies on the fact that the acid and base forms of an indicator have quite different visible absorption spectra. Using a spectrophotometer, the concentrations of each form can usually be independently measured in a solution. Thus if the dissocation constant for the indicator is known the pH is easily calculated using the familiar equation

$$pH = pK_a + \log\frac{[base]}{[acid]} \qquad [7.9]$$

Figure 7.1 shows the visible absorption spectra for the indicator phenol red in synthetic seawater solutions of two different pH values. The solution containing Tris buffer, pH 8, has a spectrum dominated by the base form of phenol red with a maximum at 558 nm, while the spectrum of the solution containing the phthalate buffer, pH 4, is dominated by the acid form, maximum at 433 nm.

The dissociation constant for phenol red in seawater media has been accurately determined as a function of temperature by Dr Robert Byrne

$$pK_a = -\frac{4054.8374}{T} + 116.6037 - 38.6645\log T \qquad [7.10]$$

A number of other suitable indicators are also available, including cresol red, *m*-cresol purple and thymol blue, for which the equivalents to [7.10] have been determined.

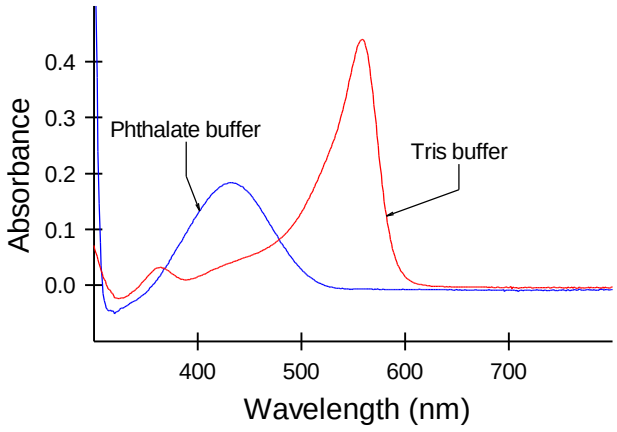

Figure 7.1 Visible absorption spectra of phenol red indicator in synthetic seawater solutions containing either Tris buffer (pH 8.072) or potassium hydrogen phthalate buffer (pH = 4.0) at 25°C.

Measurement technique

The pH measurement is made by recording the absorbances A_1 and A_2 of the seawater sample, to which a small amount of indicator has been added, at two wavelengths. Preferably, the wavelengths chosen give good separation of the acid and base peaks in the spectrum and reasonable sensitivity. The following equation is then used to calculate the pH

$$pH = pK_a + \log \frac{R - \frac{\varepsilon_1(acid)}{\varepsilon_2(acid)}}{\frac{\varepsilon_1(base)}{\varepsilon_2(acid)} - R\frac{\varepsilon_2(base)}{\varepsilon_2(acid)}} \qquad \left(R = \frac{A_1}{A_2}\right) \qquad [7.11]$$

In [7.11], ε_1 and ε_2 are the extinction coefficients of the relevant species at each of the two wavelengths and R is the absorbance ratio. The absorbance readings must be corrected for background effects using a seawater sample free of indicator. The three extinction coefficient ratios in [7.11] are not strongly dependent on temperature or salinity, and likepK_a, have been previously determined for each particular indicator with some accuracy. For the example of phenol red considered here, insertion of the known values of the ratios into [7.11] leads to the simplified equation

$$pH = pK_a + \log \frac{R - 0.0038}{2.6155 - 0.1234R} \qquad \left(R = \frac{A_1}{A_2}\right) \qquad [7.12]$$

Equivalent expressions are available for the other indicators in common use.

The spectrophotometric method may be used for both discrete samples and, more recently, for continuous surface water measurements. The discrete measurements normally involve the use of a conventional, high-quality spectrophotometer with10 cm path length cells to minimize the amount of added indicator. Continuous surface water measurements are made using a flow injection technique in which metered flows of seawater and indicator solution are mixed together and then passed through a spectrophotometer flow cell. In recent years, the use of compact charge-coupled diode array photometers with optical fibre connections has become common.

The major advantage of the spectrophotometric pH method is that unlike the use of the glass electrode, it does not require calibration. This is because it is inherently based on a precise knowledge of the thermodynamic properties of the indicator, properties that can be (and have been) accurately measured in the laboratory by skilled workers. In addition, it does not suffer from the problem of residual liquid junction potentials. It will be interesting to see if the use of spectrophotometric pH measurement can be incorporated into the alkalinity titration technique so that reliable C_T data can also be derived from this measurement.

The main drawback of the method at present is the unknown effect of the indicator on the pH of the original seawater. Some workers ignore this effect, justifying this by the use of low indicator concentrations (< 5 μmol kg^{-1}). In the discrete sample technique, some workers make several additions of indicator and then extrapolate the measured pH values to zero indicator concentration. This procedure is not entirely correct, since calculations of the expected pH shift show that it is not always linear with amount of added indicator. In fact, the pH change may even change sign as more indicator is added! The reason for this is that not only is the pH affected by

the acidity of the indicator itself, but also the indicator addition decreases the salinity of the seawater. The effect of both changes can be opposite in direction.

Temperature corrections

Generally, pH measurements made by either technique are carried out at a controlled constant standard temperature such as 25°C and require correction of the measured results back to the *in situ* temperature of the water. The correction procedure is the same for both techniques, and is done using an equilibrium model for CO_2 in seawater.

As discussed in Section 7.1, the CO_2 system is completely defined by any two composition parameters. Thus in the context of pH measurements, we need one other measured parameter. This parameter must either be temperature independent (A_T or C_T), or one that was measured at the same temperature as the pH.

If no other parameters are available, the best approach for surface waters is to estimate alkalinity from the salinity of the seawater as follows:

$$A_T = 660 + 47.6\ S \qquad [7.13]$$

This equation describes the alkalinity of surface seawaters with sufficient accuracy for temperature correction of pH. For deep waters, it will probably be possible to estimate the alkalinity from a knowledge of the oceanographic properties of the oceanic region and water depth being sampled. The temperature correction is not especially sensitive to the alkalinity value so reliable corrections can usually be made in the absence of other data.

Once a second parameter has been measured, or a suitable value assumed, this and the measured pH are used as input parameters for the calculation of the CO_2 composition, as set out in Section 7.6 below. From this, the temperature independent values of A_T and C_T are obtained. Next, these are used as input parameters to calculate the composition at the desired *in situ* temperature, thus obtaining the corrected pH value.

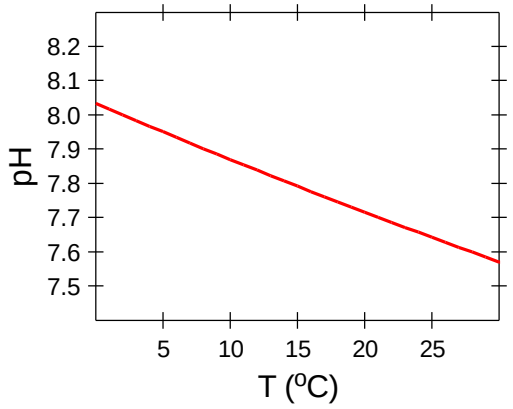

Figure 7.2 Calculated pH of seawater of salinity S = 35.00, A_T = 2300 mmol kg^{-1} and C_T = 2100 mmol kg^{-1} as a function of temperature.

Figure 7.2 shows the temperature dependence of pH for a typical seawater sample. Note that the pH increases as the temperature is lowered. This results from the changes in the equilibrium constants describing the CO_2 system, especially K_1 and K_2 for H_2CO_3*.

7.5 CO_2 Fugacity and Partial Pressure

The direct measurement of CO_2 fugacity f (CO_2) is, in principle, quite straightforward. A sample of seawater in the form of either a continuous flow, or a discrete sample, is equilibrated with a small volume of air whose CO_2 concentration is subsequently measured using either gas chromatography or infrared photometry.

Discrete Measurements by Gas Chromatography

In the GC technique, CO_2 is catalytically reduced to methane after column separation and subsequently detected using a flame ionization detector. This is generally applied to discrete samples since the high sensitivity of the flame detector means that only a small ratio of air to water is needed for analysis, thus minimizing the correction needed for loss of C_T from the seawater. Generally, samples are collected in 500 mL volumetric flasks and poisoned to prevent biological changes. At the time of analysis, the sample is equilibrated with the head space in the flask, generally by inserting a gas dispersing line that circulates the head space air through the water using a frit bubbler. A metered volume of the air is then injected into the gas chromatograph for analysis. The quantity of CO_2 in the air is calculated from the calibrated response of the GC detector.

The detector is calibrated using standard gas mixtures containing a known CO_2 mole fraction. For each sample analysis, this yields directly the mole fraction x (CO_2) in the air. This is multiplied by the measured atmospheric pressure at the time a particular sample was injected into the GC to calculate the CO_2 partial pressure in the air sample. If the air sample has been dried before GC analysis, the results must be corrected for the increase in CO_2 concentration that arises from the removal of water vapour. This is done using equations describing the vapour pressure of seawater as a function of salinity and temperature (see [7.15]).

Following this calculation, a correction is usually needed for the small amount of CO_2 that has been lost from the seawater during equilibration, which would otherwise tend to make the results lower than expected. The loss of CO_2 to the air will decrease the C_T of the original seawater without affecting its alkalinity. Thus, a mass-balance approach taking account of the volumes of air and water can then be used to make the correction. This is straightforward if either the alkalinity A_T or the C_T of the water is known.

If p_1 is the measured CO_2 partial pressure in the head space before equilibration and p_2 its value afterwards, then the change in the amount of CO_2 in the head space Δn is given by (assuming ideal gas behaviour)

$$\Delta n = \mathrm{V}\frac{p_1 - p_2}{\mathrm{RT}} \qquad [7.14]$$

where V is the head space volume. From this, the change in total CO_2 is given by

$$\Delta C_T = \frac{\Delta n}{\rho V_{sw}} \quad [7.15]$$

where V_{sw} is the volume of seawater and ρ its density.

If A_T is known, the next step is to use the measured CO_2 partial pressure p_2 along with alkalinity A_T to calculate the C_T of the equilibrated sample. This is then corrected for the loss of CO_2 using the value of [7.15]. This corrected C_T value, along with the original A_T, is then used to calculate the partial pressure before equilibration.

If C_T is known, this value is first combined with the equilibrated partial pressure p_2 to calculate A_T. Then, the correction for CO_2 loss is made to C_T and the original CO_2 partial pressure calculated.

If the result is to be used in a subsequent equilibrium model for CO_2, the measured partial pressure is usually converted to fugacity using the virial equations describing the non-ideal behaviour of CO_2 in air. However some computer programs for CO_2 equilibria have this correction built in and can accept p (CO_2) directly as an input parameter.

Continuous Measurements by Infrared Spectrometry

Continuous measurements of CO_2 partial pressure are normally carried out using infrared detection of the equilibrated CO_2 in air. Unlike in the discrete method, a fixed volume of air held at atmospheric pressure is equilibrated with a flowing stream of seawater. Since the seawater volume is essentially infinite relative to the air, this equilibration involves no measurable loss of CO_2 from the water. The air is recirculated through an infrared detector to determine its CO_2 mole fraction, which is then combined with the measured atmospheric pressure to obtain the CO_2 partial pressure. As with the dicrete method, this value may then be converted to the fugacity.

In most implementations, the air stream is dried before it enters the infrared analyser. This can be done using a solid water adsorbent, e.g. P_2O_5, or by cooling the air below its dew point. However, some recent models incorporate two channels, one of which measures water vapour, thus providing the ability to measure CO_2 in moist air.

The detector is calibrated with several standard gas mixtures of known CO_2 mole fraction. Its response is quite non-linear, so a quadratic or higher order equation is normally used to describe the detector response in terms of the amount of CO_2 in the infrared cell. If the air is dried before analysis, a correction must then be applied for the increase in CO_2 concentration caused by the removal of water vapour:

$$p\,(CO_2) = p\,(CO_2, \text{dry air}) \times (1 - VP_{SW}) \quad [7.16]$$

where VP_{SW} is the calculated vapour pressure of the seawater.

Since continuous underway measurements of p (CO_2) are normally made to evaluate air-sea exchange of CO_2 in different regions of the ocean, it is necessary to correct the value obtained back to the *in situ* seawater temperature. If the difference between the equilibrator temperature and the *in situ* temperature is not too large ($\Delta T < 2$ K), the following equation is suitable

$$p(CO_2, in\,situ) = p(CO_2, meas)\,\exp(0.0423[T_{in\,situ} - T_{meas}]) \quad [7.17]$$

Otherwise, the temperature correction must be made using the equilibrium equations for CO_2 and one other of the CO_2 system parameters. The procedure is quite similar to that described in the previous section for the temperature correction of pH.

7.6 Calculation of the CO_2 Composition

The basic concepts underlying the methods for the calculation of equilibrium systems were discussed in Chapter 5, including specific reference to the CO_2 system. A comprehensive account of available equilibrium constant data was also given in Chapter 4. In this section, we look specifically at how these concepts and data are applied to the seawater CO_2 system.

As mentioned in Section 7.1, the CO_2 system is completely specified if values for any two of the system composition parameters are adopted, usually by direct measurement. Generally, only the 4 parameters whose measurement methods have just been described are used for this purpose, viz. A_T, C_T, pH and $f(CO_2)$. Various calculation strategies are adopted depending on which of these 2 parameters are chosen as the independent input parameters. We shall examine some of the various combinations, using the first examples to introduce the terminology involved. Therefore it is better to work through the examples sequentially. In the following examples, the total proton pH scale has been used.

C_T and pH

We start by calculating $[H_2CO_3^*]$ directly

$$[H_2CO_3^*] = C_T \alpha_0 = \frac{C_T}{1 + \frac{K_1}{[H^+]} + \frac{K_1 K_2}{[H^+]^2}} \qquad [7.18]$$

From this, we can calculate $[HCO_3^-]$ and $[CO_3^{2-}]$

$$[HCO_3^-] = [H_2CO_3^*]\frac{K_1}{[H^+]} \qquad [7.19]$$

$$[CO_3^{2-}] = [HCO_3^-]\frac{K_2}{[H^+]} = [H_2CO_3^*]\frac{K_1 K_2}{[H^+]^2} \qquad [7.20]$$

$f(CO_2)$ is calculated from $[H_2CO_3^*]$ using the Henry's Law equilibrium

$$f(CO_2) = \frac{[H_2CO_3^*]}{K_0} \qquad [7.21]$$

These results for [7.19] and [7.20] allow calculation of the carbonate alkalinity A_C

$$A_C = [HCO_3^-] + 2[CO_3^{2-}] \qquad [7.22]$$

The difference between A_C and the total alkalinity A_T is the alkalinity due to all the minor species in seawater (see Section 6.8); here this is denoted A_M

$$A_M = [OH^-] - [H^+]_F - [HSO_4^-] - [HF] - [H_3PO_4] + [B(OH)_4^-] + [HPO_4^{2-}] + 2[PO_4^{3-}] + [SiO(OH)_3^-] \quad [7.23]$$

The individual terms in [7.23] are calculated from the appropriate equilibrium constants and total concentrations for each species as in [7.24]. Refer to Chapter 5 for full definitions of the degree of dissociation terms α_i used in [7.24].

$$[OH^-] = \frac{K_w}{[H^+]} \qquad [H^+]_F = \frac{[H^+]}{1 + S_T / K_S} \qquad [HSO_4^-] = \frac{S_T}{1 + K_S / [H^+]_F}$$
$$[B(OH)_4^-] = B_T \alpha_1 \qquad [SiO(OH)_3^-] = Si_T \alpha_1 \quad [7.24]$$
$$[HF] = B_T \alpha_0$$
$$[H_3PO_4] = P_T \alpha_0 \qquad [HPO_4^{2-}] = P_T \alpha_2 \qquad [PO_4^{3-}] = P_T \alpha_3$$

Notice that since HSO_4^- is defined as part of the ionic medium in the total proton scale, its contribution to the minor species alkalinity must be evaluated using its dissociation onsntant measured on the free proton pH in scale. In fact, the sum of $[H^+]_F$ and $[HSO_4^-]$ is extremely close to $[H^+]_T$.

Finally, combination of [7.2] and [7.44] allows calculation of A_T

$$A_T = A_C + A_M \quad [7.25]$$

C_T and f (CO_2)

The first step using these input parameters is to calculate $[H_2CO_3^*]$ using the Henry's Law equilibrium (cf [7.21])

$$[H_2CO_3^*] = K_0 \, f(CO_2) \quad [7.26]$$

From this point, the calculation method follows the same steps as the previous example, beginning at [7.19] and leaving out the calculation of f (CO_2) in [7.22]. The final step is to calculate C_T from the individual species

$$C_T = [H_2CO_3^*] + [HCO_3^-] + [CO_3^{2-}] \quad [7.27]$$

A_T and pH

The starting point for this method is to calculate the minor speciesalkalinity A_M using [7.23] and then calculate the carbonate alkalinity by difference

$$A_C = A_T - A_M \quad [7.28]$$

This then allows calculation of $[HCO_3^-]$

$$[HCO_3^-] = \frac{A_C}{1 + 2K_2 / [H^+]} \quad [7.29]$$

From this point, it is straightforward to calculate the remaining parameters.

C_T and A_T

This is perhaps the most common selection of input parameters. In this case, the equations cannot be solved directly and an iterative numerical method must be used. The following technique works quite effectively on a personal computer.

Firstly, assume a starting pH = 8 and calculate the minor species alkalinity A_M using [7.23]. From this, calculate A_C using [7.28]. We can now solve for a better pH estimate using [7.30] below. To simplify the notation, we define the ratio $a = A_C/C_T$.

$$[H^+] = -(a-1) + \sqrt{(a-1)^2 - 4a(a-1)\frac{K_2}{K_1}} \qquad [7.30]$$

This procedure is now repeated, from the point where A_M is calculated, until the successive estimates of A_C agree with each other within an acceptable tolerance (e.g. 10^{-9} mol kg^{-1}).

After the required A_C and $[H^+]$ have been found, the individual CO_2 species are easily calculated, starting with HCO_3^-

$$[HCO_3^-] = \frac{A_C - C_T}{\frac{K_2}{[H^+]} - \frac{[H^+]}{K_1}} \qquad [7.31]$$

followed by the use of [7.19] through [7.21] to calculate $[H_2CO_3^*]$, $[CO_3^{2-}]$ and finally $f(CO_2)$.

A similar procedure to the above may be used for calculating the composition using A_T and $f(CO_2)$ as input parameters.

7.7 Internal Consistency of the Methods

The internal consistency of the different methods for measuring the composition parameters of the CO_2 system can only be assessed by comparing a direct measurement with one calculated from any two other measured parameters. This comparison is as much a test of the reliability and consistency of the CO_2 equilibrium model as it is of the experimental methods.

Recently, Millero *et al.* examined the internal consistency using a set of seawater samples for which all 4 parameters were obtained by measurement. Their results are summarized in Table 7.3, which shows the average deviation from the experimental value for each parameter when calculated using various combinations of the others as input parameters. Results are shown for 5 different sets of equilibrium constants K_1 and K_2 for carbonic acid. These are referred to in Chapter 4.

Table 7.3 Average deviations from measured values of CO_2 parameters calculated using combinations of the other parameters as input values. The results for C_T and A_T are in mmol kg^{-1}, while those for f (CO_2) are in matm. Results for 5 different sets of K_1 and K_2 are given.

Reference	Δ pH	Δ A_T	Δ C_T	Δ *f* (CO_2)
Roy *et al.*	0.006	10.3	8.6	7.1
Goyet & Poisson	0.007	9.6	8.0	7.8
Dickson & Millero	0.011	5.4	4.3	9.4
Hansson	0.012	7.2	6.0	9.0
Mehrbach *et al.*	0.009	11.5	9.7	6.0

The results in the table show that there is reasonable internal consistency in the measurements and CO_2 model, although the results do not indicate that any particular set of values for the CO_2 dissociation constants is to be preferred over the others. However, the average deviations remain almost a factor of 10 larger than the target precision and accuracy for each parameter presented in Table 7.1. For example, the typical precision for spectrophotometric pH measurements is about ± 0.0005, which is considerably better than can be achieved by calculation from any of the other parameters.

Therefore at the present time, direct experimental measurement is to be preferred over calculation. Nonetheless, the attainment of the agreement observed in Table 7.3 must be regarded as a triumph of analytical and physical chemistry!

Further Reading

Dickson, A.G., The development of the alkalinity concept in marine chemistry, *Marine Chemistry*, *40*, 49-63, 1992.

Dickson, A.G., The measurement of pH in seawater,*Marine Chemistry*, *44*, 131-142, 1993.

Dickson, A.G., and J.P. Riley, The effects of analytical error on the evaluation of the components of the aquatic carabon dioxide system,*Marine Chemistry*, *6*, 77-85, 1978.

DOE, *Handbook of methods for the analysis of the various parameters of the carbon dioxide system in sea water*; version 2, ORNL/CDIAC-74, 1994.

Johnson, K.M., A.E. King, and J. Sieburth McN, Coulometric TCO_2 analyses for marine studies; an Introduction,*Marine Chemistry*, *16*, 61-82, 1985.

Johnson, K.M., A.E. King, and J. Sieburth McN, Total CO_2 analysis for marine studies: Automation and calibration, *Marine Chemistry*, *21*, 117-133, 1987.

Johnson, K.M., K.D. Wills, D.B. Butler, and W.K. JohnsonC.S. Wong, Coulometric total carbon dioxide analysis for marine studies : maximizing the performance of an automated gas extraction system and coulometric detector,*Marine Chemistry*, *44*, 167-187, 1993.

Millero, F., R. Byrne, R. Wanninkhof, R. Feely, T. Clayton, P. Murphy, and M. Lamb, The internal consistency of CO2 measurements in the equatorial Pacific, *Marine Chemistry*, *44*, 269-280, 1993.

Millero, F.J., The thermodynamics of the carbonate system in seawater, *Geochimica et Cosmochimica Acta*, *43*, 1651-1661, 1979.

Millero, F.J., J.-Z. Zhang, S. Fiol, S. Sotolongo, R.N. Roy, K. Lee, and S. Mane, The use of buffers to measure th pH of seawater,*Marine Chemistry*, *44*, 143-152, 1993.

Millero, F.J., J.-Z. Zhang, K. Lee, and D.M. Campbell, Titration alkalinity of seawater, *Marine Chemistry*, *44*, 153-165, 1993.

Wanninkhof, R., and K. Thoning, Measurement of fugacity of CO_2 in surface water using continuous and discrete sampling methods,*Marine Chemistry*, *44*, 189-204, 1993.

Chapter 8 CO_2 in the Oceans

This chapter uses the information and concepts developed in the preceding chapters of this book in a brief examination of the geochemical behaviour of CO_2 in the global ocean. This topic is of particular importance because of the role of the oceans in absorbing fossil fuel CO_2. Over the 50 years, there has been a significant increase in the CO_2 content of the atmosphere from this source. Yet, budgets for the likely amounts of CO_2 released by fossil fuels show that as much as half of the emitted CO_2 may have been absorbed by the oceans. Furthermore, as we shall see later in this chapter, absorption by the ocean is the long term fate of fossil fuel CO_2. The key question is, how long will it take to be absorbed?

8.1 CO_2 Composition of Typical Ocean Regions

As mentioned in Section 7.1, The CO_2 equilibrium system in seawater can be completely constrained by specifying any two of its main compositional parameters. The ensuing discussion will be based on the choice of total alkalinity A_T and total dissolved CO_2 C_T. This choice is a logical one because these are the only two parameters of the system that are conservative capacity factors. This means that both are temperature and pressure independent, a property of great usefulness given the large range in both T and p that occurs throughout the ocean. Surface waters can vary in temperature from below 0°C to over 30°C, although the temperature variation in deep waters is very much less. However, ocean waters exist at pressures ranging from 1 atm at the surface to over 1,200 atm in the deepest part of the ocean. The average depth is 3,600 m corresponding to about 3600 atm pressure.

The second useful attribute of these conservative capacity factors is that the C_T or A_T of seawater formed by the admixture of two, or more, different bodies of seawater can be directly calculated from the corresponding parameters for the constituent water types, taking into account the proportion of each in the mixture. The global ocean undergoes continuous circulation and is not homogeneous in its chemical properties. Thus the ability to predict, and rationalize, its composition in terms of the mixing of one or more water types together is of considerable value.

The Deffeyes Diagram

As mentioned, specifying both A_T and C_T completely determines the CO_2 properties of a particular seawater. From this it follows that any particular composition may be uniquely represented by a point on a diagram of A_T versus C_T. Such a diagram is termed a *Deffeyes diagram* in honour of the scientist who first suggested its utility.

Figure 8.1 shows a Deffeyes diagram upon which are marked the CO_2 compositions of major oceanic regions. The values of C_T and A_T chosen as 'typical' for construction of the diagram are also shown in Table 8.1. Our task is to explain the trends seen in these results.

Table 8.1 Typical values of total CO_2 and alkalinity in different oceanic water types. Data compiled from various sources, including the GEOSECS and WOCE Programs.

Region/Type	C_T (µmol kg^{-1})	A_T (µmol kg^{-1})
Warm surface water	1960	2306
Cold surface water	2220	2377
Deep Atlantic	2182-2204	2337-2359
Deep Pacific/Indian	2320-2366	2400-2473

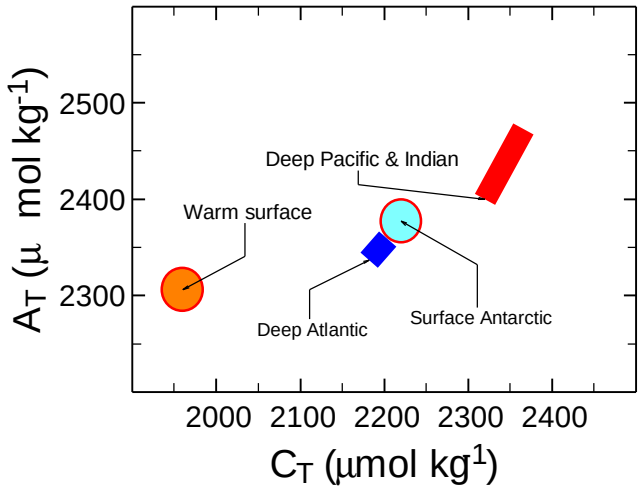

Figure 8.1 Typical values of total CO_2 and alkalinity for different oceanic water types displayed on a Deffeyes diagram. Data taken from Table 8.1.

Table 8.2 Calculated composition of various seawater types relevant to Table 8.1 and Figure 7.1. See text for explanation of the calculation conditions. In all cases, a constant salinity of S = 35.00 was assumed.

Region	C_T (µmol kg^{-1})	A_T (µmol kg^{-1})	f (CO_2) (µatm)
Surface, 25°C	1960	2300	356.1
Surface, 2°C	1960	2300	122.5
f (CO_2) = 356 µatm	2155	2300	356.0
Actual surface waters	2200	2377	348.1
Deep Atlantic	2193	2377	295.0
Deep Pacific/Indian	2343	2436	558.6

Table 8.2 shows the calculated CO_2 composition for several seawater types of relevance to explaining the experimental results seen on Table 8.1, Figure 8.1.

The first line of Table 8.2 shows results calculated assuming rounded values for C_T and A_T for warm surface waters typical of equatorial regions. For this, a temperature of 25°C was assumed. The key result of this calculation is the $f(CO_2)$ value of 356 μatm, one that is typical of the present-day (1990's) global atmosphere. Therefore, as the starting point of this discussion of the data in Table 8.1, Figure 8.1, we can say that warm surface waters, which cover all temperate and tropical latitudes, are close to equilibrium with the atmosphere.

The second line in Table 8.1 shows the calculated $f(CO_2)$ if the same seawater is translated to polar regions where surface water temperatures are much lower. The decrease in temperature to 2°C also decreases the equilibrium $f(CO_2)$ to only 122.5 μatm, a value that is much lower than the actual atmospheric fugacity. The atmosphere, as a gaseous fluid, is well-mixed compared to the ocean, and latitudinal variations in gas concentrations, including CO_2, are extremely small.

The much lower calculated $f(CO_2)$ for this hypothetical polar water would, by itself, leave the polar ocean well undersaturated with reference to atmospheric CO_2, a situation that would not remain static in the real ocean-atmosphere system. It is therefore relevant to ask what the polar water composition would be like if it were to remain in equilibrium with an atmospheric CO2 fugacity of $f(CO_2)$ = 356 μatm. The results of this model calculation are shown in the 3rd line of the table. For this calculation, input parameters of $f(CO_2)$ = 356 μatm and A_T = 2300 μmol kg^{-1} were assumed. The result is C_T = 2155 μmol kg^{-1}, a value about 10% higher than the starting point in warm surface waters.

This is not unreasonable since the Henry's Law constant increases in value from 25°C to 2°C from 0.0284 to 0.0582, an increase of about 100 %. Detailed calculations show that the expected increase in C_T resulting from this about 1/10, or 10 %.

Actual surface waters from the Antarctic region, as shown in Figure 8.1, have the composition shown in the 4th line of Table 8.2, revealing an slightly higher C_T (2200 μmol kg^{-1}) than that assumed in the 3rd line of the table, offset by a slightly higher T (2377 as opposed to 2300 μmol kg^{-1}). The equilibrium $f(CO_2)$ of this water is not significantly different from the that for the simple assumption in the 3rd line of the table.

At this point it is useful to note that the primary difference between polar and equatorial surface waters is temperature. Atmospheric CO_2 is, as indicated by the relative Henry's Law constants, about twice as soluble in polar water as warm equatorial water. We recall that the exchange of CO_2 between atmosphere and ocean takes place at constant alkalinity since the defining reference proton condition for A_T is a pure solution of CO2 in seawater. We conclude that most of the increase in C_T from warm to cold surface waters (lines 2 to 3 in Table 8.2) can be ascribed to increased CO_2 solubility. Notice that over this large range of oceanic surface waters, the alkalinity increases by only 77 μmol kg^{-1} or about 3 %.

This, by itself, is an interesting conclusion because it implies that the ocean-atmosphere system is maintained close to equilibrium by gas exchange processes as far as surface waters are concerned. It is useful to recall in this context that the present-day atmospheric concentration is considerably larger that the pre-industrial equilibrium value of about 280-290 μatm as a result of

the increases caused by fossil fuel burning and biomass alteration. Thus the characteristic time scale for equilibration of the atmosphere and the surface ocean must be shorter than the time scale of human-derived changes, i.e. 200 years. This value is consistent with the known rated of CO_2 exchange between the two reservoirs. Studies of gas exchange, and other exchange phenomena, indicate that the surface layer of the ocean comprises a layer of some 50-200 m depth that is rapidly mixed by the effects of wind. However, beneath this lie the deep waters of the global ocean, waters that occupy more than 95 % of the ocean's total volume. Exchange between these waters and the atmosphere is very much slower.

We now consider the composition ofthe deep ocean waters. At this point it is useful to note that with respect to $f(CO_2)$ being considered at present, the effects of pressure on the equilibria are rather small, and certainly not large enough to warrant consideration. Given this, one expects the $f(CO_2)$ of the deep waters to be more or less identical to those of polar surface waters. The 5th line of Table 8.1 shows that deep waters of the Atlantic ocean are indeed rather similar to polar surface waters with respect to their CO_2 composition. However, most of the global deep ocean is located in the Pacific and Indian oceans, and it is clear from the final line in the table that the CO_2 composition of these waters is considerably different. Specifically, they contain increased concentrations of both C_T and A_T, with the result that the CO_2 fugacity is at least twice than seen in any surface waters.

We note that changes in the alkalinity of seawater can only result from the addition or removal of acid-base species other than pure CO_2. Therefore we must examine possibilities for such changes in the alkalinity balance to explain the changes typified by Table 8.2. The changes observed are a consequence of the effect of biological processes on the CO_2 chemistry of seawater.

8.2 Effect of Biological Processes on CO_2

In the previous section we observed that the deep waters of the global ocean, especially in the Pacific and Indian oceans, have a different CO_2 composition from surface waters. While surface waters can be considered close to equilibrium with the atmosphere, deep waters have substantially higher A_T, C_T and $f(CO_2)$. These differences are a direct result of biological fixation of CO_2 in surface waters, some of which escapes respiration until it has escaped into the deep water reservoir, thus transporting a difference in CO_2 composition into the deep layers of the ocean.

Photosynthesis, which takes place exclusively in the euphotic zone of the surface ocean, consumes CO_2 dissolved in seawater in the production of biological organic tissue. It may be represented by the simplified equation

$$CO_2 + H_2O \rightarrow (CH_2O) + O_2 \qquad [8.1]$$

About 95 % of the CO_2 reduced to organic tissue (represented by CH_2O) undergoes respiration back to CO_2 in surface waters. Respiration is the exact reverse of [8.1], and the combination of photosynthesis and respiration obviously involves no net change in the water chemistry. However, about 5 % of the carbon that is reduced by photosynthesis escapes the surface water zone of respiration by sinking into the cold, quiescent deep layers of the ocean. However, this does not mean that it escapes the ultimate fate of oxidation back to CO_2. Indeed, virtually all of this

biological carbon that sinks into deep waters gets oxidized back to CO_2 in the deep layer. Only a very small fraction survives the passage through deep waters to become preserved in deep ocean sediments, some of which eventually becomes fossil fuel!

The transport of reduced CO_2 in the form of sinking biological tissue onto the deep ocean sets up a *biological pump* that shifts a fraction (5 %) of the products of surface water photosynthesis into deep waters. The remineralized products, i.e. CO_2, are eventually returned to surface waters as the ocean waters circulate and turn over. Thus the cycle, of which the biological pump is an integral part, is essential closed. However, the circulation process is relatively slow. Studies using radiocarbon (half-life 5780 yr) indicate that the average turnover time for oceanic deep waters is about 1600 yr. This is an important value, because it indicates the time scale over which the deep ocean and the atmosphere maintain equilibrium.

We know a lot about the action of the biological pump through the study of the vertical concentration profiles of the variuous chemical constituents of seawater, including CO_2, that are involved in the photosynthesis/respiration process. Of these, perhaps the most important are the macronutrients *nitrate* and *phosphate*, both of which are essential for photosynthesis. Nitrate is the major source of nitrogen needed for the synthesis of nitrogen-containing molecules such as amino acids, the key components of protein. Phosphate is required for the adenosine triphosphate (ATP) energy transfer system in primary organisms. Both nitrate and phosphate are in short supply in surface waters, and their low availability is often the factor that limits the total amount of net photosynthesis that can take place.

This is revealed by Figure 8.2 which shows typical vertical concentration profiles for both substances in the global ocean.

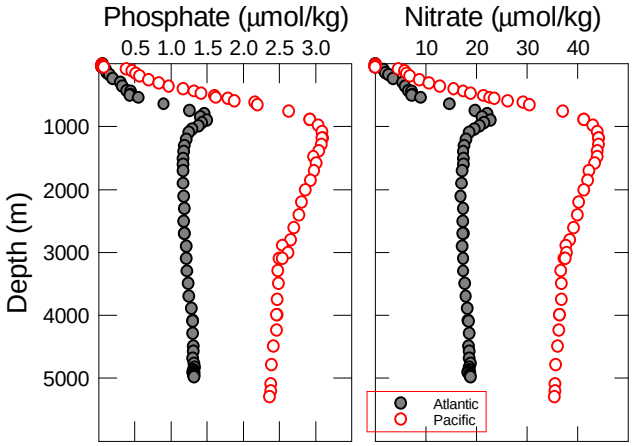

Figure 8.2 Typical vertical profiles of the macronutrients nitrate and phosphate in the Atlantic and Pacific Oceans. Drawn using data from the GEOSECS Program.

In both cases, we see that surface water concentrations of these macronutrients have been reduced to almost zero because of their efficient utilization for photosynthesis. Concentrations are maximum in deep waters as a result of the biological pump. Since the rate of return of deep waters to the surface is so slow, the macro-nutrients generated in deep waters by the oxidation of

biological material sinking down from the surface accumulate to high relative concentrations in the deep water layer. Ad the deep waters return to the surface by upwelling and diffusion, they carry with them the high nutrient concentrations, thus completing the closed cycle.

The corresponding vertical profiles for CO_2 and O_2, both of which are involved in the photosynthesis/respiration cycle (see [8.1]) are shown in Figure 8.3. These profiles show the features expected from the discussion given so far for the macro-nutrients. Total CO_2 increases from surface to deep waters by about 10 % in the Atlantic and 20 % in the Pacific (note that these relative increases are comparable to those seen for nitrate and phosphate in Figure 8.2). At the same time as C_T increases through the respiration of the sinking biological tissue, O_2 is consumed, as required by reaction [8.1]. Indeed, at mid-depths of the Pacificocean, O_2 is reduced in concentration to almost zero.

Examination of data such as those displayed in Figures 8.2 and 8.3 indicates that the stoichiometric ratios of the biological pump are approximately

$$1\ PO_4^{3-} : 15\ NO_3^- : 100\ CO_2 : 140\ O_2 \qquad [8.2]$$

These ratios are known as *Redfield ratios* in honour of Arthur Redfield, the marine scientist who first suggested their use as a description of the changes in water chemistry accompanying biological growth and respiration.

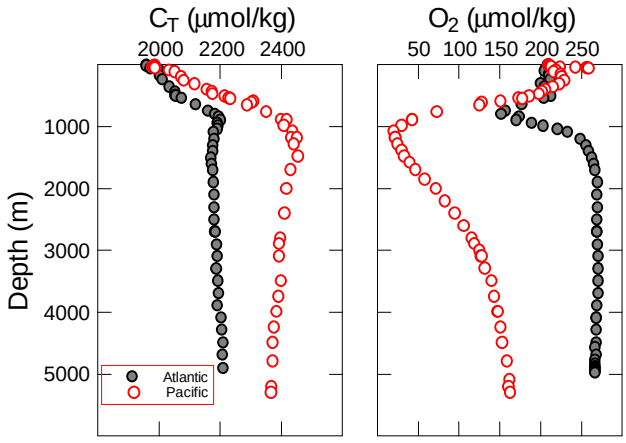

Figure 8.3 Typical vertical profiles of total CO_2 and dissolved oxygen in the Atlantic and Pacific Oceans. Drawn using data from the GEOSECS Program using the same station locations as Figure 8.2. C_T values are normalized to a constant salinity of 35.000.

Equation [8.1] is not the full story, however, because we still need to explain why the deep waters of the ocean have a higher alkalinity than at the surface. In its simplified form, [8.1] implies that photosynthesis and respiration merely remove or add neutral CO_2 , a process that would give rise to no change in A_T. Detailed investigations show that in fact there is a small *consumption* of H^+ during photosynthesis, with a corresponding *production* of H^+ accompanying respiration. Quantitatively, this amounts to about 1 H^+ for every 5 CO_2 molecules. Therefore, we would predict that the 20 % increase in C_T with depth as a result of the respiration of sinking organic tissue that is seen in the Pacific Ocean (Figure 8.3) should be accompanied by a *decrease* of about 20/5 = 4 % in A_T.

A quick glance at the results shown in Figure 8.4 shows that this is far from what is observed. In fact the trend is opposite and much larger: A_T increases significantly with depth, particularly in the Pacific Ocean where the increase is almost 10%. These changes can only be explained by an additional process accompanying CO_2 involvement in photosynthesis that acts directly on the proton balance of seawater. This process is the precipitation and dissolution of the mineral *calcite* ($CaCO_3$). Calcite is used by many of the planktonic organisms in the ocean for the construction of their mineral exoskeleton.

A large group of photosynthetic organisms that construct calcite exoskeleta is the *coccolithophoridae* (or coccoliths for short). These tiny unicellular plants build a network of interlocking calcite plates around the outside of the cell, rather like medieval armour. Figure 8.4 shows electron micrographs of typical coccolith plates. The shape and structure of the plates is different for each species and highly characteristic.

Figure 8.4 Electron micrograph of typical coccolith plates found in marine sediments.

Calcite exoskeleta are also constructed by the class of planktonic animals known as *foraminifera*. These normally construct a multi-chambered microscopic cell within which the organism lives. Foraminifera feed on bacteria and other planktonic organisms, including coccoliths. As with coccoliths, the shape and structure of the foraminifera shell is highly characteristic of the species, Examples are shown in Figure 8.5.

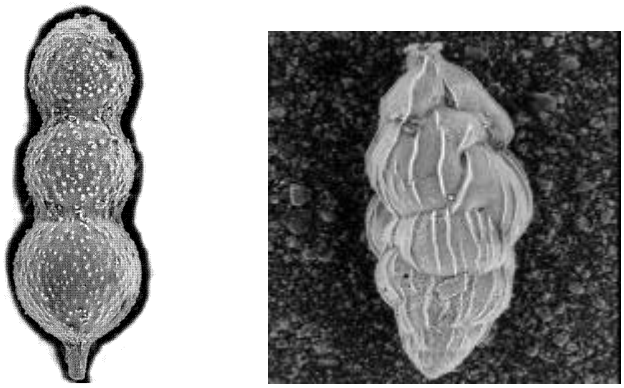

Figure 8.5 Electron micrograph of two foraminifera: Nodoseria aspera (left) and Uvigerinella californica (right).

The precipitation of calcite by marine organisms has a simple reaction stoichiometry

$$Ca^{2+} + CO_3^{2-} \rightarrow CaCO_3\,(s) \qquad [8.3]$$

This reaction consumes the alkaline species CO_3^{2-} and therefore decreases the water alkalinity (and C_T) while the reverse process generates CO_3^{2-} and increases A_T (and C_T). The $CaCO_3$ components of the biological debris sinking into deep water eventually undergo dissolution deeper in the water column, thus returning the alkalinity extracted from surface waters. This provides the source of the increase in A_T with water depth observed in Figure 8.6.

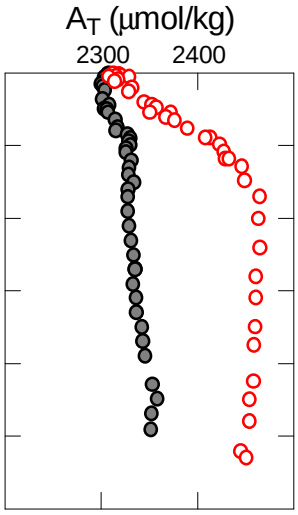

Figure 8.6 Typical vertical profiles of total alkalinity in the Atlantic and Pacific Oceans. Drawn using data from the GEOSECS Program using the same station locations as Figure 8.2. A_T values are normalized to a constant salinity of 35.000.

We are now in a position to account for all the changes observed in Tables 8.1 and 8.2. If we compare cold surface waters (line 4 of Table 8.2) with deep Pacific waters (line 6), it is clear that the combination of organic matter respiration and $CaCO_3$ dissolution gives increases in C_T and A_T of

$$\Delta C_T = 2343 - 2200 = 143\ \mu mol\ kg^{-1}$$
$$\Delta A_T = 2436 - 2377 = 59\ \mu mol\ kg^{-1} \qquad [8.4]$$

Since the alkalinity change for $CaCO_3$ dissolution is exactly twice the corresponding change in total CO_2 (because of the doubled contribution of carbonate ion to A_T), the change in C_T resulting from the $CaCO_3$ dissolution is expected to be half that of A_T, i.e. about 30 μmol kg^{-1}. Thus the net change in C_T arising only from respiration is 143 – 30 = 113 μmol kg^{-1}, or about 80% of the total change in C_T.

Naturally, the figures presented here are only a selection taken from particular regions of the ocean, and a more detailed analysis would require examination of a much more comprehensive set of results. However, the major conclusions of this analysis are sound. The biological pump exerts a strong influence on the spatial distribution of CO_2 species within the global ocean.

We now consider how these processes affect the speciation of CO_2 into its different chemical forms, and how they affect pH.

8.3 pH and f (CO_2)

For the vertical profiles of C_T and A_T shown in Figures 8.3 and 8.6, it is a simple matter to compute the remaining CO_2 composition with C_T and A_T as input parameters using the methods discussed in Chapter 7. Figure 8.7 shows calculated values for pH_T (total proton pH scale) and *f* (CO_2) for the Atlantic and Pacific Ocean sets of data used in previous figures.

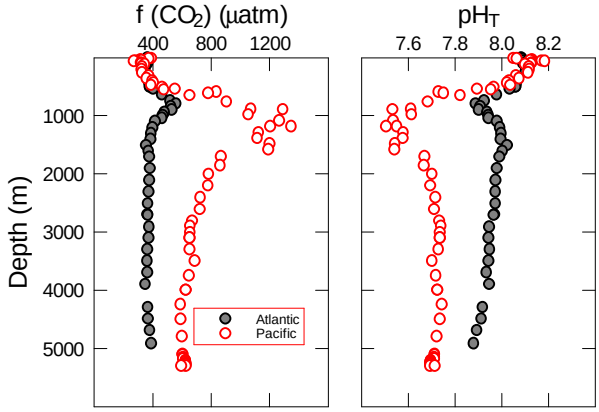

Figure 8.7 Typical vertical profiles of pH_T and CO_2 fugacity in the Atlantic and Pacific Oceans. Calculated from C_T and A_T data taken from Figures 8.3 and 8.6

The vertical trend for these two parameters is seen to be complementary: *f* (CO_2) increases steadily over the first 1000 m depth, after which it becomes relatively uniform in deep waters. The trend for pH_T is opposite to this. Clearly these opposite trends reflect the same basic changes in water chemistry. *f* (CO_2) is directly related to the concentration of H_2CO_3* through the Henry's Law equilibrium (see Chapters 4 and 7), Thus a decrease in pH, which shifts the CO_2 equilibrium system closer to this acidic species and increases its concentration, must also result in higher *f* (CO_2). The question is, therefore, why does the pH decrease with depth down the water column. To answer this, we must examine the effect on pH of the two processes that are feeding additional C_T and A_T into deep waters: biological pumping of both biological organic tissue and $CaCO_3$.

Ignoring the small alkalinity change accompanying photosynthesis and respiration, the effect of organic matter respiration is to generate dissolved CO_2 (reaction [8.3]). This will increase C_T with little change in A_T. This change, *by itself*, would cause a *decrease* in pH since a solution of pure H_2CO_3* is more acidic (pH = 5.6) than seawater itself.

On the other hand, the effect of $CaCO_3$ dissolution is the same as adding a soluble carbonate salt, e.g. Na_2CO_3, to the water. *Both* C_T and A_T will increase as a consequence of $CaCO_3$ dissolution, with A_T increasing twice as fast, on a mole basis, as C_T. Since a solution containing only carbonate ion has a *higher* pH than seawater, the effect of $CaCO_3$ dissolution is to *increase* the pH.

Both effects therefore oppose each other. It is clear that the decrease in pH from organic matter respiration overwhelms the increase in pH from $CaCO_3$ dissolution. In the previous section, we saw that the C_T and A_T profiles are consistent with about 80 % of the increase in total carbon resulting from organic matter respiration and only 20 % from $CaCO_3$ dissolution. These estimates are therefore consistent with the observed trends in pH.

The important point to note is the enormous influence of the biological pump on CO_2 composition of the atmosphere. Both Figure 8.7 and Table 8.2 make it clear that if the biological pump were not operating to maintain the concentration gradient between surface and deep waters, the equilibrium CO_2 partial pressure of the surface ocean would be significantly higher than it is. This would have with important consequences for the Earth's radiation balance and temperature. Thus the biological pump converts the ocean's surface waters into a protective 'blanket' having much lower CO_2 partial pressure than it otherwise would have. In this sense, marine plants control the climate that affects all other living things.

8.4 CO_2 Speciation

We now consider the speciation of CO_2 into the 3 chemical forms H_2CO_3*, HCO_3^- and CO_3^{2-}. The results of the calculations for the two oceanic examples are shown in Figure 8.8. Note that a logarithmic concentration axis has been used to make the results for the 3 parameters visible on the same diagram.

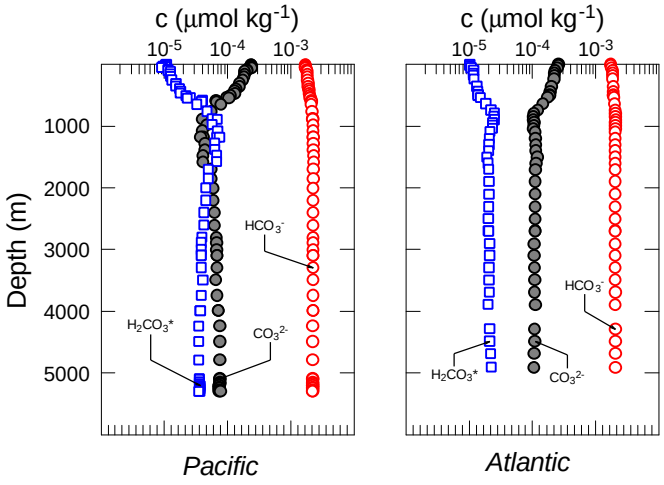

Figure 8.8 Typical vertical profiles of CO_2 speciation in the Atlantic and Pacific Oceans. Calculated from C_T and A_T data taken from Figures 8.3 and 8.6.

These results show trends that are consistent with the behaviour seen so far for the preceding parameters. The vertical profiles for $[H_2CO_3^*]$ are exactly the same as those for $f(CO_2)$, which is expected since these two parameters are linked directly through the Henry's Law equilibrium. $[H_2CO_3^*]$ increases with depth, particularly in the Pacific Ocean, consistent with the overall decrease in pH.

The vertical trend for $[HCO_3^-]$ also shows an increase with depth. Although this does not appear obvious because of the logarithmic scale used, the absolute increase for this ion is almost the same as the increase in C_T seen in Figure 8.3. It is clear that HCO_3^- is the dominant CO_2 species at all depths in the water column by at least an order of magnitude.

Finally, the vertical trend for $[CO_3^{2-}]$ is one of *decreasing* concentration, again consistent with the trend in pH. Note that $[CO_3^{2-}]$ decreases with depth even though the alkalinity is *increasing* at the same time. The reason for this is that the decrease in $[CO_3^{2-}]$ is offset by an increase in $[HCO_3^-]$ that is more than twice as great.

These concentration trends show what is happening to the end products of the biological pumping process. CO_2 generated by the respiration of biological organic tissue in the deep layer is neutralized by CO_3^{2-} generated by $CaCO_3$ dissolution

$$H_2CO_3^* + CO_3^{2-} \rightarrow 2\,HCO_3^- \qquad [8.5]$$

The equilibrium constant for this reaction has a large positive value

$$K = \frac{[HCO_3^-]^2}{[H_2CO_3^*][CO_3^{2-}]} = \frac{K_1}{K_2} \approx 10^4 \qquad [8.6]$$

Thus once the additional CO_2 generated from respiration has reacted with all carbonate ion from $CaCO_3$ dissolution, which it exceeds by about 4-fold, further reaction with the residual carbonate ion in the water will take place, decreasing the overall concentration. The net benefactor of these changes is the major species, HCO_3^-.

Comparison Between the Two Oceans

All of the trends examined above show a clear difference between the Atlantic and Pacific Oceans. For example, the increase with depth of $f(CO_2)$, and the decrease with depth of pH_T, are both greater for the Pacific Ocean than for the Atlantic. Comparison with Figures 8.2, 8.3, 8.6 and 8.8 shows the same feature. Whatever change is brought about by the biological pump, those changes are much larger in the Pacific than the Atlantic. In other words, the *efficiency* of the biological pump seems to be much greater in the Pacific Ocean.

This difference is caused by the nature of the ocean circulation system. The deep water circulation starts in the North Atlantic Ocean, where atmospheric cooling near Greenland and Scandinavia generates a downward-moving deep water current. This current flows south through to the Antarctic polar regions where further cold water is added by the same atmospheric cooling process. From there, the current flows into the Indian and Pacific Ocean.

This ocean current sets up a 'conveyor belt' for chemical materials generated by the biological pump. Thus, as biological debris containing both organic tissue and $CaCO_3$ that will soon be dissolved sinks into deep water, it hitches a ride on a current system flowing in the general direction Atlantic to Pacific. As a result, the products of dissolution build up at the end of the conveyor, in the North Pacific Ocean.

8.5 Factors affecting $CaCO_3$ Solubility

In the previous section we saw that the biological pump causes a significant decrease in the concentration of carbonate ion with depth, particularly in the Pacific Ocean. This has important consequences for the solubility equilibrium of $CaCO_3$.

$$CaCO_3\,(s) \rightarrow Ca^{2+} + CO_3^{2-} \qquad [8.7]$$

$CaCO_3$ will be stable with respect to dissolution in seawater solution if its ionic product Q_s for the particular seawater composition exceeds the value of the solubility product K_s constant for reaction [8.7]. In this case the solution is said to be *supersaturated* with respect to the solid phase.

$$Q_s = [Ca^{2+}][CO_3^{2-}] > K_s \quad \text{(supersaturated)} \qquad [8.8]$$

On the other hand if Q_s is less than K_s, the solution is *undersaturated* and $CaCO_3$ is able to dissolve spontaneously (in a thermodynamic sense)[7]

$$Q_s = [Ca^{2+}][CO_3^{2-}] < K_s \quad \text{(undersaturated)} \qquad [8.9]$$

Finally, if Q_s is equal to K_s, the solution is *saturated*, i.e. the solution and the solid phase at in equilibrium with each other

$$Q_s = [Ca^{2+}][CO_3^{2-}] = K_s \quad \text{(saturated, at equilibrium)} \qquad [8.10]$$

In seawater, the concentration of Ca^{2+} is almost constant at 0.01028 mol kg^{-1} (salinity 35). Thus the relationships in [8.8] to [8.10] can be simplified to comparing the actual carbonate ion concentration of the seawater with the equilibrium value for a saturated solution in seawater under the same conditions of temperature and pressure

$$[CO_3^{2-}]_S = \frac{K_s}{[Ca^{2+}]} \qquad [8.11]$$

Like the equilibrium constant K_s, the *saturation carbonate concentration* $[CO_3^{2-}]_S$ defined in [8.11] is a function of temperature and pressure.

Therefore, to assess the state of saturation of $CaCO_3$ at different depths in the ocean, we need only to compare the calculated values of the actual carbonate concentrations (e.g. from Figure 8.8) with values for saturated seawater of the same T and p.

The solubility product of the $CaCO_3$ mineral *calcite* (produced by most marine plankton) can be calculated from the equation

$$\begin{aligned} \log K_s = {} & -171.965 - 0077993T + \frac{2839.319}{T} + 71.595 \log T \\ & + (-0.77712 + 0.00284826T + \frac{178.34}{T})\, S^{1/2} \\ & - 0.07711\, S + 0.0041249\, S^{3/2} \end{aligned} \qquad [8.12]$$

---

[7] Whether it is *actually* able to dissolve depends on other factors, notably the rate of reaction.

The corresponding expression for the mineral form *aragonite*, which is produced by some organisms, particularly pteropods and corals, is

$$\log K_s = -171.945 - 0077993T + \frac{2903.293}{T} + 71.595 \log T + (-0.068393 + 0.0017276T + \frac{88.135}{T}) S^{1/2} - 0.10018 S + 0.0059415 S^{3/2} \quad [8.13]$$

The effect of pressure on these constants was discussed in Section 4.2. Both minerals increase slightly in solubility over the depth range of the ocean.

Figure 8.9 compares the actual carbonate concentrations with the saturation values for the example stations in the Pacific and the Atlantic. The comparison shows a clear difference between the two. In the Atlantic, both calcite and aragonite remain supersaturated at all depths (for the particular Atlantic station shown here). By contrast, in the Pacific both minerals become undersaturated in deeper waters.

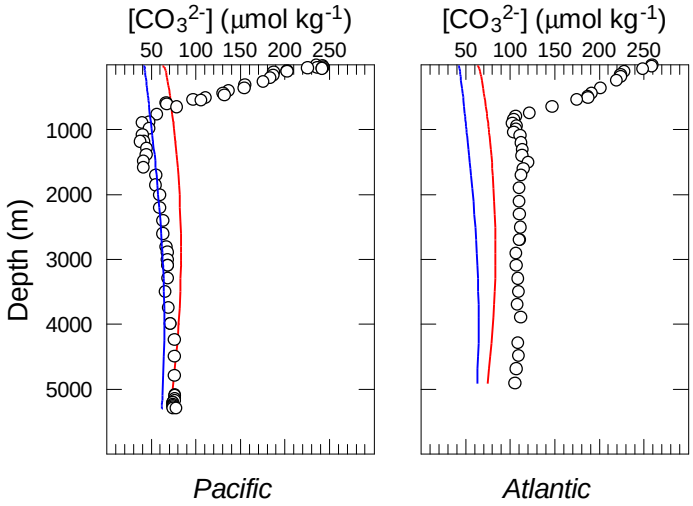

Figure 8.9 Vertical profiles of CO_3^{2-} concentration in the Atlantic and Pacific Oceans compared to the saturation carbonate concentration. [CO_3^{2-}] calculated from C_T and A_T data taken from Figures 8.3 and 8.6. Saturation values calculated as described in the text.

One should not generalize too much using results obtained for just two particular places in the global ocean. A more detailed examination of $CaCO_3$ saturation using much more data leads to the following general conclusions. Aragonite is undersaturated in the Pacific, except in shallow waters. This is consistent with the fact that deposits of aragonitic organisms, e.g. pteropods, are not found in Pacific deep waters, except during glacial transition periods when the carbonate chemistry changes temporarily. Calcite becomes undersaturated in the Pacific at a depth of about 3000 m, whereas the comparable depth in the Atlantic is somewhat shallower.

The level in the water column at which seawater and $CaCO_3$ are at equilibrium is termed the *saturation depth* (or horizon). This depth level, viewed as a surface in the water column, slopes *downwards* towards the Pacific. This slope is yet another consequence of the conveyor belt process.

In general, the depth distribution of $CaCO_3$ saturation agrees reasonably well with the known distribution of this mineral in deep ocean sediments. $CaCO_3$ is abundant in sediments where the sea bottom lies above the saturation horizon, but very rare in the deep, abyssal regions of the Pacific Ocean. In this context, the biogenic $CaCO_3$ that rains down from the ocean surface is somewhat like snow: it "melts" wherever it falls deeper than the submarine mountain tops that protrude into supersaturated water!

8.6 The Ocean-Atmosphere CO_2 Cycle

The preceding discussion shows that there are two competing processes that affect the spatial distribution of CO_2 in the ocean. The *biological pump* transports carbon fixed by photosynthesis as organic matter, plus $CaCO_3$, from surface to deep waters where they undergo re-dissolution. This sets a gradient in composition between the surface and deep layers. On the other hand, the ocean circulation system mixes surface and deep waters together on a time scale of 1000-2000 years, and serves to equalize any composition differences between the two layers created by the biological pump. We may think of the ocean circulation system as a *physical pump* that operates in both directions, unlike the one-way biological pump.

These features are easier to visualize in a *box model* such as that in Figure 8.10. This represents the atmosphere, ocean surface layer and deep layer, and the ocean sediments as *boxes*. The arrows connecting the boxes represent *fluxes* of carbon moving from one box to another. The fluxes shown in the figure are given in units of Gt of carbon per year. Superimposed on the Figure are estimates of the current rate of production of excess CO_2 by the combustion of fossil fuels.

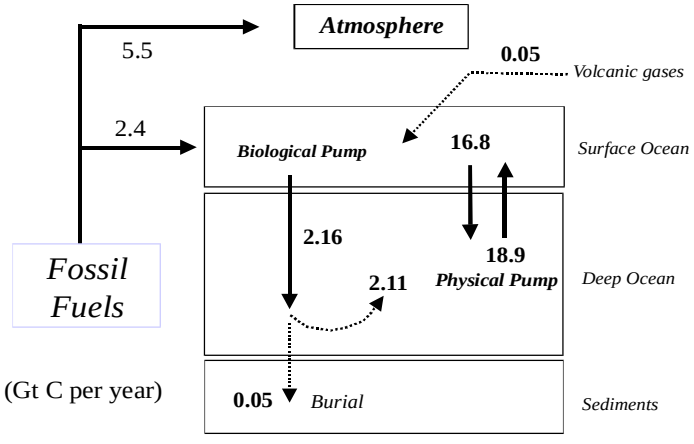

Figure 8.10 Idealized box model for the ocean-atmosphere carbon cycle. Fluxes are in Gt of C per year, where 1 Gt = 10^9 metric tonnes = 10^{12} kg.

Interpretation of the figure requires information about the amounts of carbon held in the different reservoirs. This is shown in Table 8.2 in units of Gt. To estimate the turnover time for a particular reservoir, divide the reservoir size in Gt from Table 8.2 by the correspnding flux value shown in the Figure. For example, CO_2 in the atmosphere is increasing at a rate of 3.3 Gt/yr from fossil fuel burning, and the pre-industrial atmosphere contained 600 Gt of CO_2. Therefore the turnover time for fossil fuel CO_2 input is 600 / 3.3 = 180 years. The interpretation of this value is that fossil fuel CO_2 inputs will, in the absence of any other change, double the atmospheric CO_2 concentration in a time scale of 180 years.

Table 8.2. Comparison of the amounts (in Gt of carbon) in different reservoirs of the global carbon cycle.

Carbon Reservoir	*Amount (Gt C)*
Recoverable fossil fuels	4,200
Soil organic matter	1200
Terrestrial biomass	1200
Ocean, inorganic carbon	40,000
Ocean, organic matter	4800
Ocean, living biomass	8.4
Atmosphere (1993)	820
Atmosphere (1750)	600
Atmospheric increase	220

Features of the Ocean-Atmosphere Cycle

Table 8.2 shows that oceanic carbon inventory is dominated by inorganic carbon (40,000 Gt). Of this quantity, about 2 % or 800 Gt is located in the surface layer. Therefore its size is comparable to the atmosphere, with which it maintains equilibrium through gas exchange of CO_2. Although not shown in Figure 8.10, this gas exchange flux is about 8-12 Gt/yr across the global ocean surface.

As indicated in the Table, the terrestrial and oceanic biomasses are very different in size. However, their importance in terms of carbon *flux* is about equal. This is because the average member of the oceanic biomass is a unicellular planktonic organisms having a very short lifetime (days). By contrast, the average terrestrial plant is a tree having a lifespan measured in years or decades. Although not shown in Figure 8.10, the gross rate of CO_2 fixation by marine phytoplankton in the surface ocean is about 44 Gt/yr. However, only 2.16 Gt/yr, or 5%, of this

escapes the surface layer as sinking biogenic debris. The remainder undergoes respiration in the surface layer where it was originally formed, and thus has no net effect on the carbon cycle.

The carbon cycle, as presented in Figure 8.10, is largely internal. The small loss of carbon from the deep ocean to marine sediments, which is in the form of both residual organic matter and $CaCO_3$, is more or less balanced by the input of fresh CO_2 by volcanic gases.

Carbon leaves the oceanic surface layer through both the physical pump (sinking of surface water in polar areas) and through the one-way biological pump. The flux figures show that about 10 % of the total carbon flux is accounted for by the biological pump. This is consistent with the fact that the total carbon inventory (C_T) of the surface layer is about 10 % lower than the deep ocean (Figure 8.3). Interestingly, for the limiting macro-nutrients nitrate and phosphate, transport out of the surface layer is almost completely accounted for by the biological pump. The turnover times for carbon removal from the surface layer are relatively short

$$T = \frac{800}{2.16 + 16.8} = 42 \text{ yr} \qquad [8.14]$$

Carbon leaves the deep layer primarily through the physical pump, as the carbon-enriched deeper waters complete the oceanic circulation cycle and return to the surface. Much of this takes place in specific areas of deep water *upwelling*, especially on the western boundaries of the major continents. Because this water contains very high concentrations of the macro-nutrients, upwelling areas are generally extremely fertile. A good example is the coast of Peru, home to a (sometimes) massive anchovy fishing industry. This return of macro-nutrients to the surface layer is what supports their *net* productivity, i.e. the fixation of carbon that becomes lost in the form of sinking biological material. Oceanographers often refer to this as *new production* to distinguish it from the much larger total production that goes through the complete photosynthesis-respiration cycle without leaving surface waters. The latter, as already mentioned, has no net effect on the carbon cycle budget.

The turnover time for loss of carbon from the deep layer is

$$T = \frac{41{,}200}{18.9 + 0.05} = 2200 \text{ yr} \qquad [8.15]$$

This value is consistent with measurements of the ^{14}C radiocarbon content of CO_2 taken from deep waters of the ocean, which reach as high as several thousand years in the North Pacific. It also provides a perspective on how long it will take for recently-released fossil fuel CO_2 to reach equilibrium with the deep ocean.

Of the 2.16 Gt/yr of carbon transported into deep waters as sinking biological material, 2.11 Gt/yr or 98 % undergoes re-dissolution and remains within the oceanic cycle. Only 2 % escapes to be buried on sediments. A small fraction of this carbon eventually becomes fossil fuel deposits, probably less than 1 % (0.0005 Gt/yr). This allows a crude comparison of the rate of formation of fossil fuels with the rate at which we are presently consuming them. The consumption rate is 3.3 + 2.4 = 5.7 Gt/yr, which is many orders of magnitude faster than the natural production rate.

Reference to Table 8.2 shows that the Earth system contains about 4,200 Gt of recoverable fossil fuels, of which perhaps 90 % still remain untouched. Indeed, at the present rate of consumption, these reserves would last

$$T = \frac{4{,}200 \times 0.90}{3.3 + 2.4} = 660 \text{ yr} \qquad [8.16]$$

However, 660 years is not very long, even in the context of the brief span of human history. Obviously other energy sources must be found.

Figure 8.10 also shows that the fluxes of CO_2 generated by fossil fuel burning (and other human activities such as cement manufacture, gas flaring and deforestation) are of the same order of magnitude as the natural fluxes in the ocean atmosphere system. Of the 5.7 Gt/yr of carbon as CO_2 released, only about a third (2.4 Gt/yr) manages to get into the ocean system. The rest "backs up" in the atmosphere, causing increasing concentrations of CO_2. The rate of uptake of atmospheric CO_2 by the ocean is simply not fast enough to cope with the onslaught produced by the burning of carbon-containing fuels.

Since the surface layer reservoir occupies only a small fraction of the total oceanic carbon inventory, it is clear that the entry of 2.4 Gt/yr of additional carbon to the ocean system from fossil fuels is significant in relation to the natural internal fluxes. Obviously, penetration of recent fossil fuel CO_2 into some of the deep parts of the ocean must be involved. Indeed, this can be demonstrated by very careful detailed studies of the C_T properties of deep waters. Increased C_T consistent with uptake of fossil fuel CO_2 can be found in the deep waters at the start of the circulation system having the youngest radiocarbon age. However, the measurement problems are severe, as the following argument shows. The total carbon released as fossil fuels since the mid-1700's is about 400 Gt, of which about half now remains in the atmosphere. Some of the 'missing' 200 Gt has probably ended up in increased terrestrial biomass, but it is likely that most of this 200 Gt has ended up somewhere in the deep ocean. However, although large, 200 Gt represents only about 0.5 % of the total inorganic carbon held in the ocean. Were it not for the fact that only the youngest deep waters have been affected by fossil fuel CO_2, it would not be technically possible to measure the increase!

8.6 Implications of Increasing Atmosphere CO_2 for the Ocean

We compete this analysis of CO_2 chemistry in the oceans by looking at the implications for increasing atmospheric CO_2 on ocean chemistry. The preceding discussion makes it clear that the overall uptake rate of atmospheric CO_2 by the oceans occurs on a timescale of thousands of years (the age of the oldest carbon atoms in the ocean). Therefore we shall separate our consideration of the effects of increased atmospheric CO_2 into two cases. The first is the short-term scenario in which the primary changes will be those occurring in surface waters. The second is the long-term scenario after which fossil fuels have run out, or their use has been been outlawed, and the ocean-atmosphere system can once again achieve equilibrium.

Short-Term Scenario

To examine this case, we make the assumption[8] that increasing atmospheric CO_2 concentration maintains equilibrium with the surface layer of the ocean. Since CO_2 exchange is independent of alkalinity, we calculate the C_T and CO_2 speciation using a constant A_T and increasing values of $f\ (CO_2)$ as input parameters.

The results of the calculations are depicted in Figure 8.11, which shows how some of the parameters change with an increase in $f\ (CO_2)$ from the pre-industrial value of 280 µatm to about 4 times that value. This change would theoretically use up about half of the recoverable fossil fuels reservoir.

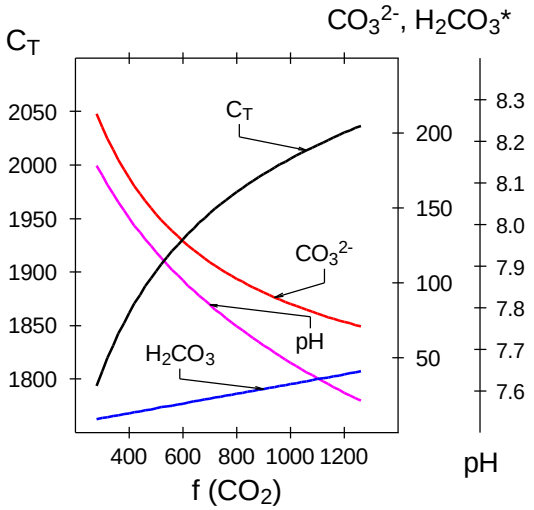

Figure 8.11 Calculated change in seawater speciation as a function of increasing atmospheric CO_2 fugacity. Assumed A_T is constant at 2100 mmol kg^{-1}.

Firstly, we note that as expected from the Henry's Law equilibrium, the concentration of H_2CO_3* increases linearly with $f\ (CO_2)$. Note also that C_T does not increase linearly, nor is its relative increase as great as that of $f\ (CO_2)$. For example, for a doubling of $f\ (CO_2)$ from 400 to 800 µatm, C_T increases from 1862 to only 1975 µmol kg^{-1}, i.e. an increase of only 6 %. In other words, oceanic C_T is strongly buffered against changes in atmospheric $f\ (CO_2)$. This was first pointed out by Roger Revelle, after whom the factor describing this effect has become known as the *Revelle buffer factor*. It is defined as follows

---

[8] This assumption is not entirely realistic because complete equilibrium between the atmosphere and the surface ocean would need to take account of the mass-balance between the 2 reservoirs. As CO_2 transfers to the surface ocean, the atmospheric concentration must decrease. This was not allowed for in the analysis.

$$RF = \frac{\frac{\partial f(CO_2)}{f(CO_2)}}{\frac{\partial C_T}{C_T}} \qquad [8.17]$$

The Revelle buffer factor has a value that depends on the CO_2 composition (as shown by the curvature in Figure 8.11), and has a typical value in the range 9-12 for present-day surface seawater. This means that the relative changes in C_T are a factor 9-12 times *lower* than the corresponding relative changes in $f(CO_2)$.

As expected from the addition of a gas whose pH in pure solution is lower than that of seawater, the increase in $f(CO_2)$ causes pH to decrease. For a doubling of $f(CO_2)$ the pH decrease is 0.26, which means that the $[H^+]$ is about doubled. This arises because virtually all of the extra CO_2 taken up by the seawater ends up as HCO_3^-, effectively forming a new H^+.

At the same time, reaction [8.5] takes place, bringing about the decrease in the concentration of carbonate ion seen in Figure 8.11. For a doubling of $f(CO_2)$, the final carbonate concentration is about half its original value. Once the $f(CO_2)$ exceeds about 1200 μatm, the diminished carbonate ion concentration begins to approach the value for $CaCO_3$ saturation, implying that $CaCO_3$-secreting organisms may not be able to precipitate this mineral in such a situation.

Long-Term Scenario

In the long-term scenario, we assume that sufficient time has elapsed for the ocean-atmosphere system to reach equilibrium. Suppose that this arises when most of the available fossil fuel reserves have been converted to CO_2. What will be the composition under these circumstances?

We begin the calculation by noting that these reserves are rather small (4,200 Gt) compared to the oceanic inorganic carbon (40,000 Gt) (Table 8.2). Therefore, we will assume as a first approximation, most of the fossil fuel CO_2 ends up in the ocean, and then see if the resulting composition indicates that a more detailed account has to be made of the mass-balance. First we start with some typical values for the modern deep ocean taken from Table 8.1 as an average for the whole ocean shown as the first line in Table 8.3

$$C_T = 2300\ \mu mol\ kg^{-1} \qquad A_T = 2400\ \mu mol\ kg^{-1} \qquad [8.18]$$

The Table shows that the equilibrium $f(CO_2)$ of such water is about 520 μatm, which would be reduced to about half that value after the effects of the biological pump have kicked in.

Next we assume that 4,200 Gt of fossil fuel carbon becomes distributed throughout the whole ocean mass (10^{21} kg of seawater). This implies an increase in C_T of 350 μmol kg^{-1} without change in alkalinity (line 2 of Table 8.3).

The third line in the Table shows the new C_T value resulting from the uptake of this additional CO_2. At constant alkalinity, we see that the equilibrium $f(CO_2)$ has increased markedly from 520 to 4600 μatm. In fact, this increase is large enough that we would need to consider the mass-balance between ocean and atmosphere.

Table 8.3 Typical values of total CO_2 and alkalinity in different oceanic water types. Data compiled from various sources, including the GEOSECS and WOCE Programs.

	C_T (μmol kg^{-1})	A_T (μmol kg^{-1})	f (CO_2)
Global ocean now	2300	2400	520
4200 Gt fossil fuel	+350	0	-
After CO_2 uptake	2650	2400	4600
$CaCO_3$ dissolution	+350	+700	-
After $CaCO_3$ dissolution	3000	3100	750

However, there is a more important factor that we have not yet accounted for. Reference to Figure 8.11 suggests that if the f (CO_2) were to increase by anything like as much as just indicated, then the equilibrium carbonate ion concentration of the whole water column would drop well below the level for saturation of $CaCO_3$. In this situation, the deposits of $CaCO_3$ on the ocean floor would begin to dissolve, consuming H_2CO_3*

$$CaCO_3\,(s) + H_2CO_3^* \rightarrow Ca^{2+} + 2HCO_3 \qquad [8.19]$$

The net result of this, if all the additional CO_2 were 'titrated' with $CaCO_3$, would be a doubling of the original increase in C_T and an equivalent increase in alkalinity. This is shown in the last two lines of the Table. The final result is a CO_2 fugacity that is not much different from the present-day scenario. In other words, the atmosphere would probably have a composition similar to that which prevailed before fossil fuel consumption began at an accelerated rate.

Is there enough $CaCO_3$ in the deep ocean to titrate the CO_2 from all available fuel reserves? The deep ocean contains millions of Gt of $CaCO_3$, but most of it is not in sufficient contact with seawater to allow reaction [8.19] to take place. Estimates of the geochemically available quantity of $CaCO_3$ vary, but are similar in magnitude to the quantity of available fuel reserves.

From this it follows that the human society is engaged in a rather uncertain, and potentially dangerous chemical experiment. If the race to generate more energy is not curtailed, or solved by methods that do not entail CO_2 emission, we may find out the hard way that the oceanic buffer reservoir of $CaCO_3$ is not sufficient to control ocean chemistry and the atmospheric CO_2 concentration will remain, more or less forever, at very high values!

Further reading

Bradshaw, A.L., P.G. Brewer, D.K. Shafer, and R.T. Williams, Measurements of total carbon dioxide and alkalinity by potentiometric titration in the GEOSECS program,*Earth and Planetary Science Letters, 55*, 99-115, 1981.

Broecker, W.S., and T.H. Peng,*Tracers in the Sea*, 98,226. pp., Eldigio Press, New York, 1982.

Broecker, W.S., T. Takahashi, H.J. Simpson, and Peng T-H, Fate of fossil fuel carbon dioxide and the global carbon budget,*Science, 206*, 409-418, 1979.

Peng, T.-H., and W.S. Broecker, Ocean life cyles and the atmospheric CO_2 content, *Journal of Geophysical Research*, *89*, 8170-8180, 1984.

Revelle, R., and H.E. Suess, Carbon dioxide exchange between atmosphere and ocean and the question of an increase of atmospheric CO_2 during past decades, *Tellus*, *9*, 18-27, 1957.